# Application of Transformed Manipulated Variables to Cascade Control Systems for Linearization and Disturbance Rejection

Masters Thesis

Callum Ross Kingstree (s1621206)



Supervisors: Sigurd Skogestad and Cristina Zotică

Chemical Engineering Overseas Research Project 5

Chemical Engineering with Management (MEng)

2020/2021

# Abstract

The field of chemical engineering provides many examples, such as chemical reactors or distillation columns, which are hard to control due to their nonlinear nature. The control of nonlinear systems is a complex task that has attracted a lot of interest in academia but has not resulted in industry adopting many of the techniques due to their complexity. This thesis analyses the application of a new nonlinear control technique, namely Transformed Manipulated Variables, to systems with a relative order greater than one. The new theory, first developed by Prof. Sigurd Skogestad, is a simple yet powerful, model-based, method to control nonlinear systems. Different control structures are presented and simulated to find the optimum configuration for a given system.

Four case studies are presented; tanks-in-series, a continuously stirred-tank reactor, a pH neutralisation problem and a semi-batch polymerisation reactor. It has been shown that the new theory is robust for a certain level of model error and time delay for systems with a relative order greater than one. Disturbance rejection and set-point tracking are compared to PI control throughout; always showing an increase in performance, without the loss of simplicity. Furthermore, perfect disturbance rejection is seen for a special case.

# Acknowledgements

I would like to thank my supervisor, Professor Sigurd Skogestad, for his willingness to take me on board with some of his current work and for the interesting discussions which we had. Furthermore, I would also like to thank my co-supervisor Cristina Zotică for her patience and willingness to invest time in me and my work. The transition to remote learning due to Covid-19 was made a more pleasant experience due to her hard work and perseverance.

# Covid-19 Impact Statement

After Covid-19 closed the world down in late March 2020 it was shortly decided after that my placement at NTNU must take place entirely remotely. This presented a number of challenges, which are detailed below.

Trying to conduct an entire project online was difficult, though I am still very appreciative for the opportunity. Simple things like trying to run a piece of code, or follow an example; if we were able to meet in person then small bugs could easily be identified and explained a lot faster - screen-sharing is not an ideal environment for this. Also, not meeting in person meant that asking what would normally be a short trivial question, would require a full email and obviously I did not want to constantly be pestering anyone. I am very grateful that I was invited to attend the group's weekly meetings as I think it kept me a little sane having some social contact, though seeing most people partake in person (at least for the most part) was difficult to see since restrictions in Norway were a lot less than those imposed in Scotland.

Furthermore, I had to complete my project while living at home with my parents. Firstly, normally when studying for a project I'd try to set myself somewhere like the library or Murchison House, away from my 'life' - so that I could easily separate work and play. On this occasion, it was impossible and this made it really hard to switch off. This meant it was difficult to focus solely on my project. Secondly, with both parents working in the NHS, they would often be working long tiresome hours, creating a stressful environment when they came home. This meant that I was not able to devote my full time to working on my project, especially at evenings and weekends.

The pandemic also threw up some challenges with regards to basic common university activities, that would normally go unnoticed. In normal times I would always take books out from the library, but this was impossible. This meant that not all resources were available to me as not all books are digitalized yet and the University of Edinburgh Library's 'Scan & Deliver' service was not available at the time of

writing. In addition to this, the transition from reading a paper book to an online pdf made it difficult for me and to fully understand content as I had to write it down myself, taking more time than expected. I did not have access to a working printer either. This has meant that the literature review section of my thesis is less complete than I would have liked it to be.

# Contents

# List of Figures

# List of Tables

# Nomenclature

## Global

### Abbreviations

| | |
|---|---|
| ADRC | = Active Disturbance Rejection Control |
| ANN | = Artificial Neural Network |
| CV | = Controlled Variable |
| CSTR | = Continuous Stirred-Tank Reactor |
| CW | = Cooling Water |
| DL | = Double Linearized |
| EKF | = Extended Kalman Filter |
| ESO | = Extended State Observer |
| FOPTD | = First-Order-Plus-Time-Delay |
| GLT | = General Linear Transform |
| IAE | = Integral of Absolute Error |
| ISE | = Integral of Squared Error |
| LHP | = Left-Hand Plane |
| MV | = Manipulated Variable |
| MPC | = Model Predictive Control |
| MRAC | = Model Reference Adaptive Control |
| MIMO | = Multiple-Input Multiple-Output |
| ODE | = Ordinary Differential Equation |
| RADRC | = Reduced-order Active Disturbance Rejection Control |
| PEMFC | = Proton Exchange Membrane Fuel Cell |
| RESO | = Reduced-order Extended State Observer |
| RHP | = Right-Hand Plane |
| SIMC | = Simple/Skogestad Internal Model Control |
| SISO | = Single-Input Single-Output |
| TF | = Transfer Function |
| UKF | = Unscented Kalman Filter |

### Parameters

$\tau_c$ = Controller tuning parameter [*time*]
$\tau_D$ = Controller derivative time [*time*]
$\tau_I$ = Controller integral time [*time*]
$K_c$ = Controller proportional gain [unit depends on system]
$u$ = System input [unit depends on system]
$v$ = General linear transformed input [unit depends on system]
$v_{L0}$ = Alternative form of general linear transformed input [unit depends on system]
$v_0$ = Static transformed input [unit depends on system]
$v_{FL}$ = Integrating transformed input [unit depends on system]
$w$ = Internal variable [unit depends on system]
$y$ = System output [unit depends on system]

## Case Study A

$T_0$ = Temperature of inlet flow [$^\circ C$]
$T_1$ = Temperature of tank 1 [$^\circ C$]
$T_2$ = Temperature of tank 2 [$^\circ C$]
$T_d$ = Temperature of disturbance flow [$^\circ C$]
$F_0$ = Inlet flow to tank 1 [$m^3\,min^{-1}$]
$F_1$ = Outlet flow of tank 1 [$m^3\,min^{-1}$]
$F_2$ = Outlet flow of tank 2 [$m^3\,min^{-1}$]
$F_d$ = Disturbance flow to tank 2 [$m^3\,min^{-1}$]
$h_1$ = Level in tank 1 [$m$]
$h_2$ = Level in tank 2 [$m$]
$A_1$ = Cross-sectional area of tank 1 [$m^2$]
$A_2$ = Cross-sectional area of tank 2[$m^2$]

## Case Study A Extension

$T_0$ = Temperature of inlet flow [$^\circ C$]
$T_1$ = Temperature of tank 1 [$^\circ C$]
$T_2$ = Temperature of tank 2[$^\circ C$]
$T_{1d}$ = Temperature of disturbance flow to tank 1 [$^\circ C$]
$T_{2d}$ = Temperature of disturbance flow to tank 2 [$^\circ C$]
$F_0$ = Inlet flow to tank 1[$m^3\,min^{-1}$]
$F_1$ = Outlet flow of tank 1 [$m^3\,min^{-1}$]

$F_2$ = Outlet flow of tank 2 $[m^3\,min^{-1}]$
$F_{1d}$ = Disturbance flow to tank 1 $[m^3\,min^{-1}]$
$F_{2d}$ = Disturbance flow to tank 2 $[m^3\,min^{-1}]$
$h_1$ = Level in tank 1 $[m]$
$h_2$ = Level in tank 2 $[m]$
$A_1$ = Cross-sectional area of tank 1 $[m^2]$
$A_2$ = Cross-sectional area of tank 2$[m^2]$

# Case Study B

$T_0$ = Reference temperature $[K]$
$T_1$ = Inlet stream temperature $[K]$
$T$ = Tank temperature $[K]$
$V$ = Volume of tank $[m^3]$
$q_1$ = Inlet stream flowrate $[m^3\,min^{-1}]$
$q_2$ = Outlet stream concentration of A $[c_{Af}]$
$Q$ = Heat provided $[kJ\,min^{-1}]$
$c_p$ = Specific heat capacity $[kJ\,kg^{-1}\,K^{-1}]$
$c_{Af}$ = Inlet stream concentration of A $[kmol\,m^{-3}]$
$c_A$ = Outlet stream concentration of A $[kmol\,m^{-3}]$
$E$ = Activation energy $[kJ\,kmol^{-1}]$
$H_{rx}$ = Heat of reaction $[kJ\,kmol^{-1}]$
$\rho$ = Density $[kg\,m^{-3}]$
$k_0$ = Reference rate constant $[min^{-1}]$
$R$ = Universal gas constant $[kJ\,kmol^{-1}\,K^{-1}]$

# Case Study C

$[q_1]$ = Concentration of stream 1 $[M]$
$[q_2]$ = Concentration of stream 2 $[M]$
$[q_3]$ = Concentration of stream 3 $[M]$
$A_1$ = Cross-sectional area of tank 1 $[cm^2]$
$A_2$ = Cross-sectional area of tank 2 $[cm^2]$
$K_{a1}$ = Equilibrium constant for reaction 1 $[-]$
$K_{a2}$ = Equilibrium constant for reaction 2 $[-]$
$K_{a3}$ = Equilibrium constant for reaction 3 $[-]$
$\theta$ = Time delay in pH measurement $[s]$
$q_1$ = Flowrate of stream 1 $[ml\,s^{-1}]$

$q_2$ = Flowrate of stream 2 $[ml\,s^{-1}]$
$q_3$ = Flowrate of stream 3 $[ml\,s^{-1}]$
$q_{1e}$ = Flowrate of stream 1e $[ml\,s^{-1}]$
$q_4$ = Flowrate of stream 4 $[ml\,s^{-1}]$
$W_{a1}$ = Reaction invariant A - stream 1 $[M]$
$W_{b1}$ = Reaction invariant B - stream 1 $[M]$
$W_{a2}$ = Reaction invariant A - stream 2 $[M]$
$W_{b2}$ = Reaction invariant B - stream 2 $[M]$
$W_{a3}$ = Reaction invariant A - stream 3 $[M]$
$W_{b3}$ = Reaction invariant B - stream 3 $[M]$
$W_{a4}$ = Reaction invariant A - stream 4 $[M]$
$W_{b4}$ = Reaction invariant B - stream 4 $[M]$
$h_1$ = Level in tank 1 $[cm]$
$h_2$ = Level in tank 2 $[cm]$
$pH$ = pH of stream 4 (and tank) $[-]$
$C_{v1}$ = Valve coefficient $[ml^{0.5}\,s^{-1}]$

# Case Study D

$m_{M,0}$ = Initial mass of monomer $[kg]$
$m_{P,0}$ = Initial mass of polymer $[kg]$
$m_{W,0}$ = Initial mass of water $[kg]$
$\rho_M$ = Density of monomer $[kg\,m^{-3}]$
$\rho_P$ = Density of polymer $[kg\,m^{-3}]$
$\rho_W$ = Density of water $[kg\,m^{-3}]$
$c_{p,M}$ = Heat capacity of monomer $[kJ\,kg^{-1}\,K^{-1}]$
$c_{p,P}$ = Heat capacity of polymer $[kJ\,kg^{-1}\,K^{-1}]$
$c_{p,W}$ = Heat capacity of water $[kJ\,kg^{-1}\,K^{-1}]$
$MW_M$ = Molecular weight of monomer $[kg\,kmol^{-1}]$
$m_c$ = Mass of coolant in jacket $[kg]$
$\dot{m}_c$ = Mass flowrate of coolant in jacket $[kg\,s^{-1}]$
$c_{p,C}$ = Heat capacity of coolant $[kJ\,kg^{-1}\,K^{-1}]$
$k_0$ = Pre-exponential rate constant $[s^{-1}]$
$k_1$ = Rate constant correction $[m\,s\,kg^{-1}]$
$k_2$ = Rate constant correction $[-]$
$E$ = Activation energy $[kJ\,min^{-1}]$
$c_0$ = Batch viscosity correction $[kg\,m^{-1}\,s^{-1}]$
$c_1$ = Batch viscosity correction $[-]$
$c_2$ = Batch viscosity correction $[-]$

| | |
|---|---|
| $c_3$ | = Batch viscosity correction $[-]$ |
| $a_0$ | = Batch viscosity correction $[K]$ |
| $-\Delta H_p$ | = Heat of polymerization $[kJ\,kmol^{-1}]$ |
| $d_0$ | = Heat transfer coefficient correction $[kW\,m^{-2}\,K^{-1}]$ |
| $d_1$ | = Heat transfer coefficient correction $[m\,s\,kg^{-1}]$ |
| $\dot{m}_M^{-in}$ | = Mass flowrate of monomer $[kg\,s^{-1}]$ |
| $[t_{M,0}^{in}, t_{M,1}^{in}]$ | = Monomer flow schedule $[s]$ |
| $T_{set}$ | = Temperature set-point $[K]$ |
| $R$ | = Universal gas constant $[kJ\,kmol^{-1}\,K^{-1}]$ |
| $(UA)_{loss}$ | = Heat loss to surroundings factor $[kW\,K^{-1}]$ |
| $\tau_p$ | = Time constant for heating/cooling $[s]$ |
| $\theta_1$ | = Time delay 1 $[s]$ |
| $\theta_2$ | = Time delay 2 $[s]$ |
| $i$ | = Impurity $[-]$ |
| $1/h_f$ | = Fouling factors $[m^2\,K\,kW^{-1}]$ |
| $T_{amb,S}$ | = Summer ambient temperature $[K]$ |
| $T_{amb,W}$ | = Winter ambient temperature $[K]$ |
| $T_{inlet}$ | = Inlet cooling water temperature $[K]$ |
| $T_{steam}$ | = Inlet steam temperature $[K]$ |
| $a_3$ | = Temperature set-point parameter $[-]$ |
| $a_4$ | = Temperature set-point parameter $[-]$ |
| $a_5$ | = Temperature set-point parameter $[-]$ |
| $B_1$ | = Reactor bottom area $[m^2]$ |
| $P$ | = Jacket perimeter $[m]$ |
| $B_2$ | = Jacket bottom area $[m^2]$ |

# Chapter 1

# Introduction

The control of a chemical process is of utmost importance. There will be many disturbances for any given system and keeping all process variables at their prescribed values is paramount to the expected operation of a plant. Not only for performance-related factors like temperature control for a specific molecular weight of polymer production, but it is also used to add a layer of safety to the plant. For example, to avoid thermal runaway of a reactor. Although it still requires a level of personnel, it is largely automated if used correctly once set up.

It may be said that every chemical process is nonlinear, some are just able to be represented by a linear model better than others. In cases where linear approximation is not accurate, conventional linear PID control cannot be used and the limitations of this started to be explored in the 1950s (Bequette, 1991). Following on from this, nonlinear process control started to receive more attention and continues to do so. Due to the simple nature of PID control, some nonlinear control techniques focus on creating a nonlinear PID controller in order to control processes. Another example is feedback linearization, whereby the nonlinear system is transformed into a linear system (Khalil, 2002, Isidori, 1995). The new nonlinear control theory discussed in this thesis - Transformed Manipulated Variables (MVs) - has had initial examples published by Zotică et al. (2020), with a more general paper currently being written. It may be seen to have similarities to feedback linearization, though also encompasses the simplicity of a PID controller. This thesis explores the application of the new nonlinear control theory to complex systems which require cascade control or other means.

## 1.1 Motivation

From the existing methods in literature, discussed in Chapter 2, it is clear to see the motivation for a new nonlinear control theory. Existing methods are either complex and rigorous, or simple but lacking performance. Many of the nonlinear control methods are scarcely applied to chemical systems, let-alone implemented in industry. A nonlinear control scheme must be as simple as possible if it is to stand a chance of being applied in reality; in particular, industry is well suited to existing PID controllers. Another point is the reliance on an accurate process model, and therefore the robustness of the system. A control scheme based solely on a process model is likely to struggle in the presence of model mis-match and unknown/unmeasured disturbances. Nevertheless, basing a control scheme on a process model results in better performance when the system is operating as expected. Therefore, a control scheme that can cope with both a degree of model mis-match and have good performance is the goal. In addition to this, stability is one of the most important parts of designing a control scheme, and therefore a stable system (i.e. poles in the left-hand plane of $Im$ vs. $Re$) is preferred to the marginally stable system (i.e. poles at the origin) as with feedback linearization.

## 1.2 Objective

The objective of this thesis was to analyse and compare different control schemes for different case studies. Both the advantages and limitations of certain control schemes were identified and the possibilities in terms of disturbance rejection and set-point changes for both accurate and in-accurate process models were studied.

## 1.3 Thesis Structure

This thesis is divided into different case studies, each presented as an isolated case. The case studies presented in this thesis are a Tanks-in-Series problem, a continuous stirred-tank reactor (CSTR) problem, a pH control problem and the Chylla-Haase reactor; a benchmark problem from literature. Nomenclature and units in each case study are isolated. The thesis is structured as follows:

**Chapter 2** provides a literature review of the published work in the field of nonlinear process control.

**Chapter 3** presents the new transformed MVs (a.k.a. transformed inputs) theory which is applied in the four case studies.

**Chapter 4 - 8** presents the studied case studies. For each case study, firstly the process models are presented, followed by the control structures used in simulations, then the results of the simulations and finally a discussion - a look into where the results fit into the bigger picture. They are organised as follows:

**Chapter 4** : Tanks-in-Series
**Chapter 5** : Tanks-in-Series Extension
**Chapter 6** : CSTR
**Chapter 7** : pH Neutralisation
**Chapter 8** : Chylla-Haase Reactor

**Chapter 9** presents the conclusion and details possible future work.

# Chapter 2

# Background

In this section, a short literature review on some of the methods for nonlinear control, with a focus on chemical processes, is presented. There is an in-depth focus on feedback linearization (Section 2.2) due to its similarities to the new input transformation theory. In addition to this, basic control theory and controller tuning used is described.

## 2.1 PID Controllers

### 2.1.1 Control Theory

For the new nonlinear control theory, a linear PI/PID controller is employed. Therefore, in this section, some of the available tuning methods are presented and the chosen tuning technique is described. Also, throughout, the term *relative order* is taken to mean the number of times the output must be differentiated in order for the input to appear directly.[1]

#### 2.1.1.1 Controller Tuning

PID controllers are widely used to control processes and return them to their set-points, these can be presented in both the time domain and the Laplacian domain. The parallel, or ideal, form is used throughout this thesis and takes the form of Eq. 2.1 and 2.2.

$$u(t) = \bar{u} + K_c \left[ e(t) + \frac{1}{\tau_I} \int_0^t e(t^*) dt^* + \tau_D \frac{e(t)}{dt} \right] \tag{2.1}$$

[1] relative degree and relative order are used interchangeably throughout depending on the theory being used

$$C(s) = K_c\left[1 + \frac{1}{\tau_I s} + \tau_D s\right] \tag{2.2}$$

$$e(t) = y_{sp}(t) - y(t) \tag{2.3}$$

Where $u(t)$ is the input, or manipulated variable (MV), to the process, $\bar{u}$ is the nominal steady-state value, $t$ is the time, $C(s)$ is the transfer function of the controller and $e(t)$ is the error entering the controller, as defined by Eq. 2.3, where $y(t)$ is the output and $y_{sp}(t)$ is the output set-point. $K_c$, $\tau_I$ & $\tau_D$ are the three tuning parameters used in a PID controller; the proportional gain, the integral time and the derivative time respectively. It is shown in block diagram form in Fig. 2.1 for an error defined in the Laplacian domain, $E(s)$, and the manipulated variable in the Laplacian domain, $U(s)$ (Seborg et al., 2010).

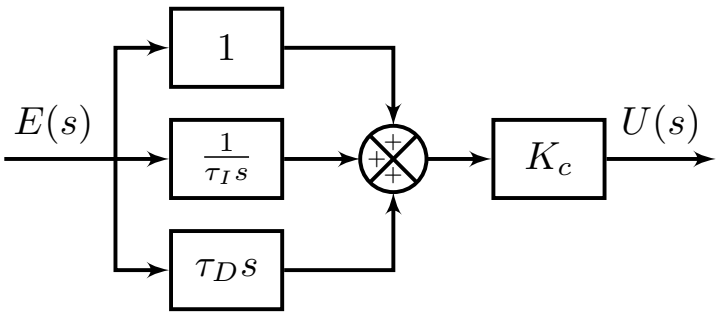


Figure 2.1: PID Controller in Parallel Form (Seborg et al., 2010)

There are multiple ways to choose tuning parameters for a PID controller, for example;

- *Ziegler-Nichols Method*: The most common Ziegler-Nichols tuning is based on a frequency domain method. A P-controller is used and the system is run with different $K_c$ values until sustained oscillation is achieved. The $K_c$ at which this is achieved is labelled $K_{cu}$ and the period of the oscillation is labelled $P_u$. This is then used in different relationships, for example for a PI controller, $K_c = 0.45K_{cu}$, $\tau_I = P_u/1.2$ (Ziegler and Nichols, 1942). However, this method is known to give an aggressive response (Skogestad, 2003; Tyreus and Luyben, 1992). It also lacks a definitive tuning parameter for the user.

- *Cohen-Coon Method*: This is based on a step-response to the open-loop system. This is then fitted to first-order-plus-time-delay (FOPTD) model to get the process gain, $K$, the process time constant, $\tau$, and any time delay, $\theta$. These values are then used in simple relationships to give controller parameters (Cohen and Coon, 1953). Although, this is based on a decay ratio of $\frac{1}{4}$ and results

are similar to the Ziegler-Nichols method (Van Der Zalm, 2004).

- *Internal Model Control (IMC) Controller Design*: This is a model-based design rather than the controller relations as above. The controller is effectively designed from the invertible part of the process model and an IMC filter, $f = \frac{1}{(\tau_c s+1)^r}$ (Rivera et al., 1986; Morari et al., 1989). $\tau_c$ is able to be used as a tuning parameter in order to be able to control how aggressive the controller is.

However, the controllers used throughout (except where explicitly stated) were tuned using SIMC (Simple/ Skogestad Internal Model Control) tuning rules (Skogestad, 2003). These rules provide a simple method to tune PID controllers, similar to the IMC controller design with a single tuning parameter, $\tau_c$, which is the closed-loop time constant. Also, similarly to the Cohen-Coon method, a step response is made and a model is fitted - this does not have to be FOPTD. For all applicable controllers in this thesis, the open-loop responses are presented in Appendix A for validation purposes. The process parameters are then used to calculate controller parameters, shown in Table 2.1. A small value of $\tau_c$ will lead to a faster response and a larger value will lead to a more stable and robust response. This analytic approach is easily applied to numerous systems while allowing the user to tune the system with a single parameter. This relies on the system having open-loop stability, but this is the case for all examples where it is used in this thesis.

Table 2.1: PID Tuning Parameters (Skogestad, 2003)

| **Process** | $g(s)$ | $K_c$ | $\tau_I$ | $\tau_D^a$ |
|---|---|---|---|---|
| First order | $k\frac{e^{-\theta s}}{\tau_1 s+1}$ | $\frac{1}{k}\frac{\tau_1}{\tau_c+\theta}$ | $\min\{\tau_1, 4(\tau_c+\theta)\}$ | – |
| Second order | $k\frac{e^{-\theta s}}{(\tau_1 s+1)(\tau_2 s+1)}$ | $\frac{1}{k}\frac{\tau_1}{\tau_c+\theta}$ | $\min\{\tau_1, 4(\tau_c+\theta)\}$ | $\tau_2$ |
| Pure Time Delay | $ke^{-\theta s}$ | 0 | $0^b$ | – |
| Integrating | $k'\frac{e^{-\theta s}}{s}$ | $\frac{1}{k'}\frac{1}{(\tau_c+\theta)}$ | $4(\tau_c+\theta)$ | – |
| Integrating with Lag | $k'\frac{e^{-\theta s}}{s(\tau_2 s+1)}$ | $\frac{1}{k'}\frac{1}{(\tau_c+\theta)}$ | $4(\tau_c+\theta)$ | $\tau_2$ |
| Double Integrating | $k''\frac{e^{-\theta s}}{s^2}$ | $\frac{1}{k'}\frac{1}{4(\tau_c+\theta)^2}$ | $4(\tau_c+\theta)$ | $4(\tau_c+\theta)$ |

[a] series form, [b] pure integral controller, $C(s) = K_I/s$, $K_I := \frac{K_c}{\tau_I} = \frac{1}{k(\tau_c+\theta)}$. g(s) = process model, $k$ = process gain, $\theta$ = process delay, $\tau_1, \tau_2$ = process time constants, $\tau_c$ = tuning parameter, $k' = k/\tau_1$, as $\tau_1 \to \infty$, $k'' = k'/\tau_2$ as $\tau_2 \to \infty$.

### 2.1.2 Using PID for Nonlinear Control

The use of a PID controller is one of the simplest ways to control a process and is, therefore, a commonly used technique. However, the performance of a conventional linear PID controller is limited when applied to a nonlinear process. Anandanatarajan et al. (2006) show the limitations of a PI controller on the nonlinear level control

of a conical tank. The performance of their PI controller is adequate for some set-point changes, but for others it creates an oscillatory response. The controller is tuned based on a linearized model of the system, but due to the nonlinear nature the gain and the time constant of the model change as the level changes. Though, Desoer and Lin (1985) claim that for a "large class of nonlinear plants" a linear PI controller will be able to provide closed-loop stability. Jha et al. (2017) control a (nonlinear) crystallization process with a simple PID controller. The concentration and temperature in the crystallizer must be kept within a given range so that a uniform crystal size distribution is achieved. The jacket temperature is taken as the manipulated variable and crystallizer temperature is the controlled variable. The responses to set-point changes exhibit overshoot and settling times that are not within acceptable performance limits.

There is no point in complicating a control system that can adequately be controlled by PI/PID control in the first place. In this sub-section, various common methods regarding the use of PI/PID controllers for nonlinear processes are discussed.

#### 2.1.2.1 Taylor Series Expansion

The simplest way to linearize a system is to use a Taylor Series expansion. The steady-state operating point is usually chosen as the reference coordinates. For a system $\frac{dy}{dt} = f(y, u)$ with steady-state conditions $(\bar{y}, \bar{u})$, truncated at first-order terms, this becomes;

$$f(y,u) \cong f(\bar{y},\bar{u}) + \left.\frac{\partial f}{\partial y}\right|_{\bar{y},\bar{u}} (y-\bar{y}) + \left.\frac{\partial f}{\partial u}\right|_{\bar{y},\bar{u}} (u-\bar{u}) \tag{2.4}$$

This means that simple, classic control techniques can be applied to the linearized version of the system, for example, PID controller tuning methods (Seborg et al., 2010). The main problem with this method is the fact that the system is linearized around a singular point; normally the steady-state operating conditions as this gives $f(\bar{y}, \bar{u}) = 0$. Therefore, the further the system deviates from this point the lower the performance that the control scheme can achieve. This also relies on an accurate model of the system to begin with.

#### 2.1.2.2 Fuzzy Logic Controller

A fuzzy logic controller, originally by Zadeh (1965), is a class of controllers that are able to control systems with a lack of information or model. Passino and Yurkovich (1998) describe fuzzy control as "a formal methodology for representing, manipulating and implementing a human's heuristic knowledge about how to control a

system". This means that the control is less model-based and more based on heuristics and rules that are applied. The system error is fed to the controller, which analyzes it, compares it to the pre-set 'rules', and then calculates the desired MV required.

Aslam and Kaur (2011) used fuzzy logic control to control the concentration in a CSTR, a nonlinear system. This was compared to P, PI and PID control and showed that using a fuzzy controller both the rise and settling times were reduced by almost ten-fold and did not show an inverse response to the same extent as the P/PI/PID controllers. Chabni et al. (2016) realised similar results, though not to the same extent when comparing PI-only control with a fuzzy controller for liquid level control in a tank. Rise time for a set-point change was reduced by five-fold for the fuzzy control.

Pitalua-Diaz et al. (2015) compare PI-only control with fuzzy logic PI control for indoor benzene concentrations, modelled by complex nonlinear models. In these simulations the response in the benzene concentration showed no real difference between the two cases. Although, the change in extractor fan speed (MV) was much more stable for the fuzzy control, whereas for the PI-only case it peaked at 100% and then quickly went back down to 0.8%.

Although fuzzy control can out-perform P/PI/PID control, it must be used with caution. If the controller is based on a human's perspective of the system more than a process model there is a fear that not all information will be taken into account (Passino and Yurkovich, 1998). Furthermore, if the process is not well known in the first place then a (rough) process model will need to be known. Tuning of the controller may be difficult as there are many parameters to be tuned and there is no systematic tuning procedure, in comparison to the numerous tuning rules for PID control that are available (Pivojika, 2000). Moreover, this technique is still centred around the steady-state values for the system, similar to the Taylor Series expansion.

## 2.2 Feedback Linearization

Covered extensively in literature, feedback linearization is a technique widely studied that transforms a nonlinear system into a fully or partially linear system that is able to be easily controlled. This comprises of two steps, one to change the coordinates and a second to provide state feedback, the order of which does not matter. Feedback linearization is summarised below, based on methods from Khalil (2002),

Isidori (1995) and Nijmeijer and van der Schaft (1990).

For a system described by Eq. 2.5, the idea is to try to find an equivalent linear system with a change of variables and state feedback control as per Eq. 2.6 and 2.7 respectively. All variables used must be measured or estimated. For systems where measurements are not available, for economic or practical reasons, methods such as using a High Gain Observer or using an Extended Kalman Filter (EKF) may be used to estimate parameters (Khalil, 2002).

$$\dot{x} = f(x) + g(x)u \tag{2.5a}$$
$$y = h(x) \tag{2.5b}$$

$$u = \alpha(x) + \beta(x)v \tag{2.6}$$
$$z = T(x) \tag{2.7}$$

This can also be described by the concept of *Lie Derivatives*.

The Lie Derivative of $h(x)$ with respect to $f(x)$ is defined by Eq. 2.8.

$$L_f h(x) = \frac{\partial h}{\partial x} f(x) \tag{2.8}$$

Lie Derivatives may be repeated, or applied in a different direction. For example, Lie Derivatives in the directions of $g(x)$ and $f(x)$ are shown in Eq. 2.8.

$$L_g h(x) = \frac{\partial h}{\partial x} g(x) \tag{2.9a}$$
$$L_g^2 h(x) = L_g(L_g h(x)) = \frac{\partial (L_g h(x))}{x} g(x) \tag{2.9b}$$
$$L_f L_g h(x) = L_f(L_g h(x)) = \frac{\partial (L_g h(x))}{x} f(x) \tag{2.9c}$$

Therefore, mathematically, for the system in Eq. 2.5, the relative degree $r$ of the system near a point $x^o$ can be defined by Eq. 2.10, where $x$ is in a neighbourhood of $x_0$ (Isidori, 1995).

$$L_g L_f^k h(x) = 0 \qquad \forall k < r - 1 \tag{2.10a}$$
$$L_g L_f^{r-1} h(x^o) \neq 0 \tag{2.10b}$$

### 2.2.1 Change of Coordinates

Assuming $r = n$, where $n$ is the order of the system, the system can be transformed to the $z$ matrix by Eq. 2.11 (if $r < n$, see Khalil (2002)).

$$z = T(x) = \begin{bmatrix} \phi_1(x) \\ \phi_2(x) \\ \vdots \\ \phi_r(x) \end{bmatrix} = \begin{bmatrix} h(x) \\ L_f h(x) \\ \vdots \\ L_f^{r-1} h(x) \end{bmatrix} \tag{2.11}$$

Therefore, the derivative of $z$ is represented by Eq. 2.12 by applying the chain rule and taking into account Eq. 2.10. From this, it can be seen that the system becomes a chain of integrators.

$$\dot{z} = \begin{bmatrix} \frac{d\phi_1}{dt} \\ \frac{d\phi_2}{dt} \\ \vdots \\ \frac{d\phi_r}{dt} \end{bmatrix} = \begin{bmatrix} \phi_2 \\ \phi_3 \\ \vdots \\ b(z) + a(z)u \end{bmatrix} \tag{2.12}$$

Where,

$$a(z) = L_g L_f^{n-1} h(T^{-1}(z))$$
$$b(z) = L_f^r h(T^{-1}(z))$$

### 2.2.2 State Feedback

The introduction of an external reference input $v$ can then be used to implement a feedback law. This is related to the input variable $u$ as per Eq. 2.13, where $a(z)$ and $b(z)$ are the same as above. Comparing this to Eq. 2.12, it can be concluded that $d\phi_r/dt = v$.

$$u = \frac{1}{a(z)}(b(z) + v) \tag{2.13}$$

Since the steps of change of coordinates and state feedback can be applied in any order, this can also be represented in terms of $x$ as in Eq. 2.14.

$$u = \alpha(x) + \beta(x)v; \tag{2.14}$$

Where,

$$\alpha(x) = -\frac{L_f^r h(x)}{L_g L_f^{r-1} h(x)}$$
$$\beta(x) = \frac{1}{L_g L_f^{r-1}}$$

As $d\phi_r/dt = v$ the system is therefore easily controlled, e.g. using $v = Kz$ where $K$ is controller gain.

### 2.2.3 Input-output linearization

Input-output linearization is a technique related to feedback linearization above, except it only linearizes the input - output equations, leaving some of the internal states as nonlinear (Isidori, 1995). This is favoured if parts of the system are non-minimum phase, i.e. contains right-hand plane zeros or time delays, since inverting these parts in feedback linearization will not give a viable system. It may also be attractive if the equations are difficult to solve analytically and input-output linearization gives a sufficient response (Hangos et al., 2006).

### 2.2.4 Disturbance Decoupling

Feedback linearization, as set out above, is based on system stabilisation; any disturbances must be decoupled from the output in order to maintain the system's performance (Isidori, 1995). However, if the disturbance is not measured then decoupling is only possible if the relative degree of the disturbance is more than, or equal to, the relative degree of the input (Henson and Seborg, 1997). The relative degree for a disturbance is the number of times the output needs to be differentiated for the disturbance term to directly appear. This case is investigated later in Chapter 6. Anyhow, stated by Henson and Kurtz (1995), in a chemical engineering context this is rarely seen and this means that unpredictable responses may be experienced.

If the disturbance $d$ is measured then it may be incorporated into the control law - a variation of Eq. 2.14 - as shown in Eq. 2.15. This, therefore, introduces a feedforward aspect to the control.

$$u = \alpha(x) + \beta(x)v + \gamma(x)d; \tag{2.15}$$

Where,

$$\alpha(x) = -\frac{L_f^r h(x)}{L_g L_f^{r-1} h(x)}$$
$$\beta(x) = \frac{1}{L_g L_f^{r-1}}$$
$$\gamma(x) = -\frac{L_p L_f^{r-1} h(x)}{L_g L_f^{r-1} h(x)}$$

The reader is referred to Henson and Seborg (1997) and Isidori (1995) for more information.

### 2.2.5 Limitations

The main limitations of these methods are that (Isidori, 1995, Khalil, 2002 & Zotică et al., 2020):

- The initial system equations must be dynamic. Due to the form of Eq. 2.5, the equations to describe the system are dynamic. This will however be realised for most chemical processes, but will not always, e.g. for pH calculation in Chapter 7, fast mixing processes or valves.
- The system is typically transformed into a chain of integrators, from Eq. 2.12. This means that the poles of the system lie at the origin, and therefore exhibit marginal stability. For many mechanical processes this will be adequate due to the right-hand-plane (RHP) poles though for the majority of chemical processes the systems will have left-hand-plane (LHP) poles anyway, so poles on the axis will not provide any benefit.
- The linearization is based on an accurate process model. Due to the reliance of the control scheme on a process model, this raises robustness issues if the *actual process* doesn't follow the *process model*.

## 2.3 Active Disturbance Rejection Control

Active disturbance rejection control (ADRC), summarised by Sira-Ramirez et al. (2017), is the theory to control nonlinear systems whereby the disturbances to the system, whether measured or unmeasured; known or unknown, are lumped into a single variable, along with unmeasured states. This variable is then estimated in real-time by an Extended State Observer (ESO) and the system is acted upon via feedback to cancel out the effect of any disturbance. This is a robust control

method that simplifies the system dynamics immensely. Although the idea was first proposed in 1939 by Schipanov (1939)- in Russian - it was not until the early 21st century that ADRC was written in English by Han (2009) and Huang et al. (2004).

ADRC was first developed outside the chemical engineering field - mainly for robotics and other mechanical systems (Gao et al., 2001). Nonetheless, it has now attracted some interest in the process control domain, albeit limited. Chen et al. (2007) simulate concentration control of two nonlinear CSTR case studies, one isothermal and one non-isothermal, with time-varying parameters such as heat transfer coefficient and activation energy. For the isothermal CSTR it is shown that ADRC out-performs feedback linearization, especially in cases of model error. For the non-isothermal CSTR, the performance of ADRC is compared to that of linear Model Predictive Control (MPC) and PID control - showing greater performance than both, in a relatively simple manner.

Brown and Zhang (2014) simulate pH control of a neutralisation process with ADRC; pH neutralisation is shown later in Chapter 7 to be a highly nonlinear process. The results show fast set-point tracking and disturbance rejection - though not perfect. In comparison to PI control, the integral of square errors (ISE) are similar for set-point tracking, whereas for disturbance rejection the increase in performance by using ADRC is evident; ISE for ADRC is only 6% of that for PI control.

Wang and Zhu (2004) apply ADRC to temperature control of a batch polypropylene reactor, both simulation and experimentally on a chemical plant. Simulations are carried out with modelling errors, and although performance is not as good, the control is robust to any changes. When tested experimentally, performance compared to PI control was greatly improved and the authors state that the plant actually accepted these changes and continued to use ADRC.

For the Chylla-Haase Reactor Case Study, Chapter 8, Li et al. (2014) use an ADRC approach, this showed very good set-point tracking and is discussed further in Section 8.2.2.

The nonlinear ADRC structure has nine parameters that are required to be tuned (Zheng et al., 2012). Clearly this is not favourable, especially for industrial application, where PID is the norm. Zheng et al. (2012) also note that using the ESO creates a phase lag, which increases with relative order. They propose using a reduced-order extended state observer (RESO), resulting in reduced-order active disturbance rejection control (RADRC) but this increases complexity, and deviates

from the original simplicity of ADRC, relative to feedback linearization. This is simulated for a distillation column and a CSTR; for both the performance of RADRC versus ADRC is improved for disturbance rejection and set-point tracking. It also must be noted that both RADRC and ADRC out-perform MPC.

## 2.4 Model Reference Adaptive Control

Model reference adaptive control (MRAC) is a type of adaptive control which is employed to nonlinear systems in order to take into account uncertainty in the process model. MRAC typically follows a block-diagram shown in Fig. 2.2.

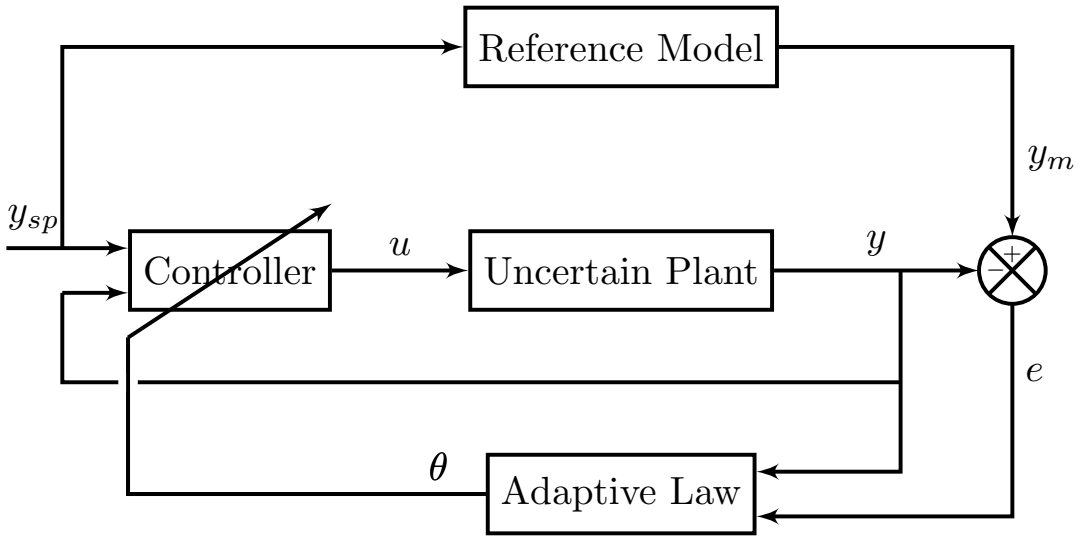


Figure 2.2: Model Reference Adaptive Control Block Diagram. Diagonal line symbolises the change of parameters. Adapted from (Nguyen, 2018)

.

Where $y$ and $y_m$ are the outputs from the actual plant and the reference plant respectively, $y_{sp}$ is the set-point, $u$ is the input and $\theta$ is a factor used to change the controller parameters. This has a cascade structure, whereby the inner loop acts like a typical feedback loop between the uncertain plant and the controller. The outer loop is based on the error between the actual output, $y$, and the reference model output, $y_m$. The adaptive law takes this into account and adjusts the controller parameters accordingly (Åström and Wittenmark, 2008). There are multiple options for the choice of controller and adaptive law, e.g. linear versus nonlinear controller or linear time-varying versus nonlinear adaptive law (Nguyen, 2018). The design of the system depends on robustness and performance requirements. For systems with a relative degree of one, the reference model can be selected to be first order and then the task is to find a set of controller parameters that makes the system follow

that model; in a similar manner to the new Transformed MVs theory.

Although first developed for the aerospace domain, Åström and Wittenmark (2008) label chemical reactors as "potential candidates for adaptive control" due to the many parameters which change with time, for example catalyst activity. In literature there are a number of examples of chemical engineering applications of MRAC, both historically and recently; showing the continued work in the field.

Ahlgren and Stevens (1971) simulate a CSTR with a drifting rate constant: to simulate changing catalyst activity, and a changing cooling water temperature: to simulate between day and night temperatures. The application of MRAC provided a stable system, which was not the case for an unadapted system. However, trial and error was used for the reference system which would be time consuming and add extra complexity to already labour-intensive calculations. Though, to this end, Najim et al. (1985) conclude that MRAC is simpler than linear controllers as not a lot of process knowledge is required a priori and parameters do not need to be retuned periodically. Furthermore, in 1981 a chemical plant in Germany transitioned to MRAC and saved 10% in energy, compared to PID control.

Han et al. (2019) presented MRAC applied to proton exchange membrane fuel cell (PEMFC). Providing a robust control strategy for PEMFCs is difficult due to changes in parameters, disturbances and lack of an accurate model. Compared to nominal feedback control, MRAC was simulated to show less control action required, meaning less wear on the compressor, as well as a lower overshoot. Interestingly, Patel et al. (2020) also use MRAC to control a fuel cell, though looking at microbial fuel cells rather than PEMFCs. With no control action, it is shown that at steady-state there is a constant error between the reference system and the actual system. Applying MRAC ensured no steady-state offset, and the error was minimised to zero for both the anode and cathode outlets.

Bastin and Dochain (1990) present a similar approach to MRAC, which also has similarities to feedback linearization and the transformed MVs theory. They use a system input-output model, where the derivative order is equal to the relative degree of the input, and combine this with a stable linear reference model to give a control law, which linearizes the feedback loop. The reference model is chosen depending on how the user wishes the tracking error to decrease. Shown by Chen et al. (1995) is the application of this approach, where a control scheme for the control of ethanol production during yeast production is presented.

## 2.5 Backstepping Control

Backstepping control is a model-based non-linear control technique based on "a known feedback law for a known Lyapunov function" (Kokotović, 1992). It is a more systematic method to controlling a system in comparison to nonlinear geometric techniques, e.g. feedback linearization (Kanellakopoulos et al., 1992). So-called 'backstepping' is achieved when a system in form of Eq. 2.16, is represented by Eq. 2.17. where $u$ is the control input and $[\eta^T, \xi]^T$ is the state (Khalil, 2002).

$$\dot{\eta} = f(\eta) + g(\eta)\,\xi \tag{2.16a}$$
$$\dot{\xi} = u \tag{2.16b}$$

$$\dot{\eta} = [f(\eta) + g(\eta)\phi(\eta)] + g(\eta)z \tag{2.17a}$$
$$\dot{z} = u - \dot{\phi}(\eta) = v \tag{2.17b}$$

$\phi$ is represented by Eq. 2.18, i.e. it is calculated from known quantities.

$$\dot{\phi} = \frac{\partial \phi}{\partial \eta}[f(\eta) + g(\eta)\,\xi] \tag{2.18}$$

The state feedback law is then derived using the Lyapunov function and substituting in the values from Eq. 2.17 and this creates an asymptotically stable system (Khalil, 2002 & Vaidyanathan and Azar, 2021). This may be applied multiple times for higher-order systems.

In literature there are very limited examples of backstepping being used for chemical engineering applications. Monroy-Loperena and Alvarez-Ramirez (2004) use backstepping control in a cascaded manner for batch distillation columns - renowned for being hard to control due to the flexibility and lack of a steady-state. The control of the output composition is achieved by cascade control; the outer controller providing a tray temperature set-point from the output composition and the inner controller changes the reflux rate in order to minimise the error in tray temperature. The outer controller is of low-gain type. The inner controller utilises backstepping control with a model error estimator. Output composition control shows good performance, and is further enhanced when multiple slave controllers are used on different trays of the column.

Hua et al. (2009) apply backstepping control to CSTRs in series, with time delay

and a recycle. The authors claim that this is the only effective method for the given process model, and the results show a global asymptotically stable system is achieved for the given nonlinear controller. Bošković and Krstić (2002) use back-stepping control for control of chemical tubular reactors. This again achieves global asymptotic stability.

# Chapter 3

# New Proposed Method for Input Transformation

## 3.1 Theory

### 3.1.1 New Transformed Input Theory

The new transformed input theory was developed within the Process Systems Engineering group at Norwegian University of Science and Technology, culminating so-far, at the time of writing, with the publication by Zotică et al. (2020). There is currently a more theoretical paper being prepared. This theory is a powerful tool that can be used to control nonlinear systems, in particular in the process control domain. In comparison with previous nonlinear control techniques, this is very simple and can be implemented to a process with relative ease.

A system with input $u$, output $y$, internal variable $w$ and disturbance variable(s) $d$, represented by Eq. 3.1, can be transformed into a first-order, linear system which can offer perfect disturbance rejection and decoupling for multiple-input, multiple-output (MIMO) systems (Perfect disturbance rejection is defined as $y = y_{sp}\ \forall\ t$ in the presence of a disturbance). By introducing the transformed input, $v_L$, and a tuning parameter, $A$, as per Eq. 3.2 , this is achieved. The transform in this form is called the general linear transform (GLT) and is often referred to as $v$ due to its general nature. Fig. 3.1 illustrates the effect of feedback linearization and the new transformed input theory on the poles of the system; poles on the y-axis will create a marginally stable system and poles on the left-hand-plane will create a stable system. If the original system is on the left-hand plane then it is clear that feedback linearization will not be favoured, whereas for an original system on the right-hand plane then feedback linearization will provide marginal stability but the new theory will provide true stability.

$$\frac{dy}{dt} = f(y, u, w, d) \tag{3.1}$$

$$v_L = f(y, u, w, d) - Ay \tag{3.2}$$

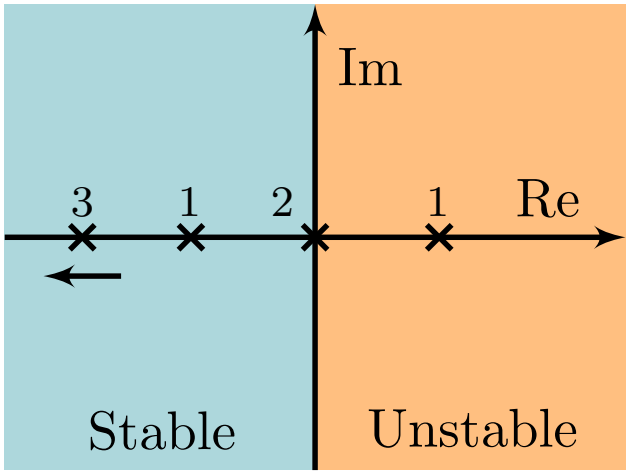


Figure 3.1: Comparison of Poles. 1: possible locations of original system poles; 2: location of feedback linearization poles; 3: location of the new theory's poles.

The value of $A$ is usually chosen such that $A = \left(\frac{df}{dy}\right)^*$, where the $^*$ indicates steady-state conditions. Choosing $A$ this way means there is no feedback at the nominal steady-state condition as $v$ is independent of $y$. Transforming the model into a first-order system yields the transfer function Eq. 3.3. It can be seen that the gain of the system is equal to the negative of the reciprocal of $A$, as is the time constant. This shows that the choice of value for $A$ will affect the speed of response, i.e. it can be used as an additional tuning parameter. It is therefore clear that the more negative the value of $A$ is, the smaller $\tau$ is; leading to a faster response, and vice versa for a less negative value. The value of $A$ must be non-positive to give a realisable time constant, and the special case of $A = 0$ is detailed below.

$$G(s) = \frac{y(s)}{v(s)} = \frac{-1/A}{(-1/A)s + 1} = \frac{K}{\tau s + 1} \tag{3.3}$$

The assumptions used in the theory are as follows;

***Assumption 1:*** Relative order of the system must be $\leq 1$

***Assumption 2:*** All variables required in the process model are measured

***Assumption 3:*** Number of inputs = number of outputs; $n_u = n_y$

***Assumption 4:*** The equation for the transformed input (Eq. 3.2) is invertible

If these assumptions do not hold then the theory can still be used under considerations, as explained in this thesis. If the assumptions hold then the system can be easily implemented using the block diagram in Fig. 3.2. It is clear to see the ease with which this is applied in comparison with the feedback linearization method presented in Section 2.2.

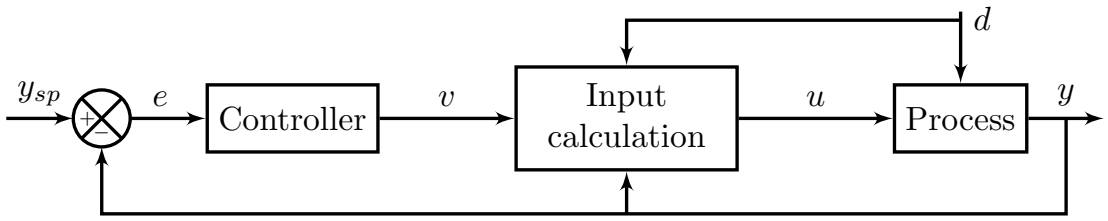


Figure 3.2: Basic Transformed Input Control Scheme

The feedback loop is not necessarily required for a system in the presence of disturbances if there is no model mis-match between the calculation block and the process. In the case of a mis-match then this is required for the system to return to the nominal steady-state. The set-point may also be changed with no feedback loop by calculating the corresponding value of $v$ as an input to the calculation block.

#### 3.1.1.1 Integrating Transformation

As mentioned above there is a special case if $A = 0$. This means that the transformed system becomes an integrator, the same as seen in feedback linearization. This is denoted by a subscript $FL$ on the transformed input $v_{FL}$. The transformed input system becomes Eq. 3.4 and has marginal stability.

$$\frac{dy}{dt} = f(y, u, w, d) = v_{FL} \tag{3.4}$$

#### 3.1.1.2 Static Transformation

The static transform can be used for either a static system, for a dynamic system - the dynamics of the system are simply disregarded ($dy/dt = 0$) or for a dynamic system where a steady-state model of the system is known but a dynamic model is not. The static transformed input is symbolised by subscript 0 as $v_0$. For a system taken as Eq. 3.5, $v_0$ is calculated by Eq. 3.6, where $y = r(u, d)$ solves Eq. 3.5. At steady-state $v_0 = y$, but not always dynamically.

$$\frac{dy}{dt} = 0 = f(y, u, w, d) \tag{3.5}$$

$$v_0 = r(u, d) \tag{3.6}$$

#### 3.1.1.3 Alternative Form of General Linear Transformation

Another special case is changing the form of the GLT so that it has a gain of 1. For this case the subscript $L0$ is used for the transformed input as $v_{L0}$. This is shown in Eq. 3.7, where $\mathcal{T} = -A^{-1}$. This would be undefined in the case of $A = 0$. In this case $y = v_{L0}$ at steady-state, and a set-point change is able to be achieved without the need for additional calculation - the set-point of $v_{L0}$ is equal to the set-point of $y$. Although, the GLT may work better than this special case when using a controller as there is less dynamic coupling.

$$\mathcal{T}\frac{dy}{dt} = \mathcal{T}f(y, u, w, d) = -y + v_{L0} \tag{3.7}$$

### 3.1.2 Cascade Control

There are a number of reasons to use cascade control versus the basic transformed input control scheme;

1. The relative order is greater than one - *Assumption 1* does not hold.
2. The model equation for $dy/dt$ is not invertible - *Assumption 4* does not hold - or inverting it is not favoured.
3. Using it to numerically invert the transformation to give the input $u$ for a desired value of $v$.

Cascade control is achieved either in a general cascade structure, or an alternative cascade structure; Fig. 3.3 and 3.4 respectively. For the general cascade structure, Fig. 3.3, the outer controller outputs the set-point for the transformed input, $v_{sp}$, from the difference between $y_{sp}$ and $y$, while the calculation block calculates the current value of $v$. The inner controller acts on the difference between $v_{sp}$ and $v$, giving the required input to the system, $u$.

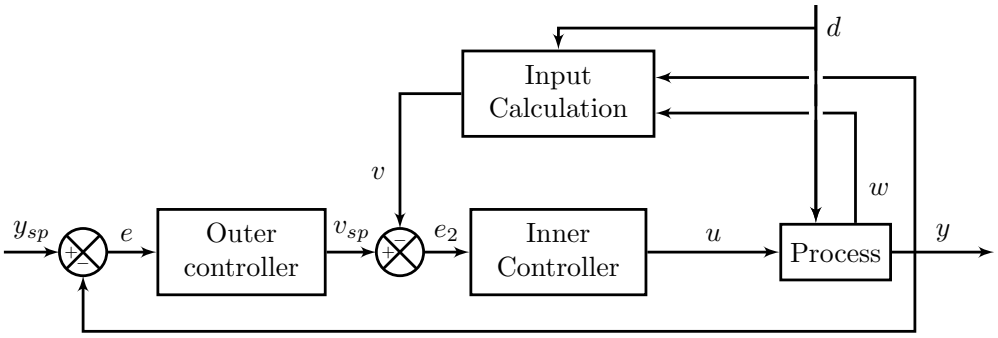


Figure 3.3: General Cascade Structure

For the alternative cascade structure, Fig. 3.4, the outer controller acts in the same way as the general cascade structure, although this time the $v_{sp}$ enters the calculation block to give a set-point for the internal variable, $w_{sp}$. The difference between $w_{sp}$ and the measured internal variable, $w$, is acted upon by the inner controller in order to give the required input to the system, $u$.

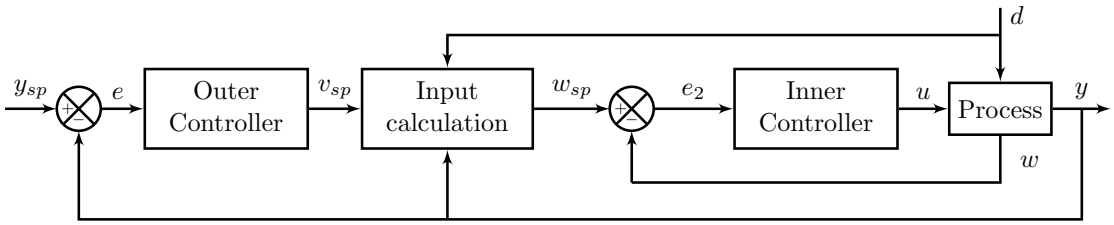


Figure 3.4: Alternative Cascade Structure

There should not be any difference in performance between the two different control structures if the system is invertible - this is investigated in Chapter 4. The general cascade has to be used for a system that can't be inverted, and will also be favoured if it requires a lengthy numerical solver. Though, the alternative cascade may appear more intuitive, as it has a feedback loop on both the output, $y$ and the internal variable, $w$, both of which are normally realisable quantities. In both cases, using cascade control in this form will see the loss of perfect disturbance rejection.

Furthermore, the cascade system is also safer than the basic transformed system (Fig. 3.2) if the internal variable, $w$, depends on the input, $u$. There is potential for instability if the transformed input is a function of the internal variable when using the basic transformed input control scheme. In addition to this, if one chooses to"cheat", and does not want to invert the equation for $v$ to find $u$, the cascade structure can be used to calculate the input to the system. This assumes that the inner loop is sufficiently fast, however this comes with the loss of perfect disturbance rejection.

An additional benefit of the alternative cascade structure is the possibility that perfect disturbance rejection can be resurrected. For a system where the disturbance directly affects the internal variable, $w$, if an additional inverse calculation block is introduced, as per Fig. 3.5, then perfect disturbance rejection will be achieved. This is named a double-linearized (DL) cascade system due to the presence of two calculation blocks.

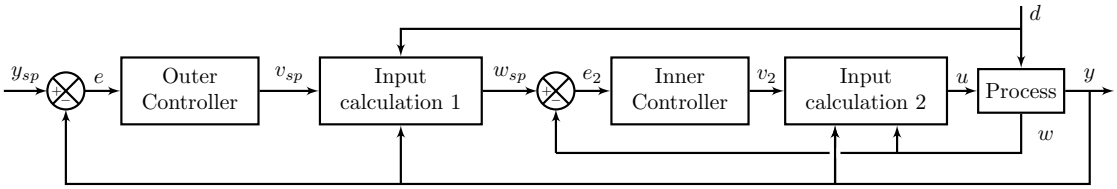


Figure 3.5: Double-linearized Cascade System

### 3.1.3 Chain of Transforms

For systems with a relative order greater than one, the chain of transforms can also be applied. In a similar configuration to feedback linearization where the system is transformed into a chain of integrators, the so-called chain of transforms is a system transformed into a chain of first-order transfer functions, shown in Fig. 3.6. Input calculation 1 is the same as the transforms above, and $v_{A0}$ is the internal variable, $w$, which satisfies the first transform equation, acting as a type of $w_{sp}$. Input calculation 2 is in the form of Eq. 3.8 and is solved to give the input to the system with given controller output $v$, measured outputs $y$ and $w$, and disturbances $d$. $A_w$ is again used as a tuning parameter.

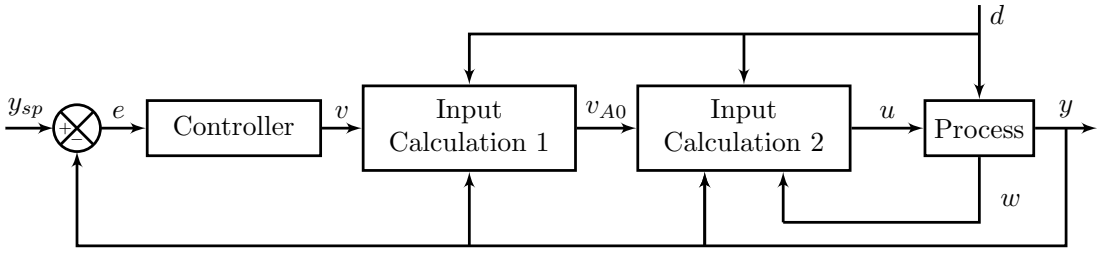


Figure 3.6: Chain of Transforms System

$$\frac{dw}{dt} = g(y, u, d, w) = A_w(w - v_{A0}) \tag{3.8}$$

This can be used if the internal variable, $w$, is known and a model is available. This also has the possibility of perfect disturbance rejection for disturbances that

directly affect the internal variable and not the controlled variable as will be shown in Chapter 6.

### 3.1.4 Output Transformation

An output transformation can be used when the variable of interest is not known, or needs to be calculated from other values, but is still important in the control of the system - shown in Chapter 5. It is applied via a simple calculation block, which contains any equation the user sees fit to calculate, or estimate in some cases, the variable of interest. It may also be used in the case of a system nonlinear in the outputs, seen in Chapter 7. Shown in Fig. 3.7 is the case of a system where the dynamics for both $y$ and $w$ are known, but the value of $w$ cannot be measured. By neglecting the dynamics for $y$, i.e. $dy/dt = 0$, the value of $w$ can be estimated from measured values in the output calculation blocks.

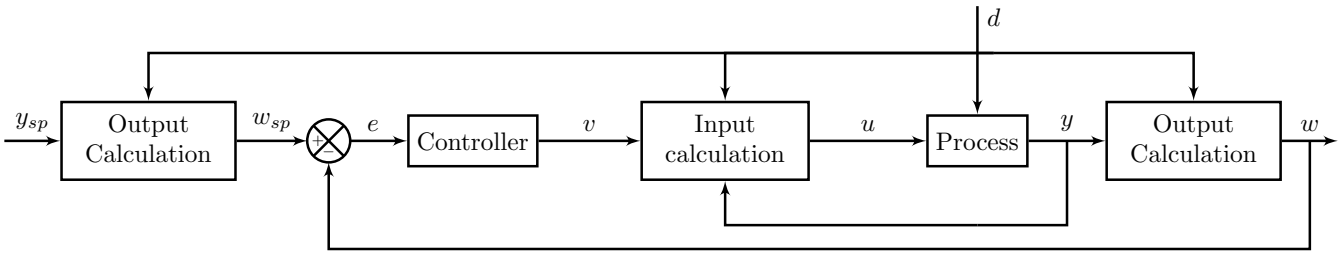


Figure 3.7: Output Transform Example Case

## 3.2 Simulation Set-up

All simulations were performed on MATLAB ® and Simulink ® R2020a with an automatic ODE solver selection, maximum step size selection and minimum step size selection.

### 3.2.1 Disturbance Mis-match

In order to test robustness in some of the case studies, a disturbance mis-match is simulated. In reality, this may happen if a measurement sensor is malfunctioning, or if there are unmeasured disturbances also affecting the system. To simulate this, a different value is used in the transformation block to the process model, governed by Eq. 3.9. The 'real' disturbance is represented by $d_r$, this is the value used in the process model. The measured disturbance is represented by $d_m$, this is the value used in the transformation block. Gain $D$ serves as a parameter to dictate the relative

amount of deviation between the measured disturbance value $d_m$ and the nominal disturbance value $d^*$. This is able to test the robustness of the control systems.

$$d_r = d^* + D(d_m - d^*) \tag{3.9}$$

# Chapter 4

# Case Study A: Outlet Temperature Control for Tanks-in-Series

The first case study presented is a two-tanks-in-series model. The aim of this was to validate the new theory, to show both of the possible cascade control schemes and also to show the effect of the static and integrating transforms. The goal was to control the temperature leaving the last tank by changing the temperature of the flow to the first tank.

## 4.1 Process Model

The tanks-in-series simulations follow the diagram shown in Fig. 4.1. Nomenclature and nominal values are shown in Table 4.1.

Derived from mass and energy balances around the tanks, Eq. 4.1 - 4.4, which are bi-linear, are used to model the process. Full derivations are provided in Appendix B.1.

Assumptions used;

*A1*: Perfect mixing in both tanks

*A2*: Constant density, $\rho$, and specific heat, $c_p$.

*A3*: Inlet temperature, $T_0$, may be manipulated sufficiently fast by the heat added, $Q$.

*A4*: Constant pressure and volume

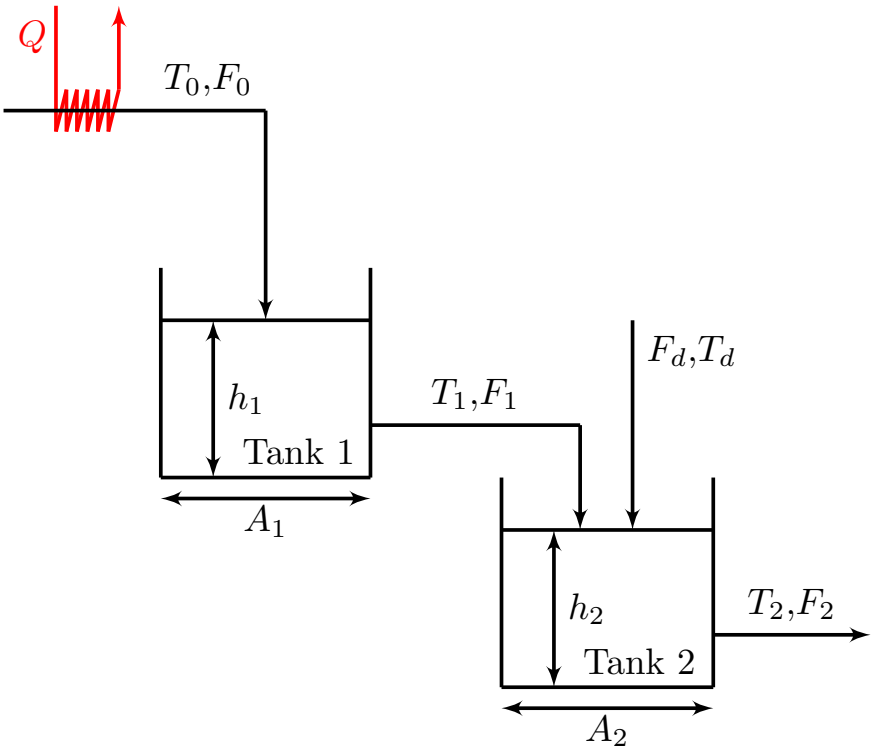


Figure 4.1: Tanks-in-Series Model

Table 4.1: Nomenclature and nominal values for Tanks in Series

| **Variable** | **Symbol** | **Unit** | **Steady-state value** |
|---|---|---|---|
| Temperature of inlet flow | $T_0$ | $^{\circ}C$ | 70 |
| Temperature of tank 1 | $T_1$ | $^{\circ}C$ | 70 |
| Temperature of tank 2 | $T_2$ | $^{\circ}C$ | 60 |
| Temperature of disturbance flow | $T_d$ | $^{\circ}C$ | 40 |
| Inlet flow to tank 1 | $F_0$ | $m^3\,min^{-1}$ | 1 |
| Outlet flow of tank 1 | $F_1$ | $m^3\,min^{-1}$ | 1 |
| Outlet flow of tank 2 | $F_2$ | $m^3\,min^{-1}$ | 1.5 |
| Disturbance flow to tank 2 | $F_d$ | $m^3\,min^{-1}$ | 0.5 |
| Level in tank 1 | $h_1$ | $m$ | 1 |
| Level in tank 2 | $h_2$ | $m$ | 0.5 |
| Cross-sectional area of tank 1 | $A_1$ | $m^2$ | 4 |
| Cross-sectional area of tank 2 | $A_2$ | $m^2$ | 6 |

$$\frac{dh_1}{dt} = \frac{1}{A_1}(F_0 - F_1) \tag{4.1}$$

$$\frac{dh_2}{dt} = \frac{1}{A_2}(F_d + F_1 - F_2) \tag{4.2}$$

$$\frac{dT_1}{dt} = \frac{F_0(T_0 - T_1)}{h_1 A_1} = g(u, d, w) \tag{4.3}$$

$$\frac{dT_2}{dt} = \frac{F_1(T_1 - T_2) + F_d(T_d - T_2)}{A_2 h_2} = f(y, u, d, w) \tag{4.4}$$

## 4.2 Control Structure

In this case study, the controlled variable (CV) was the temperature of the second tank, $y = T_2$. The manipulated variable (MV) was the temperature of the inlet flow, $u = T_0$. The disturbances to the system ($d$) are the inlet flow, $F_0$, the disturbance flow, $F_d$, and the temperature of the disturbance flow, $T_d$. The internal variable for this system is the temperature of the flow out of the first tank, $w = T_1$. All states are $x = [T_1\, T_2\, h_1\, h_2]$. The level in both tanks, $h_1$ & $h_2$ is also to be controlled to ensure tanks do not become empty or overflow. This was achieved by P-controllers, with a process gain of the reciprocal of the cross-sectional area of each tank respectively and the tuning parameter, $\tau_c$, is taken as one-quarter of the tank residence time.

The relative order of the system is greater than 1, i.e. the output $T_2$ needs to be differentiated twice before the input $T_0$ appears explicitly. This means that *Assumption 1* of the transformed input theory, Section 3.1.1, does not hold true. Therefore a cascade structure must be used; there are two possible control schemes, Fig. 4.2 and 4.3. The transformed input labels for GLT, integrating case and static case, i.e. $v$, $v_{FL}$ & $v_0$, may be used interchangeably in the block diagrams.

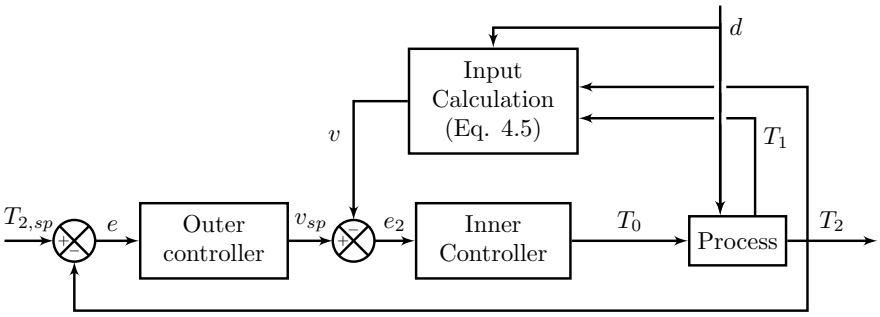


Figure 4.2: General Cascade Block Diagram

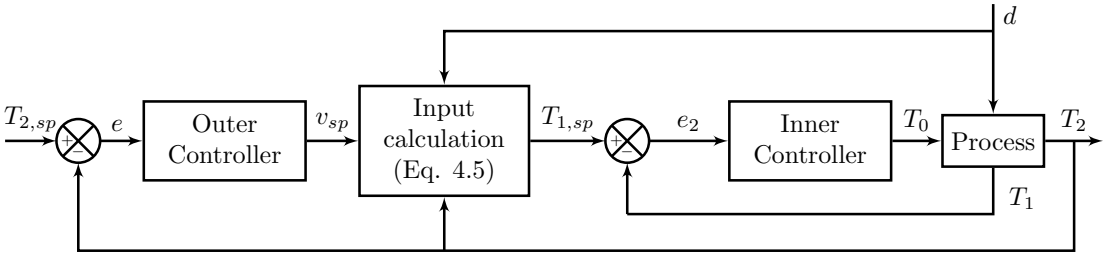


Figure 4.3: Alternative Cascade Block Diagram

The transformed input, $v$, is calculated as per Eq. 4.5:

$$v = f(y, w, u, d) - AT_2 = \frac{F_1(T_1 - T_2) + F_d(T_d - T_2)}{A_2 h_2} - AT_2 \tag{4.5}$$

Where, for the general linear transform;

$$A = \left(\frac{df}{dT_2}\right)^* = \left(-\frac{F_1 + F_d}{A_2 h_2}\right)^* = -0.5\, min^{-1} \tag{4.6}$$

and $f(y, w, u, d)$ is described in Eq. 4.4. The value of A is the reciprocal of the negative residence time of the tank which is no coincidence. The transformed system, $f(y, w, u, d) = v + AT_2$ gives a transfer function $G(s) = \frac{T_2(s)}{v(s)} = \frac{K}{\tau s+1}$, where $K = \tau = -1/A$. Therefore, intuitively the time constant is equal to the residence time. For the integrating system $A = 0\, min^{-1}$. The static system uses $v_0 = r(u, d)$, where $T_2 = r(u, d)$ solves $f(y, w, u, d) = 0$.

### 4.2.1 Controller Tuning

The controllers were tuned using SIMC tuning rules (Skogestad, 2003). For the inner controller of the alternative cascade structure, the transfer function is calculated by taking the Laplacian of Eq. 4.3, giving Eq. 4.7.

$$\frac{T_1(s)}{T_0(s)} = \frac{1}{\frac{A_1 h_1}{F_0} s + 1} = \frac{1}{\tau s + 1} \tag{4.7}$$

Therefore, SIMC rules can easily be applied. This will not always be the case for the alternative cascade structure and depends on the equations for each specific case. For the inner controller of the general cascade structure and the outer controllers for all cascade structures, an open-loop response is used to fit an approximate FOPTD transfer function to the system. The gain and time constants for all cases (delay is taken to be zero for all cases) are summarised in Table 4.2 along with the tuning parameters, where $K$ is the process gain, $\tau$ is the process time constant, $\tau_c$ is the SIMC tuning parameter which results in the proportional gain, $K_c$ and integrating time $\tau_I$; the full open-loop response graphs are shown in Appendix A.1.

Table 4.2: Process and Tuning Parameters for all Tank-in-Series Cases. († : Integrating process $\therefore \tau \to \infty$, $K = K' = \frac{\Delta y}{\Delta t \Delta u}$. Values with no units are dimensionless)

| Case | | $K$ | $\tau$ | $\tau_c$ | $K_c$ | $\tau_I$ |
|---|---|---|---|---|---|---|
| Pure Feedback | Inner | 1 | 4 $min$ | 3 $min$ | 1.3 | 4 $min$ |
| | Outer | 0.66 | 5.6 $min$ | 6 $min$ | 1.4 | 5.6 $min$ |
| General (GLT) | Inner | 0.3 $min^{-1}$ | 4.1 $min$ | 2.5 $min$ | 5.47 $min$ | 4.1 $min$ |
| | Outer | 2 $min$ | 4.4 $min$ | 6.5 $min$ | 0.34 $min^{-1}$ | 4.4 $min$ |
| Alternative (GLT) | Inner | 1 | 4 $min$ | 3 $min$ | 1.33 | 4 $min$ |
| | Outer | 2 $min$ | 4.9 $min$ | 6.5 $min$ | 0.38 $min^{-1}$ | 4.9 $min$ |
| Alternative (Static) | Inner | 1 | 4 $min$ | 2 $min$ | 2 | 4 $min$ |
| | Outer | 2 $min$ | 4.2 $min$ | 6 $min$ | 0.35 $min^{-1}$ | 4.2 $min$ |
| Alternative (Integrating) | Inner | 1 | 4 $min$ | 2 $min$ | 2 | 4 $min$ |
| | Outer† | 0.48 | – | 8 $min$ | 0.26 $min^{-1}$ | 32 $min$ |

## 4.3 Results

### 4.3.1 Comparison of General Cascade, Alternative Cascade and Pure Feedback Systems

Results for simulations of the general cascade system and the alternative cascade system are presented in Fig. 4.4, along with a comparison to an un-transformed cascade system, i.e. pure feedback. Simulations for disturbances of $F_0$, $F_d$ and $T_d$ and also a set-point change are presented.

Firstly, it must be noted that perfect disturbance rejection is not achieved. The relative order to the output $T_2$, from both disturbances, is one whereas the relative order from the input is two. This means that the disturbances affect the system before the input, so it is physically impossible to achieve perfect disturbance rejection. For $T_2$ to be controlled, the disturbances require a change in $T_1$ - which subsequently is achieved by a change in $T_0$. The dynamics in tank 1 slow this down and means perfect disturbance rejection cannot be achieved. Although, from this it is clear to see the advantage that the transformation makes to the system, the response is faster for all three disturbances in comparison to the feedback only case. This is no surprise as the transformation block delivers feedforward action, in addition to the feedback aspect achieved from the feedback loop and the two controllers. For a set-point change it can be seen that the responses for both of the transformed systems are very similar to that for the feedback only system. This is expected and is witnessed because the transformation is not a function of the set-point, and therefore any set-point change is acted upon solely by the outer and inner controllers - the same as in the feedback only case. The results also show that both the general cascade structure and the alternative cascade structure behave very similarly and

any slight differences may be attributed to controller tuning.

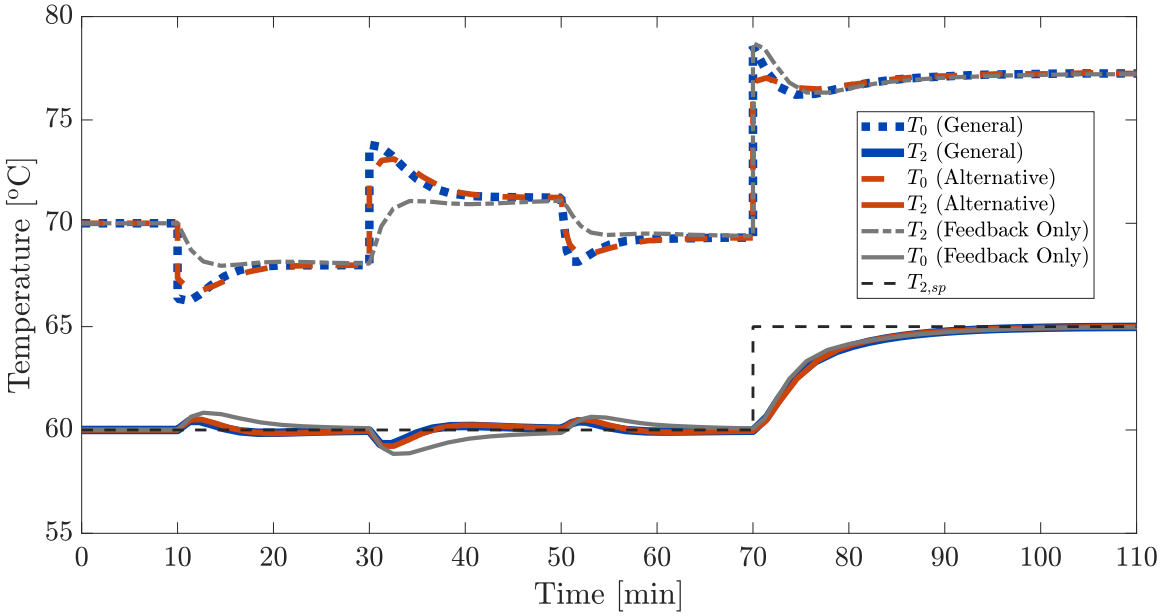


Figure 4.4: Comparison of the General Cascade Structure, the Alternative Cascade Structure, an a Feedback Only Cascade Structure, with no transform. $\Delta F_0 = +0.2\ m^3/min$ at $t = 10\ min$; $\Delta F_d = +0.2\ m^3\, min^{-1}$ at $t = 30\ min$; $\Delta T_d = +4\ ^\circ C$ at $t = 50\ min$; $\Delta T_{2,sp} = +5\ ^\circ C$ at $t = 70\ min$.

### 4.3.2 Comparison of General Linear Transform, Static Transform and Integrating Transform

In order to show the differences of the possible transforms on the cascade control structure, the general linear (GLT), integrating and static transforms are applied to the tanks-in-series problem. For these simulations, the alternative cascade structure is used. Nonetheless, it has been shown above that both the general cascade structure and the alternative cascade structure will behave similarly anyway.

The integrating transform is the case where the tuning parameter, $A$ in Eq. 4.5, is chosen to be 0. This means that the pole of the transformed system lies at the origin and there is marginal stability. This may be seen as a similarity to feedback linearization, where the system is transformed into integrating processes in series. The static transform is the case where the dynamics of the system are neglected, this may be used in a case where the process model is complicated or if the dynamics of the system are unknown. Furthermore, when the process itself is static, the static transform is clearly used. The transformed input, $v_0$ is chosen to be equal to $r(u, d)$,

where $T_2 = r(u, d)$ solves Eq. 4.8. At steady-state $v_0 = T_2$, but this will not always hold dynamically.

$$\frac{F_1(T_1 - T_2) + F_d(T_d - T_2)}{A_2 h_2} = f(y, u, d, w) = 0 \tag{4.8}$$

The results for the three systems can be seen in Fig. 4.5 for the disturbances described. From this it can be seen that for disturbances, the integrating system is always the slowest, and the static system is slightly faster at regaining $T_2$ at its set-point. The general linear transform achieves a similar performance to the static transform for disturbances, but achieves set-point tracking much faster.

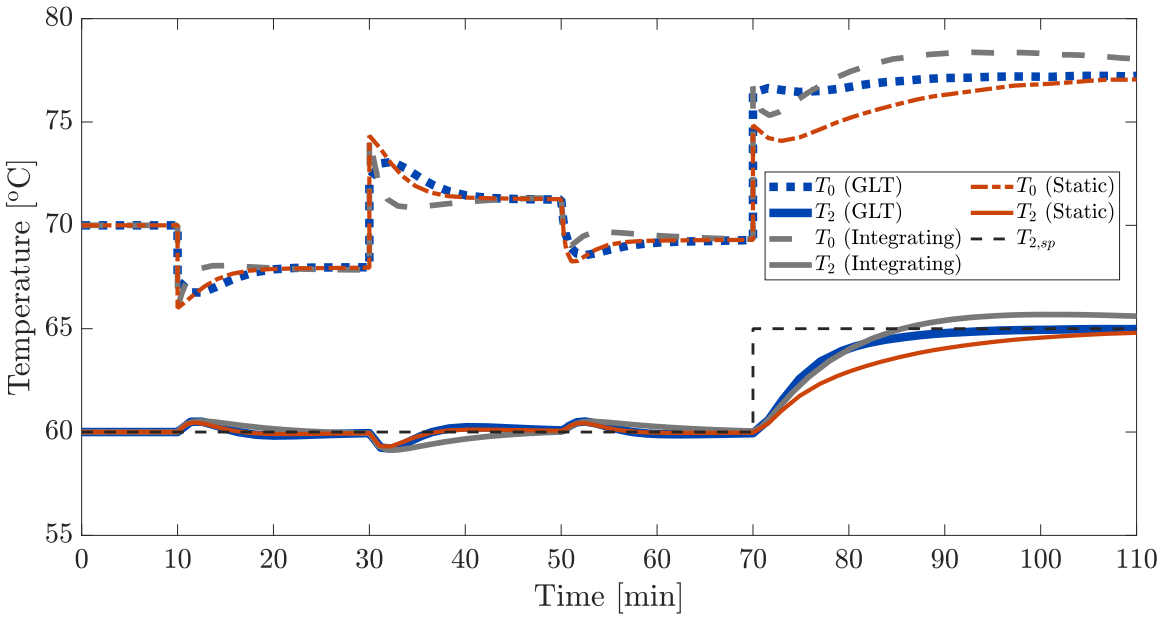


Figure 4.5: Comparison of General Linear Transform, Integrating Transform and Static Transform for Alternative Cascade System. $\Delta F_0 = +0.2m^3/min$ at $t = 10\ min$; $\Delta F_d = +0.2m^3\,min^{-1}$ at $t = 30\ min$; $\Delta T_d = +4°C$ at $t = 50\ min$; $\Delta T_{2,sp} = +5°C$ at $t = 70\ min$.

## 4.4 Case Study Discussion

In this case study, simulations have been used to prove multiple facts about the new input transformation, and possibilities for extension.

Firstly, it has been shown that if *Assumption 1* has been broken; if the relative order of the system is greater than one then a cascade implementation can be used to control the system. In this case the relative order was 2, if the system was of a higher-order then the inner loop could be changed to incorporate another transform

block if required.

Secondly, it has been shown that both of the transformed systems behave better than a regular, feedback only system, as expected. This shows a key benefit that the new transformed input theory brings.

Thirdly, both the General Cascade Structure, Fig. 4.2, and the Alternative Cascade Structure, Fig. 4.3, have been shown to be stable, and have good performance. They are directly comparable and the user can decide which to chose for a given system. The advantage of the general system is that it does not require the inversion of the transform in the calculation block. In this case study the transform is simple to solve and could be achieved analytically, though some systems may require a numerical solver, increasing difficulty and computation time. The advantage of the alternative system may be that it seems more intuitive, both controllers act on realizable quantities, the controlled variable and the internal variable. This means that tuning for the inner controller may be easier if a model equation for the internal variable is known. Nevertheless, depending on a given system's process model, either can be chosen.

Fourthly, it has been shown that the general linear transform performs best in general, for both disturbance rejection and set-point tracking, compared to the static and integrating transform. This has also shown that $A$ can be used as a tuning parameter; the integrating case has $A = 0\,min^{-1}$, compared to the general linear case with $A = -0.5\,min^{-1}$. This agrees with the fact expressed in Section 3.1.1, that the time constant for the transform is equal to $-1/A$. Therefore increasing $A$ makes $\tau$ larger, until $\tau \to \infty$ as $A \to 0\,min^{-1}$.

Introduced in Section 3.1.3, this example could also be controlled using the chain of transform, although not simulated in this chapter. No improvement in performance would be expected for disturbances of $F_d$ or $T_d$ as they have a relative order (to the output) of 1, meaning that perfect disturbance rejection would still not possible as the relative order of the input, $T_0$ is 2. Nonetheless, better performance may be achieved for a disturbance of $F_0$ as this also has a relative order of 2, meaning that the input may be changed before the disturbance affects the system. This phenomenon is explored in Chapter 6. The chain of transforms for this system would be implemented as per Fig. 4.6. Input calculation 1 is the same transform as used above, Eq. 4.5, though it is solved for $T_1$. This gives a desired set-point for $T_1$, labelled as $v_1$, shown in Eq. 4.9. Input calculation 2 solves Eq. 4.10 for the input to the system, $T_0$. $B$ is used to replace $A$ as the tuning parameter to avoid confusion.

$$v = \frac{F_1(v_1 - T_2) + F_d(T_d - T_2)}{A_2 h_2} - AT_2 \tag{4.9}$$

$$g(u, d, w) = \frac{F_0(T_0 - T_1)}{h_1 A_1} = B(T_1 - v_1) \tag{4.10}$$

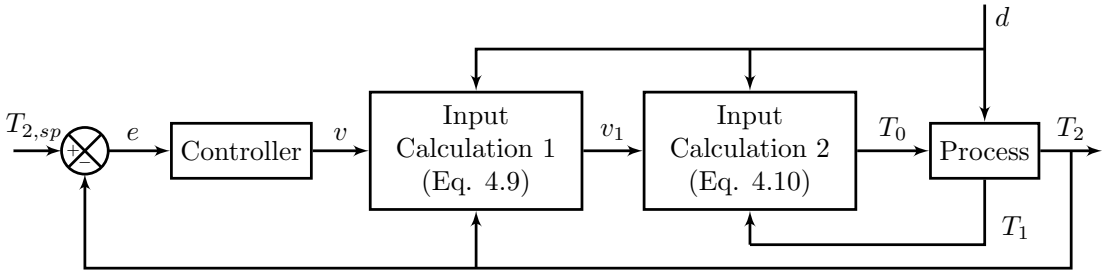


Figure 4.6: Chain of Transforms Block Diagram

# Chapter 5

# Case Study A: Extension

In Chapter 4 it was shown that the input transformation theory can be applied in a cascade nature, though this assumed that all quantities were able to be measured; *Assumption 2* in the theory. However, in an industrial setting this will not always be the case and therefore poses control limitations. It is usually a reasonable assumption that the input and output to the system are measured. Known disturbances are also typically able to be measured, whereas unknown, or unmeasured, disturbances, may be dealt with by the feedback loop. However, if the internal variable $w$ is not measured, then the cascade structures described in Chapter 4 will not be able to be implemented directly. In this chapter new methods are applied in order to overcome this, these are implemented on the tanks-in-series model again, with the same CV and MV.

## 5.1 Process Model

For this case study, a similar process model to Case Study A is used. The only difference is that there is an additional flow into the first tank, this adds an extra disturbance to the system in the form of $T_{1d}$. The new system is described by Eq. 5.1 to 5.4, which are derived from mass and energy balances. Full derivations are found in Appendix B.2. The process is shown in Fig 5.1.

$$\frac{dh_1}{dt} = \frac{1}{A_1}(F_0 + F_{1d} - F_1) \tag{5.1}$$

$$\frac{dh_2}{dt} = \frac{1}{A_2}(F_{2d} + F_1 - F_2) \tag{5.2}$$

$$\frac{dT_1}{dt} = \frac{F_0(T_0 - T_1) + F_{1d}(T_{1d} - T_1)}{h_1 A_1} \tag{5.3}$$

$$\frac{dT_2}{dt} = \frac{F_1(T_1 - T_2) + F_{2d}(T_{2d} - T_2)}{A_2 h_2} = f(y, u, d, w) \tag{5.4}$$

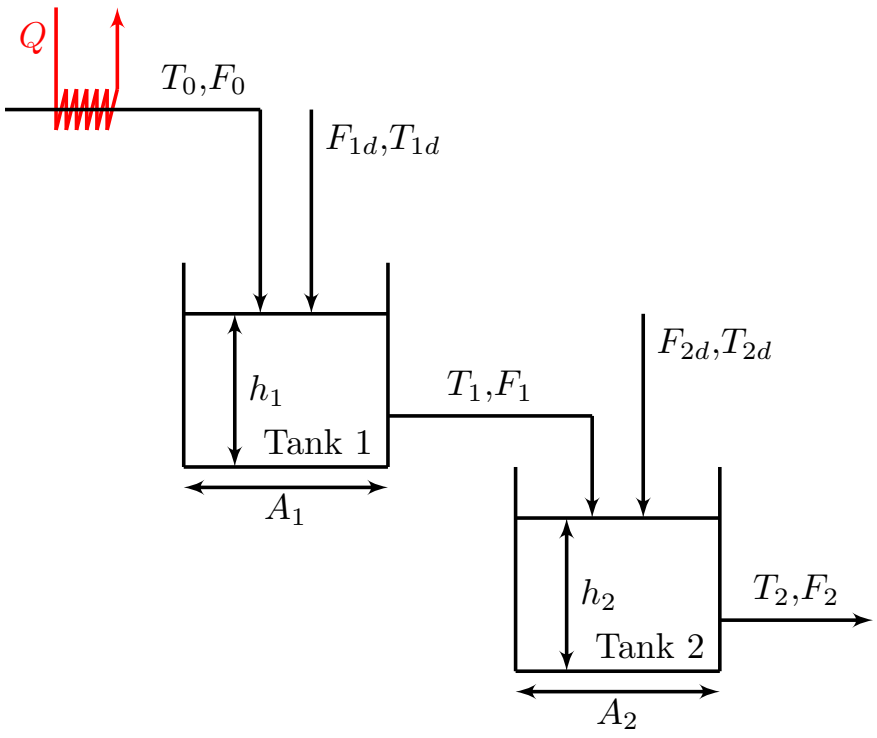


Figure 5.1: Tanks-in-Series Extension Diagram

The assumptions for this case study are the same as in Chapter 4:

*A1*: Perfect mixing in both tanks

*A2*: Constant density, $\rho$, and specific heat, $c_p$.

*A3*: Inlet temperature, $T_0$, may be manipulated sufficiently fast by the heat added, $Q$.

*A4*: Constant pressure and volume

For the extension to this case study, three different sizes of systems were simulated, these are summarised in Table 5.1. System 1 is the same as the system described in Chapter 4, with the addition of the disturbance stream, and runs the same at steady-state. System 2 is a system that has a very small tank 1 relative to tank 2, with a larger disturbance flow to Tank 2. System 3 is vice versa, where there is a very small tank 2 relative to tank 1 and a larger disturbance flow to tank 1. System 2 and 3 are used to show the effect of the extremities, changing both the size of the systems and the dynamics of the systems. System 1 is used as a more realistic example.

Table 5.1: Parameters and Steady-State Values for all three sized systems

| Parameter | Symbol | Unit | System 1 | System 2 | System 3 |
|---|---|---|---|---|---|
| Inlet Temperature | $T_0$ | $^{\circ}C$ | 70 | 70 | 70 |
| Tank 1 Temperature | $T_1$ | $^{\circ}C$ | 70 | 70 | 70 |
| Tank 2 Temperature | $T_2$ | $^{\circ}C$ | 60 | 47.5 | 68.5 |
| Tank 1 Disturbance Temperature | $T_{1d}$ | $^{\circ}C$ | 70 | 70 | 70 |
| Tank 2 Disturbance Temperature | $T_{2d}$ | $^{\circ}C$ | 40 | 40 | 40 |
| Inlet Flow | $F_0$ | $^{\circ}C$ | 0.8 | 0.8 | 0.8 |
| Tank 1 Outlet Flow | $F_1$ | $m^3\,min^{-1}$ | 1 | 1 | 3.8 |
| Tank 2 Outlet Flow | $F_2$ | $m^3\,min^{-1}$ | 1.5 | 4 | 4 |
| Tank 1 Disturbance Flow | $F_{1d}$ | $m^3\,min^{-1}$ | 0.2 | 0.2 | 3 |
| Tank 2 Disturbance Flow | $F_{2d}$ | $m^3\,min^{-1}$ | 0.5 | 3 | 0.2 |
| Level in Tank 1 | $h_1$ | $m$ | 1 | 0.025 | 5.7 |
| Level in Tank 2 | $h_2$ | $m$ | 0.5 | 4 | 0.067 |
| Cross-sectional Area of Tank 1 | $A_1$ | $m^2$ | 4 | 4 | 4 |
| Cross-sectional Area of Tank 2 | $A_2$ | $m^2$ | 6 | 6 | 6 |

## 5.2 Control Structure

If the internal variable cannot be measured then it must be estimated. To achieve this there are two cases that can be considered; the dynamics of the temperature in tank 1 can be disregarded, or the dynamics of the temperature in tank 2 can be disregarded. For this case study the same CV and MV are used as in Chapter 4; $T_2$ and $T_0$ respectively. The cascade control structure, similar to that presented in Chapter 4, is used as a benchmark for this case study. The level control as used in Chapter 4 is also used here.

### 5.2.1 Case 1: Fast Dynamics in Tank 1

For Case 1, the dynamics of tank 1 are neglected, i.e. $\frac{dT_1}{dt} = 0$. This means that, from Eq. 5.3, $T_1$ can be estimated from measured variables, seen in Eq. 5.5.

$$T_1 = \frac{T_0F_0 + T_{1d}F_{1d}}{F_1} \tag{5.5}$$

The dynamics of the second tank are therefore approximated by Eq. 5.6, replacing the actual $T_1$ with the approximation of $T_1$. This equation is now in a form that would be expected for an energy balance over a single tank with inlet streams of $F_0$, $F_{1d}$ and $F_{2d}$ and the outlet stream $F_2$.

$$\frac{dT_2}{dt} = \frac{T_0F_0 + T_{1d}F_{1d} + T_{2d}F_{2d} - T_2F_2}{A_2h_2} \tag{5.6}$$

The control scheme can then be arranged in the same way as the basic transformed

input control scheme, shown in Fig. 5.2. The general linear transform is applied to Eq. 5.6, giving Eq. 5.7, where $A = -0.5\,min^{-1}$ as before. This suggests that perfect disturbance rejection may be possible for disturbances directly affecting tank 1 ($F_{1d}$, $T_{1d}$ and $F_0$) since they will be taken into account by a change in $T_0$ before the effect is passed onto tank 2.

$$v = \frac{T_0F_0 + T_{1d}F_{1d} + T_{2d}F_{2d} - T_2F_2}{A_2h_2} - AT_2 \tag{5.7}$$

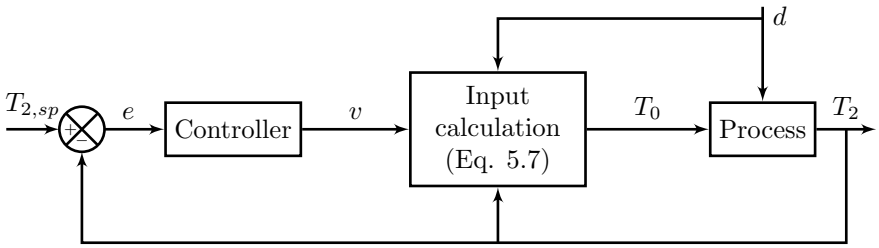


Figure 5.2: Control Scheme for Case 1

### 5.2.2 Case 2: Fast Dynamics in Tank 2

For Case 2, the dynamics of tank 2 are neglected, i.e. $\frac{dT_2}{dt} = 0$. Therefore Eq. 5.4 can be re-arranged to approximate $T_1$, as in Eq. 5.8.

$$T_1 = \frac{T_2F_2 - T_{2d}F_{2d}}{F_1} \tag{5.8}$$

Different from the approximation for Case 1, this approximation relies on values that are themselves affected by $T_1$, i.e. they come 'after' $T_1$ in the process. This acts as an output transformation and can be implemented according to Fig. 5.3.

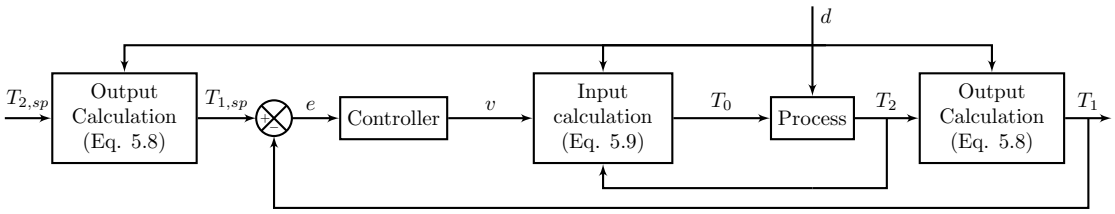


Figure 5.3: Control Scheme for Case 2

The general linear transform, in this case, is applied to the equation for $\frac{dT_1}{dt}$, Eq. 5.3 and $T_1$ is described by Eq. 5.8. This essentially changes the transformed system from $\frac{dT_2}{dt} = AT_2 + v$ to $\frac{dT_1}{dt} = AT_1 + v$; i.e. acting on the approximated internal variable, rather than the output variable. The full transform is shown in Eq. 5.9. This

also suggests that perfect disturbance rejection may be possible for disturbances directly affecting tank 1 since the internal variable is directly acted upon by the input transformation.

$$\frac{dT_1}{dt} = \frac{F_0(F_1T_0 - T_2F_2 + T_{2d}F_{2d}) + F_{1d}(T_{1d}F_1 - T_2F_2 + T_{2d}F_{2d})}{F_1A_1h_1} = v + AT_1 \quad (5.9)$$

### 5.2.3 Controller Tuning

Controllers are again tuned using SIMC rules (Skogestad, 2003). As before, for all three of the cascade structures, the inner controller is tuned using the known $T_1(s)/T_0(s)$, as in Eq. 5.10.

$$\frac{T_1(s)}{T_0(s)} = \frac{1}{\frac{A_1h_1}{F_0+F_{1d}}s + 1} = \frac{1}{\tau s + 1} \quad (5.10)$$

For all other controllers, open-loop step responses are used to fit the responses to an approximate FOPTD equation. All controller parameters are reported in Table 5.2, and detailed open-loop step response graphs can be found in Appendix A.2.

Table 5.2: Process and Tuning Parameters for all Cases and Systems. Case refers to the control scheme; system refers to the state parameters used. (Cases 1 and 2 only have one controller, values with no units are dimensionless)

| Case | System | Controller | $K$ | $\tau$ | $\tau_c$ | $K_c$ | $\tau_I$ |
|---|---|---|---|---|---|---|---|
| Cascade | 1 | Inner | 1 | 4 *min* | 2 *min* | 2 | 4 *min* |
| | | Outer | 2 *min* | 4.87 *min* | 10 *min* | 0.24 $min^{-1}$ | 4.87 *min* |
| | 2 | Inner | 1 | 0.1 *min* | 2 *min* | 0.05 | 0.1 *min* |
| | | Outer | 6 *min* | 8.93 *min* | 10 *min* | 0.15 $min^{-1}$ | 8.93 *min* |
| | 3 | Inner | 1 | 6 *min* | 2 *min* | 3 | 6 *min* |
| | | Outer | 0.1 *min* | 9.57 *min* | 10 *min* | 9.52 $min^{-1}$ | 9.57 *min* |
| Case 1 | 1 | - | 2 *min* | 6.19 *min* | 20 *min* | 0.15 $min^{-1}$ | 6.19 *min* |
| | 2 | - | 6 *min* | 6.14 *min* | 5 *min* | 0.20 $min^{-1}$ | 6.14 *min* |
| | 3 | - | 0.1 *min* | 5.95 *min* | 20 *min* | 2.96 $min^{-1}$ | 5.95 *min* |
| Case 2 | 1 | - | 4 *min* | 6.03 *min* | 5 *min* | 0.30 $min^{-1}$ | 6.03 *min* |
| | 2 | - | 0.1 *min* | 6.35 *min* | 5 *min* | 12.7 $min^{-1}$ | 6.35 *min* |
| | 3 | - | 6 *min* | 6.08 *min* | 5 *min* | 0.20 $min^{-1}$ | 6.08 *min* |

## 5.3 Results

The results for each case and system is presented in the form of the integral absolute error (IAE) in Table 5.3, where $IAE = \int_0^\infty \mid e(t) \mid dt$ and $e(t) = T_{2,sp} - T_2$. The unit for IAE in this case is *degree celsius minutes* [$^\circ C\,min$] but in literature the units for the IAE are typically omitted by convention, so this will be done from hereon. The

lower the IAE value for a simulation, the greater the performance. N.B. System refers to the different size of tanks and Case refers to the different approximation applied.

Table 5.3: IAE Values for various disturbances applied at $t = 10\,min$

| Case Number | Disturbance | IAE | | |
|---|---|---|---|---|
| | | System 1 | System 2 | System 3 |
| Case 1 | $\Delta F_0 = +0.1\,m^3\,min^{-1}$ | 5.3339 | 0.1266 | 2.8824 |
| Case 2 | | 3.1357 | 2.7454 | 0.1834 |
| Cascade | | 1.7444 | 1.2484 | 0.2408 |
| Case 1 | $\Delta F_{1d} = +0.2\,m^3\,min^{-1}$ | 10.8573 | 2.2447 | 5.7433 |
| Case 2 | | 5.9178 | 5.3637 | 0.3589 |
| Cascade | | 3.9925 | 3.0522 | 0.5341 |
| Case 1 | $\Delta T_{1d} = +2\,^\circ C$ | 0 | 0 | 0 |
| Case 2 | | 0 | 0 | 0 |
| Cascade | | 0.6299 | 0.2286 | 9.0793 |
| Case 1 | $\Delta F_{2d} = +0.1\,m^3\,min^{-1}$ | 9.3594 | 1.1447 | 5.1281 |
| Case 2 | | 6.2763 | 0.9152 | 3.4889 |
| Cascade | | 3.8174 | 0.4262 | 5.0742 |
| Case 1 | $\Delta T_{2d} = +2\,^\circ C$ | 3.49073 | 0.1006 | 0.7190 |
| Case 2 | | 3.3341 | 7.5 | 0.5 |
| Cascade | | 1.9540 | 3.4294 | 0.7189 |
| Case 1 | $\Delta T_{2,sp} = +10\%$ of set-point | 119.8626 | 23.75 | 136.8823 |
| Case 2 | | 30 | 23.75 | 34.25 |
| Cascade | | 55.9998 | 47.4990 | 68.4999 |

For the disturbances in $F_0$ and $F_{1d}$, it can be seen that for System 2 that Case 1 is the best, and for System 3 that Case 2 is the best. This is as expected since System 2 was the system with small tank 1, relative to tank 2 - therefore using the approximations in Case 1, neglecting the dynamics in tank 1, gives the best response. The system is treated as if it is one big tank, therefore any disturbance to the first tank is almost immediately fixed by a change in MV. For System 3 (small tank 2 relative to tank 1) the approximations in Case 2, neglecting dynamics in tank 2, are better and give lower IAE values, and therefore better performance. For System 1, where the two tanks are of similar size, neither Case 1 or Case 2 have lower IAE values than cascade control, though they both remain stable. This is a good outcome considering they both operate without the measurement of the internal variable, $T_1$, in comparison to the cascade control which does.

For both Case 1 System 2 and Case 2 System 3, perfect disturbance rejection is expected from the form of the transform equations. This is not realised as the system also has level controllers included, therefore any disturbance which changes the flow of material through the system will need to be acted upon by the P-controllers.

In comparison to this, all Systems simulated with either Case 1 and Case 2 for a disturbance of $T_{1d}$ have perfect disturbance rejection. The system is able to change $T_0$ as soon as there is a measured $T_{1d}$ change, meaning $T_1$, and consequentially $T_2$, do not change. Both of the cases presented in this chapter actually perform better than the cascade system, even though they have one less measurement.

No perfect disturbance rejection can be expected for either $F_{2d}$ or $T_{2d}$ since in both cases there will be some level of dynamics in tank 1, therefore any change in $T_0$ will need to be propagated through to $T_1$ and ultimately $T_2$, meanwhile $F_{2d}$ and $T_{2d}$ deviate $T_2$ from its set-point. For Case 1, the transform is modelled on a single tank, made up of a combined tank 1 and tank 2. This means that a disturbance of $F_{2d}$ or $T_{2d}$ behave similarly, but not identically, to $F_0$, $F_{1d}$ or $T_{1d}$. The difference is caused by the dynamics of the first tank slowing down the response. For Case 2 the disturbances to tank 2, $F_{2d}$ and $T_{2d}$, behave considerably differently to those which directly affect tank 1. For these disturbances, a different $T_1$ is required to get $T_2$ back to set-point, whereas for disturbances directly to tank 1, the same $T_1$ as the nominal value is required to get $T_2$ back to the set-point. A comparison of the effect of $T_{1d}$ and $T_{2d}$ on $T_1$ is shown graphically in Fig. 5.4 - a disturbance of $T_{2d}$ or $F_{2d}$ are actually similar to a direct $T_1$ set-point change. For Case 2, as described in Section 5.2.2, it is essentially a transformed system acting on the internal variable $T_1$. Therefore, for a $T_1$ set-point change the feedback loop is required, which will work with the transformation to get $T_2$ back to set-point. This is not optimal as normally the system should not rely on feedback for a disturbance and the transform should take care of the response. This means the system performance relies greatly on the controller tuning - seen by the relatively high IAE value of 7.5 for a disturbance of $\Delta T_{2d}$ for Case 2 System 2.

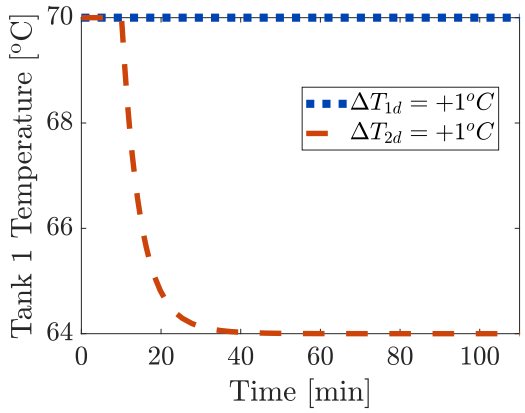


Figure 5.4: Comparison of disturbances for Case 2 System 2

## 5.4 Case Study Discussion

In the transformed input theory set out in Chapter 3, *Assumption 2* states that all variables required in the process model are measured. In this chapter, Case Study A has been extended to see if the transformed input theory can be amended to break this assumption. A conventional cascade control structure could not handle this since the inner controller acts on the internal variable error, if it is not measured then this is not possible. Feedback linearization could not handle this either, unless an estimator, such as a Kalman filter, is used.

There are two possible cases to apply to systems if the internal variable cannot be measured. One of these disregards the dynamics of the internal variable, i.e. $dw/dt = 0$, and the other disregards the dynamics of the controlled variable, i.e. $dy/dt = 0$. It has been shown that for systems nearer to extremities than the nominal model in Chapter 4, the choice of case should be chosen according to which dynamics, that of the output variable or that of the internal variable, play a bigger role. In the case of System 1, the same model as Chapter 4, the cascade system performs better than the two approximation cases for all disturbances, except the special case of perfect $T_{1d}$ disturbance rejection. This is expected, though without a key measurement the two approximated cases do perform well, and at least are stable. For a system that has more realistic parameters it is not as clear about which case should be used, but both are stable. This chapter has, therefore, shown that even when *Assumption 1* and *Assumption 2* of the original transformed input theory are broken, the system can be easily adapted by using a cascade system and by approximating the internal variable.

# Chapter 6

# Case Study B: Outlet Concentration Control of a Continuously Stirred-Tank Reactor

The second case study was a first-order continuously stirred-tank reactor (CSTR) model. This is less trivial than the Tanks-in-Series example with an increased complexity, where the concentration of reactant leaving the reactor is to be controlled by manipulating the heat added. Unlike in Chapter 4, some of the disturbances do not directly affect the controlled variable and this gives rise to possible improvements to the cascade structures presented.

## 6.1 Process Model

The CSTR simulations follow the ODEs described by Eq. 6.1 and 6.2, derived from molar and energy balances over the tank, Fig. 6.1 with the following assumptions;

*B1*: Perfect volume control, i.e. $q_1 = q_2$

*B2*: Constant density, $\rho$, and specific heat, $c_p$

*B3*: Control of heat added is sufficiently fast

*B4*: Perfect mixing within tank

*B5*: Constant pressure and volume

*B6*: Negligible shaft work

Full derivations are found in Appendix B.3. The liquid-phase reaction in the tank is first-order and described by $A \rightarrow B$.

$$\frac{dc_A}{dt} = \frac{q_1}{V}c_{Af} - \Big(\frac{q_1}{V} + k(T)\Big)c_A = f(y, d, w) \tag{6.1}$$

$$\frac{dT}{dt} = \frac{q_1}{V}(T_1 - T) - \frac{H_{rx}k(T)c_A}{\rho c_p} + \frac{Q}{V\rho c_p} = g(y, d, w, u) \tag{6.2}$$

Where,

$$k(T) = k_0 e^{-\frac{E}{R}(\frac{1}{T} - \frac{1}{T_0})}$$

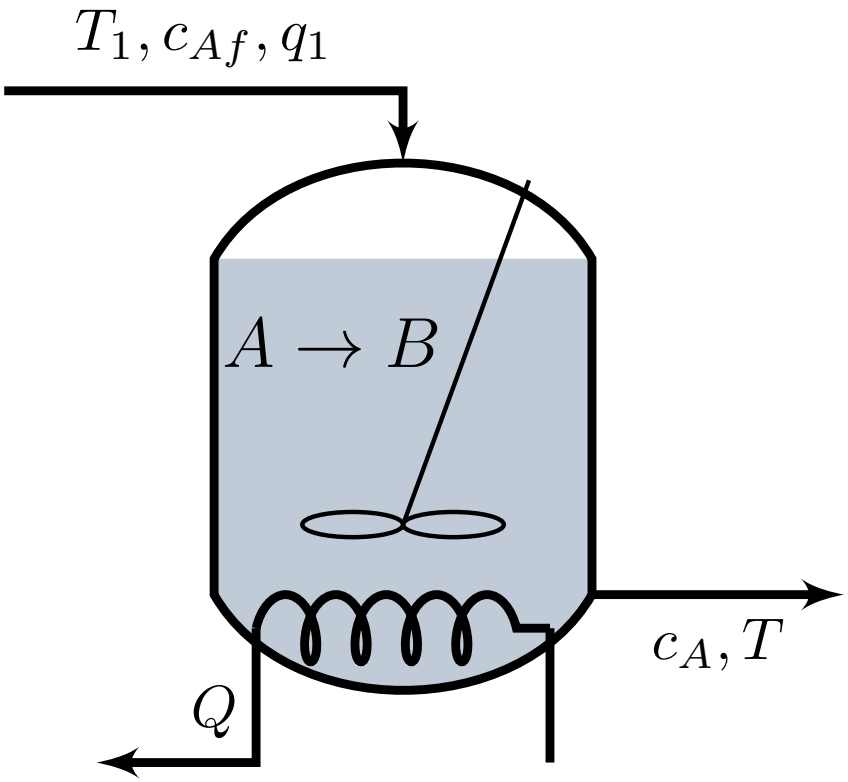


Figure 6.1: CSTR Model

Parameters and steady-state values can be found in Table 6.1.

Table 6.1: Nomenclature and nominal values for CSTR

| Variable | Symbol | Unit | Steady-state value |
|---|---|---|---|
| Reference Temperature | $T_0$ | $K$ | 400 |
| Inlet Stream Temperature | $T_1$ | $K$ | 350 |
| Tank Temperature | $T$ | $K$ | 400 |
| Volume of Tank | $V$ | $m^3$ | 4 |
| Inlet Stream Flowrate | $q_1$ | $m^3\,min^{-1}$ | 1 |
| Outlet Stream Flowrate | $q_2$ | $m^3\,min^{-1}$ | 1 |
| Heat Provided | $Q$ | $kJ\,min^{-1}$ | 5000 |
| Specific Heat Capacity | $c_p$ | $kJ\,kg^{-1}\,K^{-1}$ | 0.150 |
| Inlet Stream Concentration of A | $c_{Af}$ | $kmol\,m^{-3}$ | 2 |
| Outlet Stream Concentration of A | $c_A$ | $kmol\,m^{-3}$ | 2/3 |
| Activation Energy | $E$ | $kJ\,kmol^{-1}$ | 20000 |
| Heat of Reaction | $H_{rx}$ | $kJ\,kmol^{-1}$ | $-1875$ |
| Density | $\rho$ | $kg\,m^{-3}$ | 1000 |
| Reference Rate Constant | $k_0$ | $min^{-1}$ | 0.5 |
| Universal Gas Constant | $R$ | $kJ\,K^{-1}\,kmol^{-1}$ | 8.314 |

## 6.2 Control Structure

In this case study, the controlled variable (CV) is the concentration of $A$ in the outlet flow of the tank, $y = c_A$. The manipulated variable (MV) is the heat supplied to the tank, $u = Q$. The disturbances ($d$) to the system are the temperature, concentration and flowrate of the inlet stream to the tank; $T_1$, $c_{Af}$ and $q_1$ respectively. The internal variable for this case study is the temperature of the reactor, $w = T$.

### 6.2.1 Possible Configurations

In addition to the general and alternative cascade systems implemented in Chapter 4, introduced in this chapter are simulations of the two closely related structures, stemming from the alternative cascade structure; namely a 'double-linearized' system, and a chain of transforms.

#### 6.2.1.1 General and Alternative Cascade Systems

For this system, the transform is applied as per Eq. 6.3 for both the general cascade and alternative cascade systems, described in Fig. 6.2 and 6.3 respectively. The alternative cascade structure is also known as the 'fitted' case, so that it is not confused with the variations of the alternative cascade structure below.

$$v = f(y, d, w) - Ac_A = \frac{q_1}{V}c_{Af} - \left(\frac{q_1}{V} + k(T) + A\right)c_A \tag{6.3}$$

Where,

$$A = \left(\frac{df}{dc_A}\right)^* = -\left(\frac{q_1}{V} + k(T)\right)^* = -0.75\,min^{-1}$$

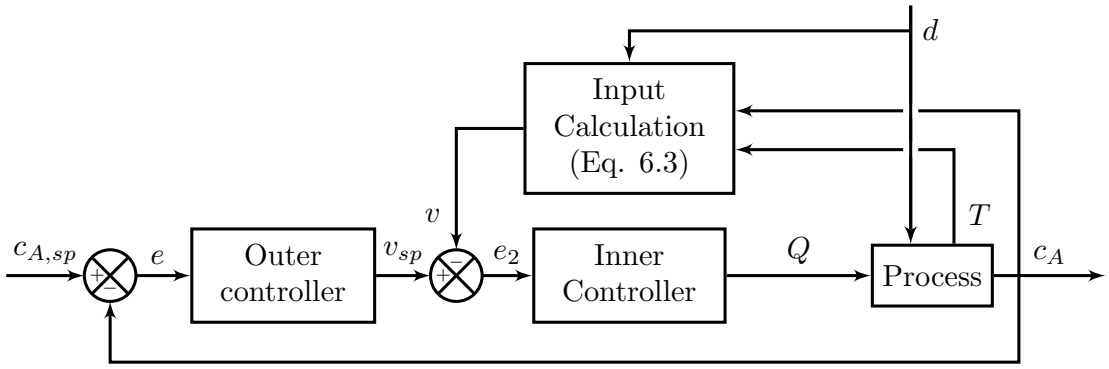


Figure 6.2: General Cascade Structure

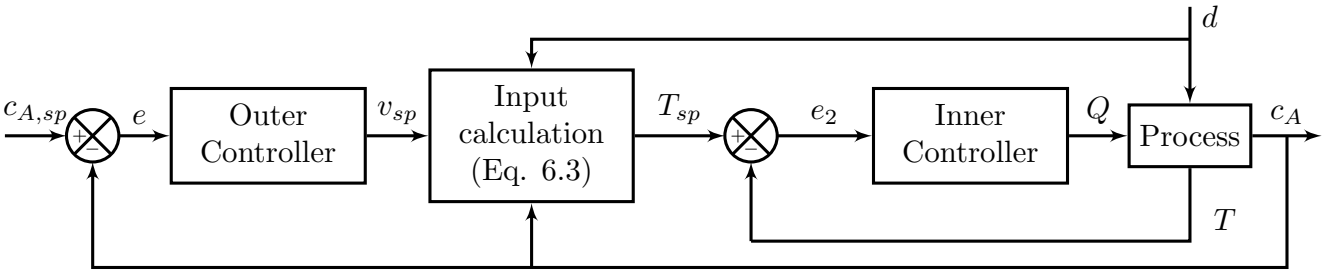


Figure 6.3: Alternative (Fitted) Cascade Structure

#### 6.2.1.2 Double-Linearized System

For the so-called 'double-linearized' system, the transform above, Eq. 6.3, is used in addition to a second transform on the internal variable - in this case the temperature of the tank $T$. The transform is applied as per Eq. 6.4. In this case the variable $B$ is introduced in place of the usual $A$ tuning parameter to avoid confusion. The double-linearized system is shown in Fig. 6.4.

$$v_2 = g(y, d, w, u) - BT = \frac{q_1}{V}(T_1 - T) - \frac{H_{rx}k(T)c_A}{\rho c_p} + \frac{Q}{V\rho c_p} - BT \tag{6.4}$$

Where,

$$B = \left(\frac{dg}{dT}\right)^* = -0.1874\,min^{-1}$$

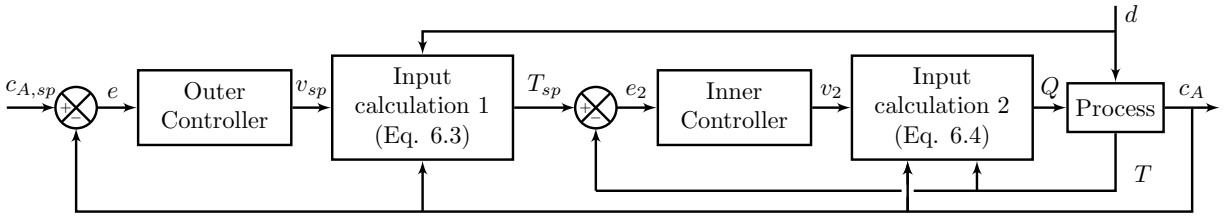


Figure 6.4: Double-Linearized System

#### 6.2.1.3 Chain of Transforms

The chain of transforms, similar in some respects to the chain of integrators in feedback linearization, is able to control the system with no controller if the model is perfect and all disturbances are measured. This uses the first transform, Eq. 6.3 to solve for $v_{A0}$, where $v_{A0} = T$ , so this gives a type of set-point for the tank temperature. This is then used in the second transformation block to give the input, $Q$, in Eq. 6.5. The value of $B$ is chosen to be the same as above. The system is described in Fig. 6.5.

$$\frac{dT}{dt} = \frac{q_1}{V}(T_1 - T) - \frac{H_{rx}k(T)c_A}{\rho c_p} + \frac{Q}{V\rho c_p} = B(T - v_{A0}) \tag{6.5}$$

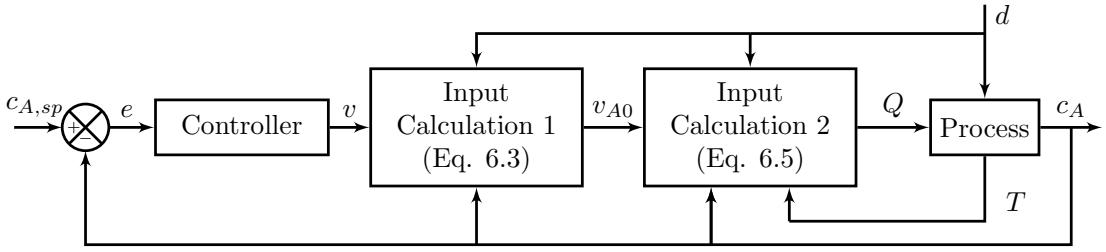


Figure 6.5: Chain of Transform System

### 6.2.2 Controller Tuning

All controllers are tuned using SIMC tuning rules (Skogestad, 2003). Process parameters from open-loop step responses and controller tuning parameters are found in Table 6.2, all graphs can be found in Appendix A.3.

Table 6.2: Process and Tuning Parameters for all CSTR Cases. (Chain requires only one controller)

| Case | Controller | $K$ | $\tau$ | $\tau_c$ | $K_c$ | $\tau_I$ |
|---|---|---|---|---|---|---|
| Chain | - | $1.33\,min$ | $7.32\,min$ | $10\,min$ | $0.55\,min^{-1}$ | $7.32\,min$ |
| Double-Linearized | Inner | $5.34\,min$ | $5.35\,min$ | $2\,min$ | $0.5\,min^{-1}$ | $5.34\,min$ |
| | Outer | $1.33\,min$ | $3.66\,min$ | $10\,min$ | $0.27\,min^{-1}$ | $3.66\,min$ |
| Fitted | Inner | $7.3 \times 10^{-3}\,K\,min\,kJ^{-1}$ | $4.33\,min$ | $2\,min$ | $296.58\,kJ\,K^{-1}\,min^{-1}$ | $4.33\,min$ |
| | Outer | $1.33\,min$ | $3.61\,min$ | $10\,min$ | $0.27\,min^{-1}$ | $3.61\,min$ |
| General Cascade | Inner | $-3.7 \times 10^{-5}\,kmol\,m^{-3}\,kJ^{-1}$ | $4.26\,min$ | $2\,min$ | $-5.76 \times 10^{4}\,m^{3}\,kJ\,kmol^{-1}$ | $4.26\,min$ |
| | Outer | $1.33\,min$ | $3.50\,min$ | $10\,min$ | $0.26\,min^{-1}$ | $3.50\,min$ |
| Feedback Only | Inner | $7.3 \times 10^{-3}\,K\,min\,kJ^{-1}$ | $4.27\,min$ | $2\,min$ | $292.47\,kJ\,K^{-1}\,min^{-1}$ | $4.27\,min$ |
| | Outer | $-7.4 \times 10^{-3}\,kmol\,m^{-3}\,min^{-1}\,K^{-1}$ | $3.65\,min$ | $10\,min$ | $-49.32\,m^{3}\,min\,K\,kmol^{-1}$ | $3.65\,min$ |

## 6.3 Results

### 6.3.1 Comparison of Control Structures

The results for disturbances of $\Delta T_1 = +17.5\,K$, $\Delta c_{Af} = +0.1\,kmol\,m^{-3}$ and $\Delta q_1 = +0.1\,m^3\,min^{-1}$ and a set-point change of $\Delta c_{A,sp} = +2/15\,kmol\,m^{-3}$ are presented separately in Fig. 6.6. In Fig. 6.7 the same disturbances and set-point changes have been simulated, except without an outer controller. Open-loop (O-L) responses have been added to show the effect on the system with no control scheme in place.

For the first disturbance (Figs. 6.6a and 6.7a), it can be seen that perfect disturbance rejection is achieved for both the chain of transforms and the double-linearized systems. This is achieved by the step-change in input, $Q$, which the system uses to offset the effect of the disturbance. For the general cascade structure and the original alternative cascade structure, named 'fitted' here, perfect disturbance rejection is not achieved and results are almost identical to that for a feedback only system.

For the second and third disturbances (Figs. 6.6b, 6.6c, 6.7b and 6.7c) the advantage of the transformed systems is very clear, even though perfect disturbance rejection is not achieved. The responses from all transformed systems are faster than that of feedback only. The general cascade structure, fitted alternative cascade structure and double-linearized alternative cascade structure all behave very similarly, with the double-linearized simulation behaving slightly faster for disturbance 3. The chain of transforms is the slowest of the transformed systems for both disturbances 2 and 3.

As seen in Chapter 4, all systems behave very similarly to set-point changes, seen in Fig. 6.6d and 6.7d. This is expected since the transforms are only functions of measured process variables, rather than the set-point variables. N.B. for a change in set-point for the systems with no outer controller, the controller bias is controlled directly to reflect the same change.

Comparing Fig. 6.6 to Fig. 6.7, i.e. cascade structure versus only an inner controller, it can be seen that the systems respond differently. For all the disturbance simulations with the cascade, where perfect disturbance is not achieved, the concentration overshoots the set-point. Whereas, for an inner controller only, the concentration always settles to the set-point with no overshoot and is usually faster to reach steady-state, even though the time for a response is typically longer.

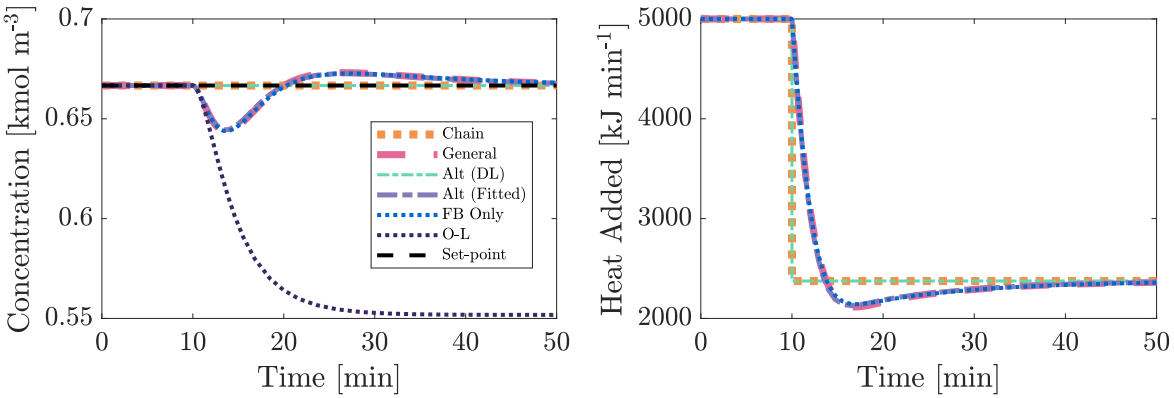


(a) Disturbance Rejection 1: $\Delta T_1 = +17.5\,K$ at $t = 10\,min$

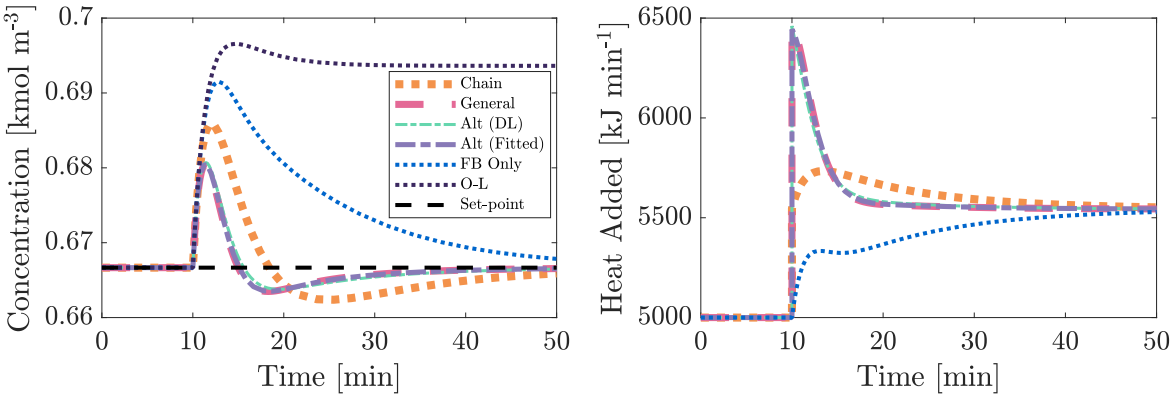


(b) Disturbance Rejection 2: $\Delta c_{Af} = +0.1\,kmol\,m^{-3}$ at $t = 10\,min$

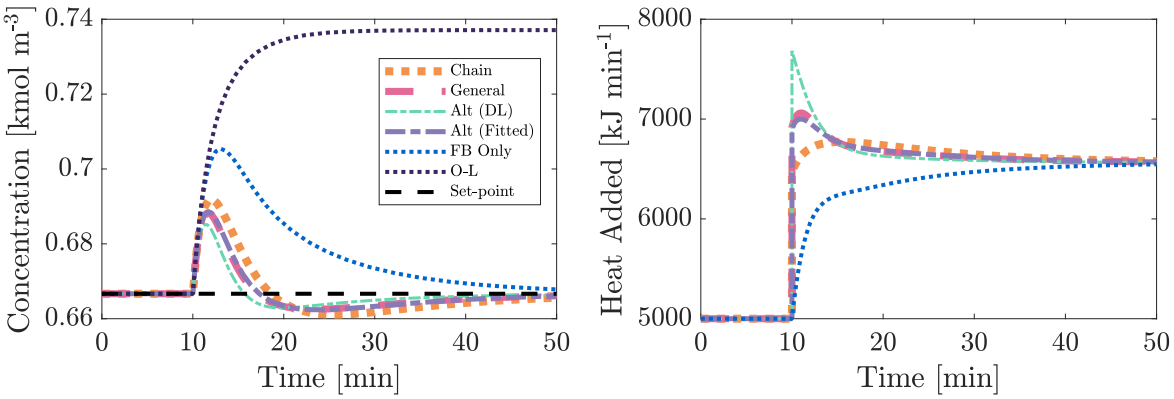


(c) Disturbance Rejection 3: $\Delta q_1 = +0.1\,m^3\,min^{-1}$ at $t = 10\,min$

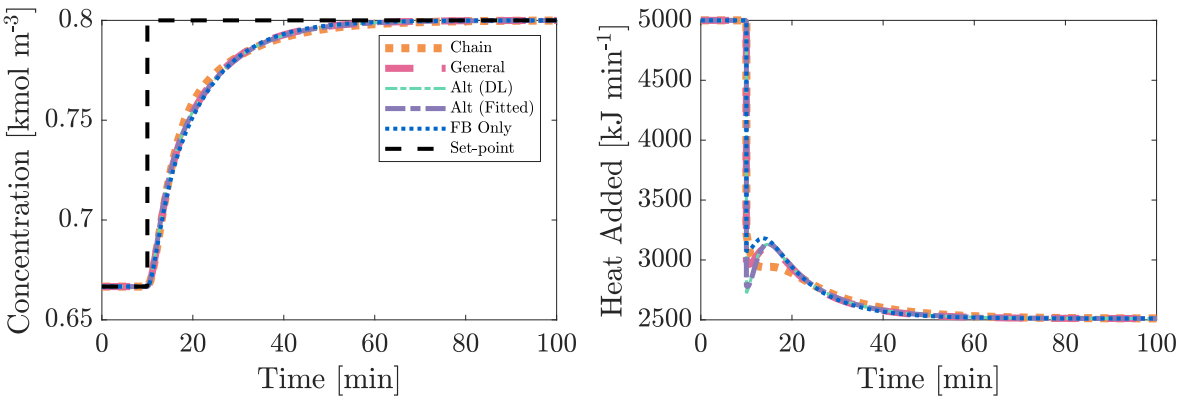


(d) Set-point Tracking: $\Delta c_{A,sp} = +2/15\,kmol\,m^{-3}$ at $t = 10\,min$ (note time-scale)

Figure 6.6: Results for Cascaded Control Structures on CSTR. (DL = double-linearized)

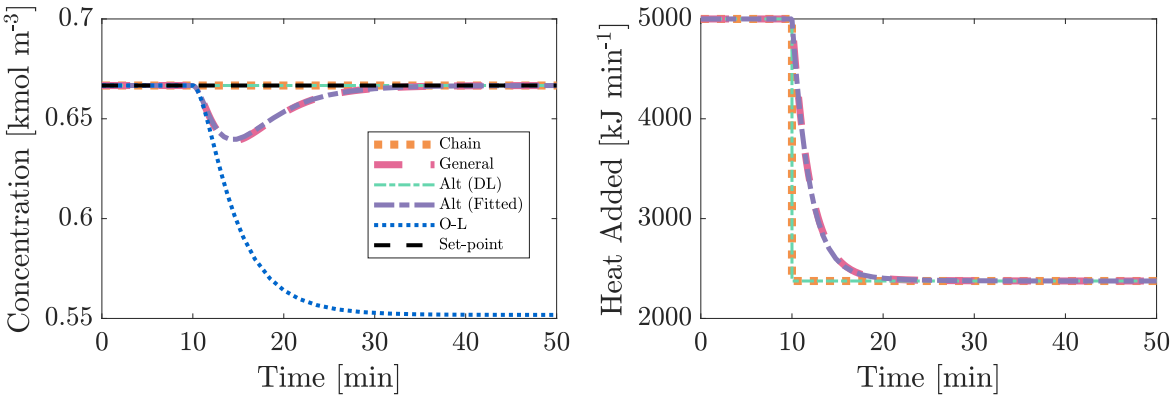


(a) Disturbance Rejection 1: $\Delta T_1 = +17.5\,K$ at $t = 10\,min$

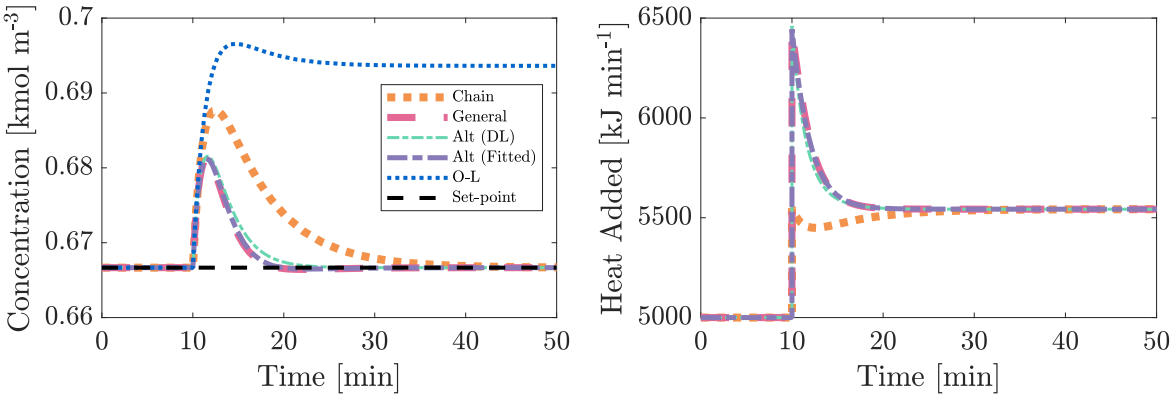


(b) Disturbance Rejection 2: $\Delta c_{Af} = +0.1\,kmol\,m^{-3}$ at $t = 10\,min$

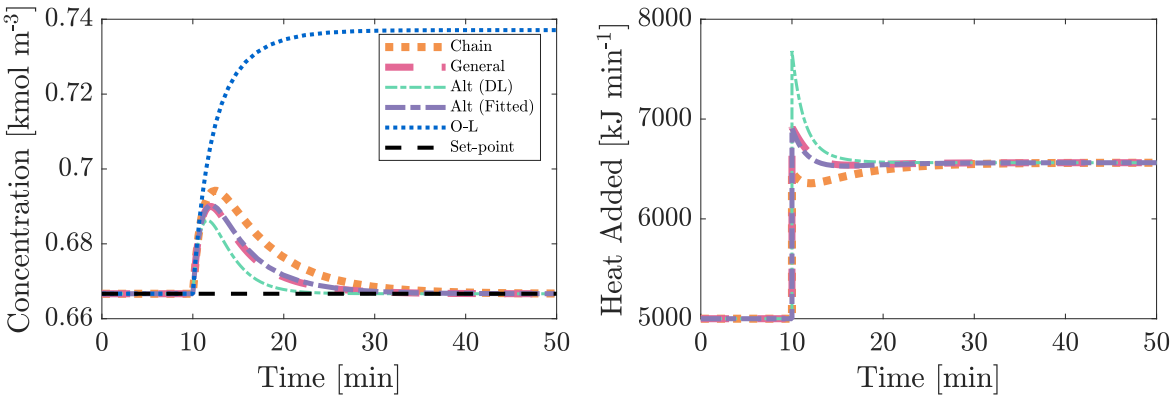


(c) Disturbance Rejection 3: $\Delta q_1 = +0.1\,m^3\,min^{-1}$ at $t = 10\,min$

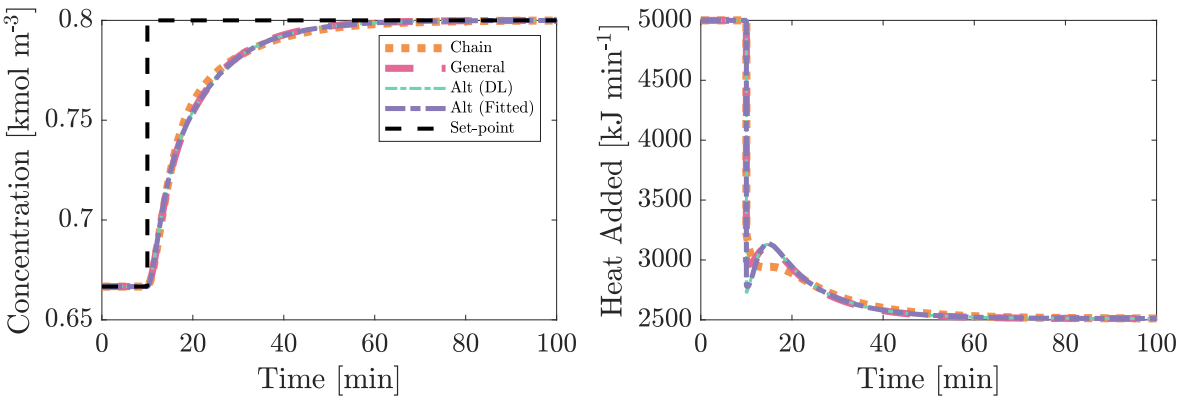


(d) Set-point Tracking: $\Delta c_{A,sp} = +2/15\,kmol\,m^{-3}$ at $t = 10\,min$ (note time-scale)

Figure 6.7: Results for Control Structures on CSTR with No Outer Controller. (DL = double-linearized)

### 6.3.2 Disturbance Mis-match

It was shown above that systems with no outer controller respond to disturbances better, though this assumes a perfect process model. In reality, this will not always be the case, for example due to unmeasured disturbances. As shown in Fig. 6.8, the double-linearized system is used to simulate disturbance mis-match, as described in Section 3.2.1. The gain $D$ is used as a measure of the amount of disturbance error relative to the nominal value.

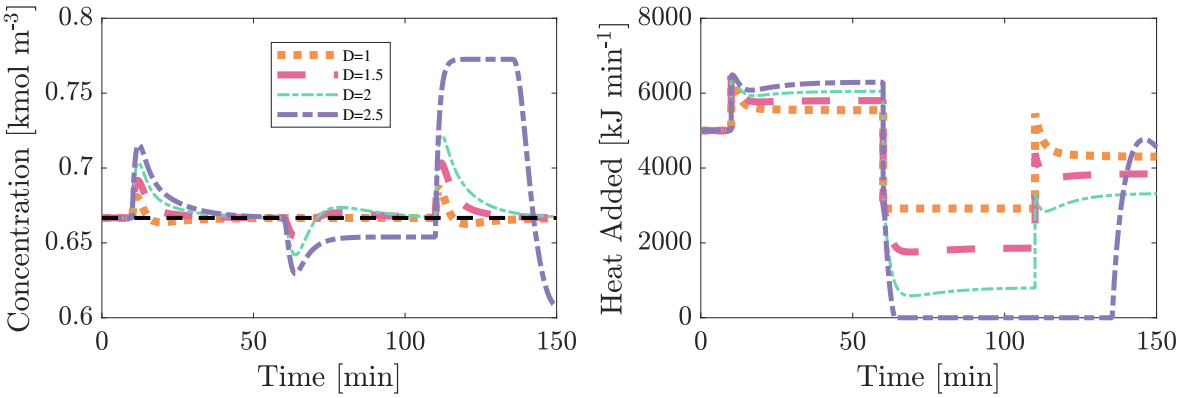


(a) Disturbance Mis-match for Cascade System

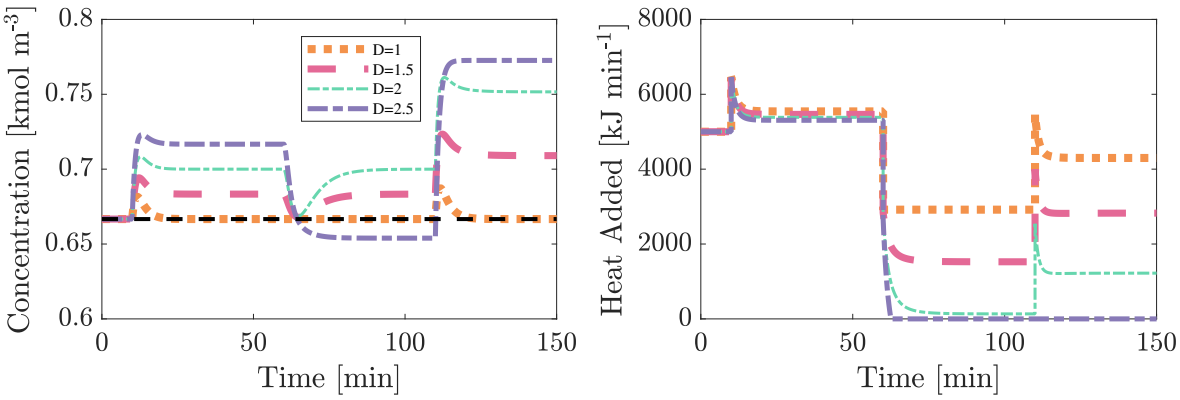


(b) Disturbance Mis-match for Inner controller only

Figure 6.8: Results for Disturbance Mis-match on CSTR with Double-Linearized System: $\Delta c_{Af} = +0.1\ kmol\,m^{-3}$ at $t = 10\ min$; $\Delta T_1 = +17.5\ K$ at $t = 60\ min$; $\Delta q_1 = +0.1\ m^3\,min^{-1}$ at $t = 110\ min$.

From Fig. 6.8a, it can clearly be seen that the system is able to hand with disturbance mis-matches of reasonable proportion. Obviously the case with $D = 1$ responds fastest to the disturbances since the actual disturbance value is the same as the measured disturbance value, and this is used in the transformation calculation. It is shown that the control scheme still works for $D = 1.5$ and $D = 2$, albeit slower than the nominal case as expected. Unfortunately, saturation of the system occurs at 60 *mins* when $D = 2.5$, and subsequently the system winds up. This is an extreme case and is not due to the control scheme. An anti-wind-up PI controller

may be implemented if the real system constantly undergoes this behaviour.

In Section 6.3.1, it was seen that a system that did not have the outer controller responded better to disturbances; both faster and with no overshooting. However, it can be seen in Fig. 6.8b that the system cannot handle disturbance mis-match when there is no outer controller present. The systems merely settle at a new steady-state value, determined by the value of the nominal value of the transformed input, $v$, and the value of the wrongly measured disturbances. From this it can be seen that in the case of disturbance mis-match the outer control loop is of utmost importance; the transformation cannot work solely.

## 6.4 Case Study Discussion

In this case study, it is seen that for *certain* disturbances perfect disturbance rejection can be achieved. But what is required for this to be the case and why not all the time? It was seen that perfect disturbance rejection was only achieved for a disturbance of $T_1$, and not for $c_{Af}$ or $q_1$. This is explained by the fact that $T_1$ appears **only** in the ODE representing the internal variable, $T$, Eq. 6.2. Mathematically, the relative order for the disturbance is the same as the relative order for the input. Therefore, a disturbance of $T_1$ does not directly affect the controlled variable, $c_A$, immediately. This means that the set-point of $T$ remains constant for a disturbance of $T_1$. Therefore the second transformation block for the double-linearized and chain of transform systems is able to handle this disturbance before it impacts $c_A$. These are the only two transformed systems which make use of the $dT/dt$ equation in a calculation block.

The disturbance $q_1$ appears in both the ODE for the controlled variable, $c_A$, and the ODE for the internal variable, $T$. This means that $T_{sp}$ changes, and $T$ itself is also directly affected. The second calculation block in the double-linearized system is able to handle the variation in $T$, owing to the faster response for a disturbance of $q_1$ in Fig. 6.6c and 6.7c. The chain of transforms does not handle this as well since there is a lack of inner controller acting on the error between $T_{sp}$ and $T$.

The disturbance $c_{Af}$ appears only in the ODE for the controlled variable, $c_A$, and therefore all systems, except for the chain of transforms, act almost identically. This is due to the fact that the second transform plays a minimal role in the response. The chain of transforms slower again due to the lack of an inner controller.

It was presented that a perfect system with no outer controller is better than one

with a full cascade structure, though it was also shown that an outer controller does not handle any sort of mis-match. For a real-life industrial system the chance that a model is completely known, and acts perfectly throughout operation, is very slim. A model describing dynamics completely correctly may be very complex too, increasing complexity of the transform and the calculations required. If a transformed system uses an outer feedback loop then this opens the possibility of using a simplified model for the transform and letting the feedback loop settle any mis-match that there is. An example of this in use is shown by Zotică et al. (2020) for a heat exchanger. This robustness is something that feedback linearization lacks and cannot handle well.

# Chapter 7

# Case Study C: pH Control of a Reactor

This case study is an example of a system that is nonlinear in the output, since pH is not a linear measurement. Therefore, the standard cascade structures which have been used in previous chapters will not work. The pH is manipulated by controlling the flowrate of a basic stream into the reactor.

## 7.1 Process Model

All nominal values and equations used for this case study are by Henson and Seborg (1994) and Hall and Seborg (1989). The system is presented in Fig. 7.1. The manipulated variable is the input flow of base stream $q_3$ ($0.003M$ $NaOH$ and $0.0005M$ $NaHCO_3$) and the controlled variable is the pH of the tank - measured in $q_4$ with the assumption of perfect mixing in the tank. The flowrates of acid stream $q_1$ ($0.003M$ $HNO_3$) and buffer stream $q_2$ ($0.03M$ $NaHCO_3$) are measured disturbances to the system.

The equations to describe the system are derived from conservation equations and the equilibrium relations from reactions in Eq. 7.1. The two reaction invariants for each stream ($i \in [1\ 4]$) are defined by Eq. 7.2.

$$H_2CO_3 \rightleftharpoons HCO_3^- + H^+ \tag{7.1a}$$

$$HCO_3^- \rightleftharpoons CO_3^{2-} + H^+ \tag{7.1b}$$

$$H_2O \rightleftharpoons H^+ + OH^- \tag{7.1c}$$

$$W_{ai} = [H^+]_i - [OH^-]_i - [HCO_3^-]_i - 2[CO_3^{2-}]_i \tag{7.2a}$$

$$W_{bi} = [H_2CO_3]_i + [HCO_3]_i + [CO_3^{2-}]_i \tag{7.2b}$$

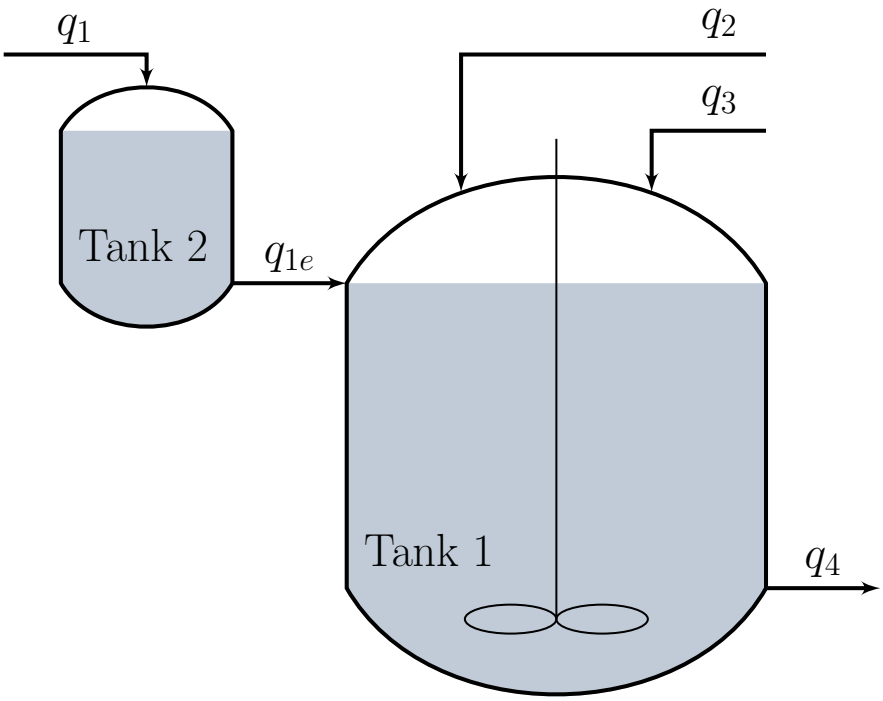


Figure 7.1: pH Neutralisation System. Adapted from Henson and Seborg (1994).

$W_a$ is a charge related quantity, whereas $W_b$ represents the concentration of $CO_3^{2-}$ ions. The values of the reaction invariants for streams 1-3 are constant as the concentration of ions within these streams does not change throughout the simulation. The values of $W_{a4}$ and $W_{b4}$ are described by the following equations;

$$\frac{dW_{a4}}{dt} = \frac{1}{A_1 h_1}\Big(q_{1e}(W_{a1}-W_{a4})+q_2(W_{a2}-W_{a4})+q_3(W_{a3}-W_{a4})\Big) = f(u,w,d) \tag{7.3a}$$

$$\frac{dW_{b4}}{dt} = \frac{1}{A_1 h_1}\Big(q_{1e}(W_{b1}-W_{b4})+q_2(W_{b2}-W_{b4})+q_3(W_{b3}-W_{b4})\Big) = g(u,w,d) \tag{7.3b}$$

The concentration of $[\mathrm{H}^+]$ in stream $i$, and subsequently the pH, is calculated by solving the equation below;

$$W_{bi}\frac{\frac{K_{a1}}{[H^+]} + \frac{2K_{a1}K_{a2}}{[H^+]^2}}{1 + \frac{K_{a1}}{[H^+]} + \frac{K_{a1}K_{a2}}{[H^+]^2}} + W_{ai} + \frac{K_w}{[H^+]} - [H^+] = 0 \tag{7.4}$$

The flowrate of the stream leaving tank 2, $q_{1e}$ is calculated by Eq. 7.5, where $h_2$ is described by the ODE in Eq. 7.6.

$$q_{1e} = C_{v1} h_2^{0.5} \tag{7.5}$$

$$A_2 \frac{dh_2}{dt} = q_1 - q_{1e} \tag{7.6}$$

Nomenclature and steady-state values are shown in Table 7.1.

Table 7.1: Nomenclature and nominal values for pH Neutralisation. (Henson and Seborg, 1994)

| **Variable** | **Symbol** | **Unit** | **Steady-state value** |
|---|---|---|---|
| Concentration of Stream 1 | $[q_1]$ | $M$ | 0.003 $HNO_3$ |
| Concentration of Stream 2 | $[q_2]$ | $M$ | 0.03 $NaHCO_3$ |
| Concentrations of Stream 3 | $[q_3]$ | $M$ | 0.003 $NaOH$ and 0.0005 $NaHCO_3$ |
| Cross-sectional Area of Tank 1 | $A_1$ | $cm^2$ | 207 |
| Cross-sectional Area of Tank 2 | $A_2$ | $cm^2$ | 42 |
| Equilibrium Constant for Reaction 1 | $K_{a1}$ | – | $4.47 \times 10^{-7}$ |
| Equilibrium Constant for Reaction 2 | $K_{a2}$ | – | $5.62 \times 10^{-11}$ |
| Equilibrium Constant for Reaction 3 | $K_w$ | – | $1.00 \times 10^{-14}$ |
| Delay in pH Measurement | $\theta$ | $s$ | 10.0 |
| Flowrate of Stream 1 | $q_1$ | $ml\,s^{-1}$ | 16.6 |
| Flowrate of Stream 2 | $q_2$ | $ml\,s^{-1}$ | 0.55 |
| Flowrate of Stream 3 | $q_3$ | $ml\,s^{-1}$ | 15.6 |
| Flowrate of Stream 1e (from Tank 2) | $q_{1e}$ | $ml\,s^{-1}$ | 16.6 |
| Flowrate of Stream 4 | $q_4$ | $ml\,s^{-1}$ | 32.8 |
| Reaction Invariant A - Stream 1 | $W_{a1}$ | $M$ | $3.00 \times 10^{-3}$ |
| Reaction Invariant B - Stream 1 | $W_{b1}$ | $M$ | 0.00 |
| Reaction Invariant A - Stream 2 | $W_{a2}$ | $M$ | 0.03 |
| Reaction Invariant B - Stream 2 | $W_{b2}$ | $M$ | 0.03 |
| Reaction Invariant A - Stream 3 | $W_{a3}$ | $M$ | $-3.05 \times 10^{-3}$ |
| Reaction Invariant B - Stream 3 | $W_{b3}$ | $M$ | $5.00 \times 10^{-5}$ |
| Reaction Invariant A - Stream 4 | $W_{a4}$ | $M$ | $4.32 \times 10^{-4}$ |
| Reaction Invariant B - Stream 4 | $W_{b4}$ | $M$ | $5.28 \times 10^{-4}$ |
| Level in Tank 1 | $h_1$ | $cm$ | 14.0 |
| Level in Tank 2 | $h_2$ | $cm$ | 3.0 |
| pH of Stream 4 (& Tank) | $pH$ | – | 7.0 |
| Valve Coefficient | $C_{v1}$ | $ml^{0.5}\,s^{-1}$ | 9.58 |

## 7.2 Control Structure

As mentioned previously, in this case study the controlled variable is the pH of the system, and the manipulated variable is the flowrate of stream 3, $q_3$. The disturbances to the system are the flowrate of stream 1, $q_1$, and the flowrate of stream 2, $q_2$.

Firstly, as pH is a nonlinear measurement, it is not easy, nor desirable, to base the control structure on the pH. It is much easier to transform it to a linear measurement, such as the hydrogen ion concentration, $[H^+]$. This is an output transformation

rather than the normal input transform for linearization which is defined as $v$. In this case the output transform is simple and described by Eq. 7.7.

$$[H^+] = 10^{-pH} \tag{7.7}$$

### 7.2.1 Standard Transformed System

If the transform is applied in the same manner as in previous case studies, i.e. in a cascade manner, it is realised that there are two internal variables for which there are ODEs for, and appear in the equation for the output; both $W_{a4}$ and $W_{b4}$. Therefore for the general cascade, alternative cascade and the chain of transform structures there is no 'correct' way to apply the transformation theory. For the general cascade and alternative cascade the static transform must follow Eq. 7.4 with $i = 4$, where $v = [H^+]$. This is solved by using an I-controller with a small $\tau_c$; a sub-system with set-point of 0, which loops, changing the value of $[H^+]$,$W_{a4}$ or $W_{b4}$ (depending on the control scheme chosen) until $f([H^+]) = 0$, as per Eq. 7.4. This is also known as dynamic inversion and is very fast compared to the other controllers and the system dynamics. The output can be chosen to be either $W_{a4}$ or $W_{b4}$, resulting in the general linear transform Eq. 7.8 or 7.9 respectively, solved to give $q_3$.

$$v_2 = f(u, w, d) - AW_{a4} = \frac{q_{1e}(W_{a1} - W_{a4}) + q_2(W_{a2} - W_{a4}) + q_3(W_{a3} - W_{a4})}{A_1 h_1} - AW_{a4} \tag{7.8}$$

or

$$v_2 = g(u, w, d) - AW_{b4} = \frac{q_{1e}(W_{b1} - W_{b4}) + q_2(W_{b2} - W_{b4}) + q_3(W_{b3} - W_{b4})}{A_1 h_1} - AW_{b4} \tag{7.9}$$

Where,

$$A = \left(\frac{df}{dW_{a4}}\right) = \left(\frac{dg}{dW_{b4}}\right) = -\frac{q_{1e} + q_2 + q_3}{A_1 h_1} = -0.0113\, s^{-1}$$

For the chain of transforms, the static transform, Eq. 7.4 is again used to give a transformed variable $v_2$, by solving for either $W_{a4}$ or $W_{b4}$. This is then used in the transform in either Eq. 7.10 or 7.11 to give the input, $q_3$.

$$\frac{dW_{a4}}{dt} = \frac{q_{1e}(W_{a1} - W_{a4}) + q_2(W_{a2} - W_{a4}) + q_3(W_{a3} - W_{a4})}{A_1 h_1} = A(W_{a4} - v_2) \tag{7.10}$$

$$\frac{dW_{b4}}{dt} = \frac{q_{1e}(W_{b1} - W_{b4}) + q_2(W_{b2} - W_{b4}) + q_3(W_{b3} - W_{b4})}{A_1 h_1} = A(W_{b4} - v_2) \quad (7.11)$$

The three configurations may be arranged according to Fig. 7.2 - 7.4. Clearly in simulations all variables are known, and this may look like the block diagrams are converting $[H]^+$ to pH, just to change it back again. For this reason, it has been marked on the diagram which variables would actually be known in a real scenario, which would be calculated and which are unknown.

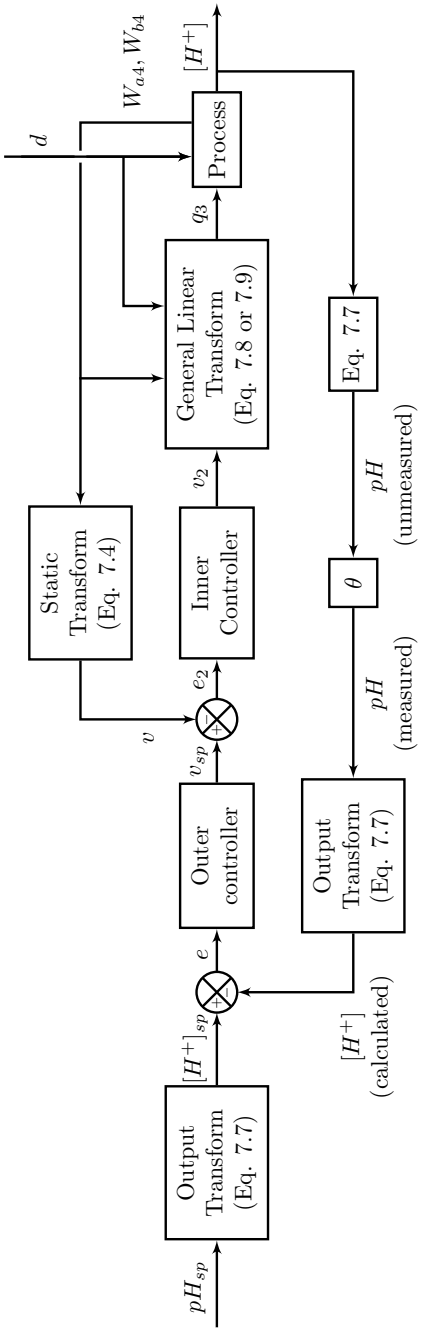


Figure 7.2: General Cascade Block Diagram

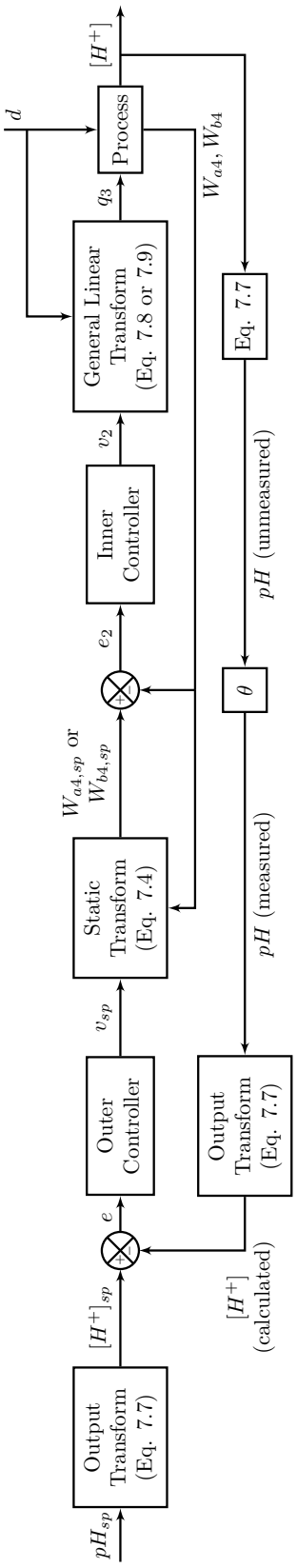


Figure 7.3: Alternative Cascaded Block Diagram

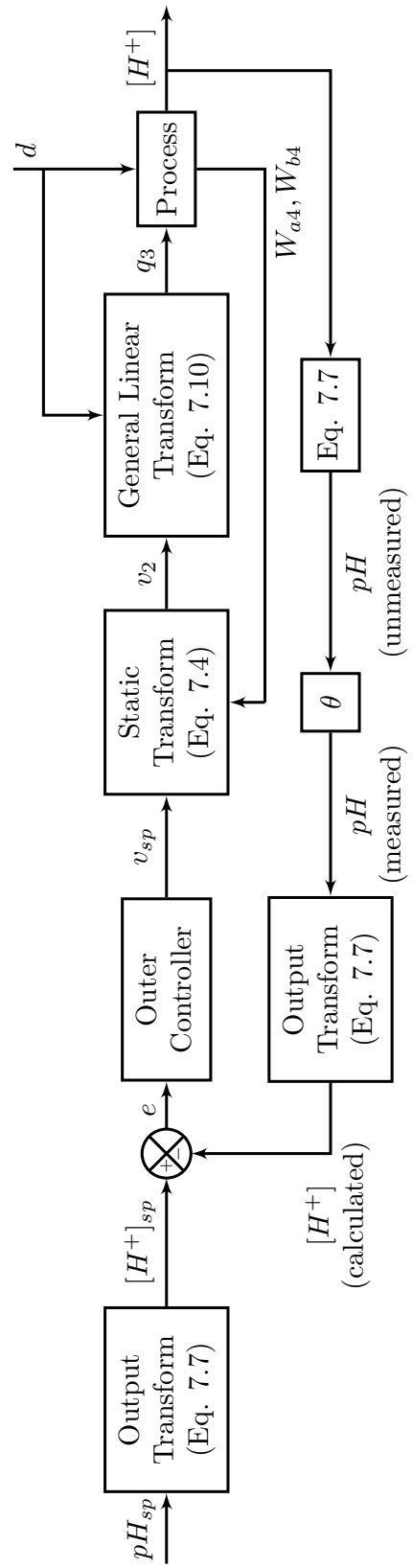


Figure 7.4: Chain of Transforms Block Diagram

### 7.2.2 Special Case

Due to the form of the equations describing the system, they can be manipulated and arranged in a different form. Considering Eq. 7.4 to calculate [H$^+$]; if the first two terms, containing $W_{ai}$ and $W_{bi}$ are grouped together to create a new variable $W_i$, defined by Eq. 7.12. To exactly reproduce the equations, the coefficient $c_1$ must contain the actual [H$^+$], but the effect of using the set-point for [H$^+$] is also simulated for this case study.

$$W_i = W_{bi}\frac{\frac{K_{a1}}{[H^+]} + \frac{2K_{a1}K_{a2}}{[H^+]^2}}{1 + \frac{K_{a1}}{[H^+]} + \frac{K_{a1}K_{a2}}{[H^+]^2}} + W_{ai} = c_1 W_{bi} + W_{ai} \tag{7.12}$$

This means that Eq. 7.3a and 7.3b may be combined to give Eq. 7.13.

$$A_1 h_1 \frac{dW_4}{dt} = q_{1e}(W_1 - W_4) + q_2(W_2 - W_4) + q_3(W_3 - W_4) \tag{7.13}$$

This, therefore, gives a single internal variable to which a general linear transform can act on, rather than having both $W_{a4}$ and $W_{b4}$. The static transform may also be removed due to the fact that it has no dynamics. The system can then be arranged as Fig. 7.5, where the general linear transform is described by Eq. 7.14; $\mathcal{T} = -1/A$ and $A$ is the same as above. The alternative form of the general linear transform is used as this allows easier set-point manipulation with no controller. This is a much simpler implementation than the generic transformed structures in Fig. 7.2 and 7.4. From hereon it is defined as the 'combined' system.

$$v_{L0} = \mathcal{T}\frac{dW_4}{dt} + W_4 = \mathcal{T}\frac{q_{1e}(W_1 - W_4) + q_2(W_2 - W_4) + q_3(W_3 - W_4)}{A_1 h_1} + W_4 \tag{7.14}$$

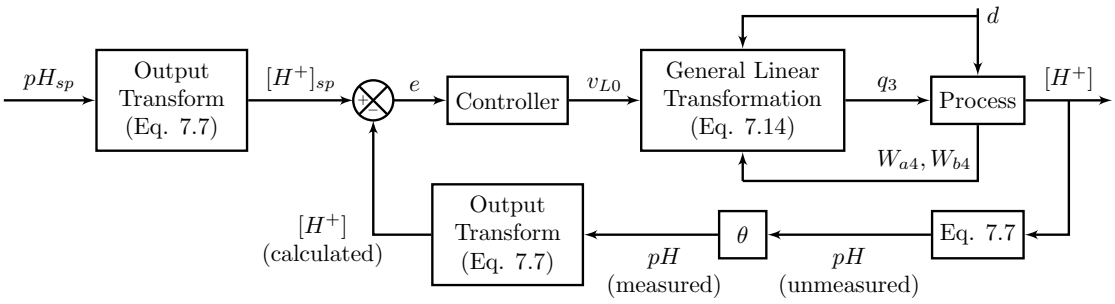


Figure 7.5: Special Case Block Diagram

### 7.2.3 Controller Tuning

Controllers were tuned using SIMC rules (Skogestad, 2003). All fitted models from open-loop responses and tuning parameters can be seen summarised in Table 7.2. All open-loop response graphs can be found in Appendix A.4.

Table 7.2: Process and Tuning Parameters for all pH Cases. (Chain and Combination require only one controller, values with no units are dimensionless)

| Case | Controller | $K$ | $\tau$ | $\tau_c$ | $K_c$ | $\tau_I$ |
|---|---|---|---|---|---|---|
| General | Inner | $0.12\,s^{-1}$ | $78.07\,s$ | $85\,s$ | $7.65\,s^{-1}$ | $78.07\,s$ |
| | Outer | 1 | $93.4\,s$ | $150\,s$ | 0.58 | $93.4\,s$ |
| Alternative on $W_{a4}$ | Inner | $88.62\,s$ | $88.62\,s$ | $105\,s$ | $9.5 \times 10^{-3}\,s^{-1}$ | $88.62\,s$ |
| | Outer | 1 | $90.4\,s$ | $500\,s$ | 0.18 | $90.4\,s$ |
| Alternative on $W_{b4}$ | Inner | $88.62\,s$ | $88.62\,s$ | $105\,s$ | $9.5 \times 10^{-3}\,s^{-1}$ | $88.62\,s$ |
| | Outer | 1 | $24.2\,s$ | $500\,s$ | $9.5 \times 10^{-3}$ | $24.2\,s$ |
| Chain | - | 1 | $131.81\,s$ | $100\,s$ | 1.32 | $131.81\,s$ |
| Combination | - | 0.24 | $91\,s$ | $75\,s$ | 5.06 | $91\,s$ |

## 7.3 Results

The results for the standard transformed simulations, that is those set out in Section 7.2.1, can be seen in Fig. 7.6.

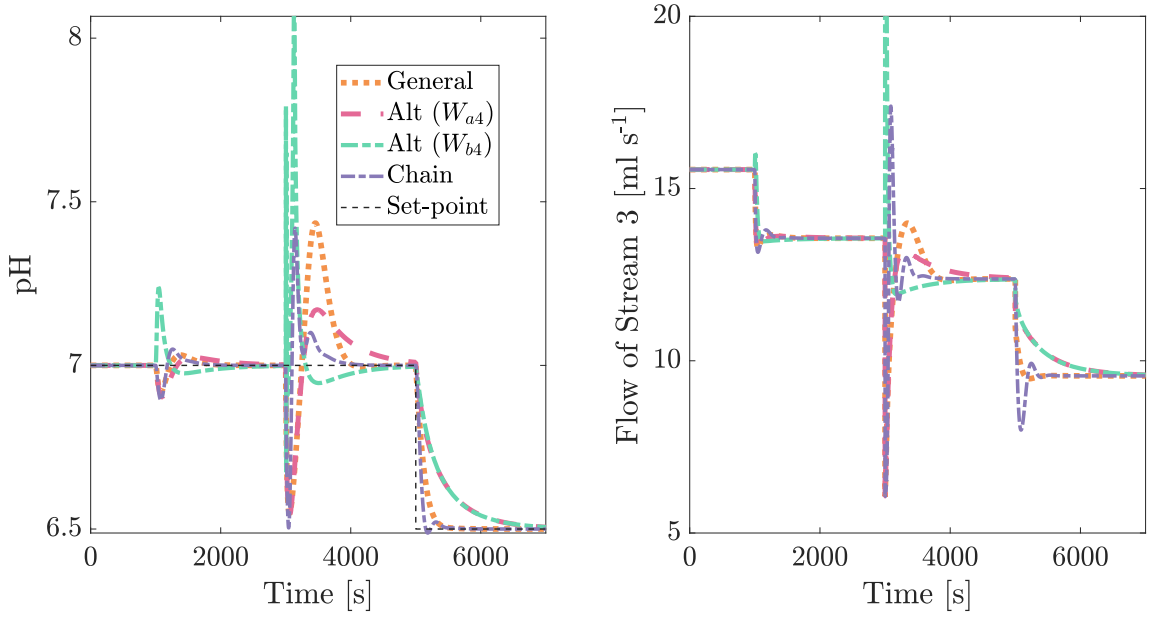


Figure 7.6: Response to disturbances and set-point changes for regular transformed systems. $\Delta q_1 = -2\ ml\,s^{-1}$ at $t = 1000\ s$; $\Delta q_2 = 0.65\ ml\,s^{-1}$ at $t = 3000\ s$; $\Delta pH_{sp} = -0.5$ at $t = 5000\ s$.

It can be seen that for the disturbance of $q_1$ at $t = 1000\ s$ the pH in all systems is perturbed, though the MV, $q_3$, has a step-like response. A perfect step is what would have been expected for perfect disturbance rejection. For the disturbance of $q_2$, a base with a stronger concentration than the acid of $q_1$, the response in the pH is not acceptable, particularly for the alternative cascade on $W_{b4}$. The MV response like-wise; a valve controlling this flow would not handle well. All systems do however return to steady-state. For a set-point change the systems respond well and more as expected in comparison to the disturbances.

For this system, perfect disturbance rejection would be expected since the disturbance directly affects only $W_{a4}$ and $W_{b4}$, and not $[H^+]$ directly. This is the same effect as seen for disturbance $T_1$ in the CSTR case study - it only directly affected $T$ and not $c_A$. Therefore, if $q_1$ and $q_2$ are measured then the control scheme should be able to change $q_3$ before any effects are propagated to the pH. However, this is not what is seen in these results. This is due to the fact that for all three systems the transforms specify values for the input, not taking into account other process variables will change. This is easiest explained when considering the alternative cascade structure, Fig. 7.3. The static equation outputs a set-point for $W_{a4}$, that is the value that $W_{a4}$ must be in order to keep the system at pH 7, assuming all other values in the static transform remain constant. Though all other values do not remain constant, as soon as $q_3$ changes in response to a disturbance, the value of $W_{b4}$ changes as well, and therefore changing the value of $W_{a4,sp}$ from the static equation. The hydrogen ion concentration also changes, affecting the static equation once again. The system, therefore, needs to rely more on the feedback loops in order to correct this, rather than the transform as desired. This also happens for the general cascade structure and the chain of transforms. The CV and MV vary more for the second disturbance, $q_2$, due to two reasons. The first is the fact that stream 1 enters a holding tank before entering the main tank, therefore $q_{1e}$ does not change in a perfect step. The second, and more important, is the fact that $q_2$ has a concentration ten times that of $q_1$. Therefore the system is more perturbed. The set-point change is dealt with well as this uses the feedback system rather than the transformed inputs in order to create a change.

The results for the cases where the equations are combined, as set out in Section 7.2.2, can be seen in Fig. 7.7. It can be seen that for all three cases there is perfect disturbance rejection. This is due to the fact that both $q_1$ and $q_2$ appear in the general linear transform for $W_4$. This encompasses both $W_{a4}$ and $W_{b4}$ and means that neither need be explicitly selected. This means that the MV makes step-changes in response to the disturbances, maintaining the pH at 7 as desired.

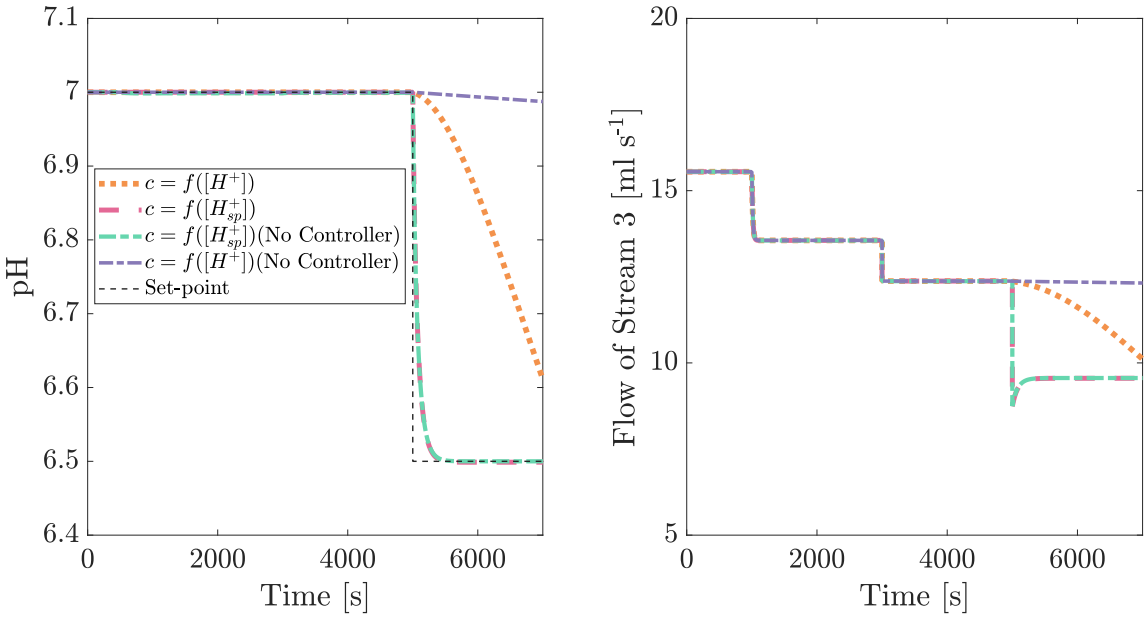


Figure 7.7: Response to disturbances and set-point changes for the combination transformed systems. $\Delta q_1 = -2\ ml/s$ at $t = 1000\ s$; $\Delta q_2 = 0.65\ ml/s$ at $t = 3000\ s$; $\Delta pH_{sp} = -0.5$ at $t = 5000\ s$.

For a set-point change, the two systems with $c = f([H^+_{sp}])$ respond better than the case where $c = f([H^+])$. The case where $c = f([H^+])$, with a controller, is oscillatory and doesn't settle until $t = 3 \times 10^5 s$ . The cases where $c = f([H^+])$ don't work well for the same reason as explained for the 'standard' transformed systems; as the value of $c$ changes, the output of the general linear transform changes, even if the input would remain constant. Therefore the feedback loop needs to compensate for this, which is not desired. It is also interesting that the case with no controller at all, i.e. changing set-point by changing the value of the transformed input directly, has an identical response to the system that does have a controller. Therefore this shows that the controller is theoretically not required for this system at all, assuming it is perfectly modelled. Though, due to the model mis-match problems as discussed in Chapter 6, a controller would be used in order to complete the feedback loop if required. This is confirmed in Fig 7.8c and 7.8d; these represent an unmeasured disturbance, i.e. the change in $q_1$ and $q_2$ does not enter the transform block, but still enters the process model. This means that the feedback loop is required. It is seen that for both cases the simulations with a controller perform better, and also when $c = f([H^+]_{sp})$.

From Fig. 7.8a and 7.8b it can be seen that most systems perform well for time delay in the measurements of $W_{a4}$, $W_{b4}$ and $h_2$. Perfect disturbance rejection is

almost achieved, the pH is kept within $4 \times 10^{-5}$ of set-point, for all cases except that for $c = f([H^+])$ with the controller. This system becomes unstable in the presence of the delay for the disturbance of $q_1$, which is not acceptable.

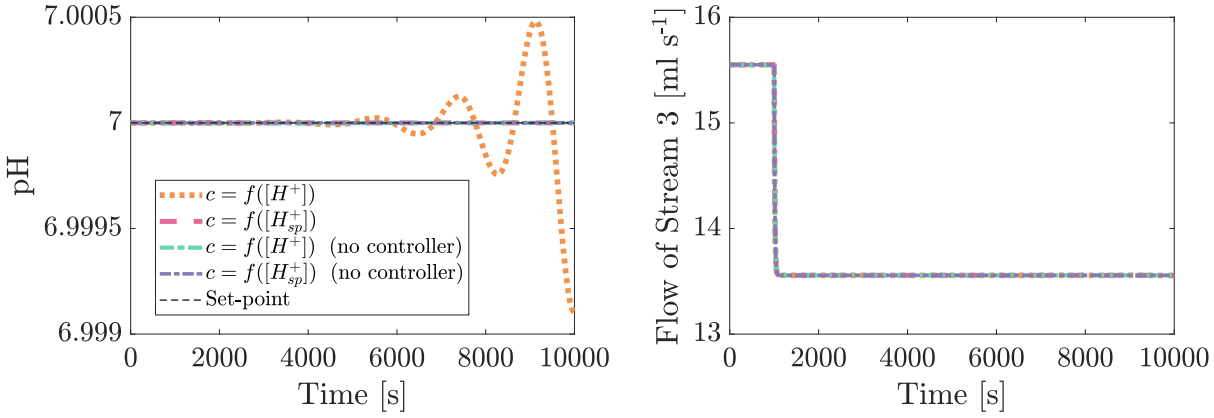


(a) Delay of $500s$: $\Delta q_1 = -2\ ml/s$ at $t = 1000\ s$

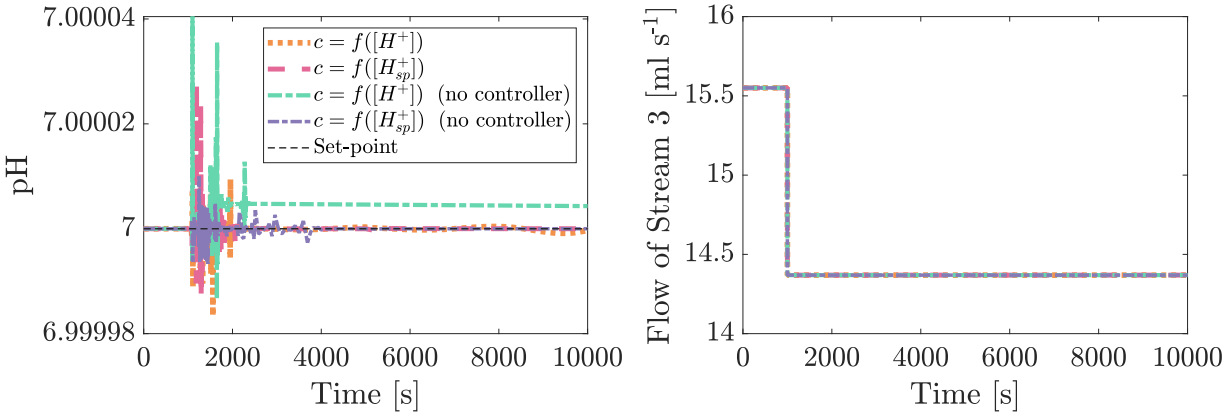


(b) Delay of $500s$: $\Delta q_2 = +0.65\ ml/s$ at $t = 1000\ s$

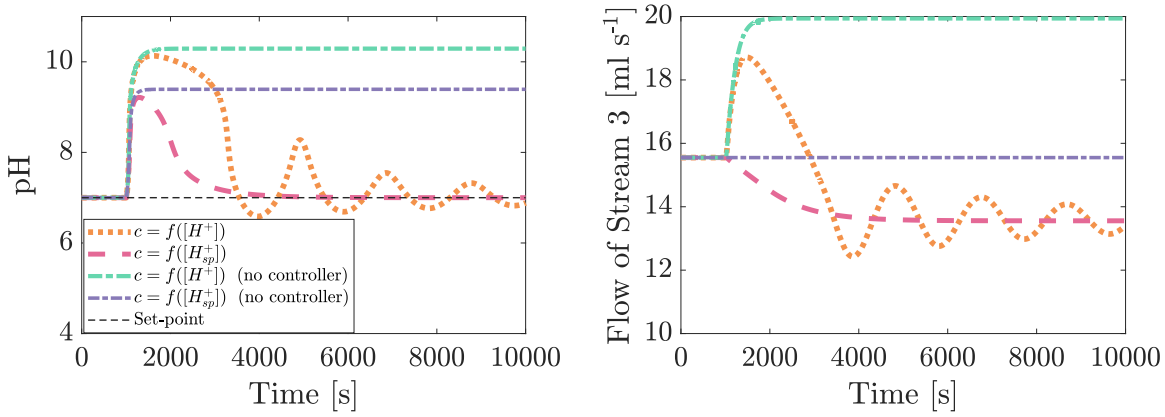


(c) Unmeasured Disturbance:$\Delta q_1 = -2\ ml/s$ at $t = 1000\ s$

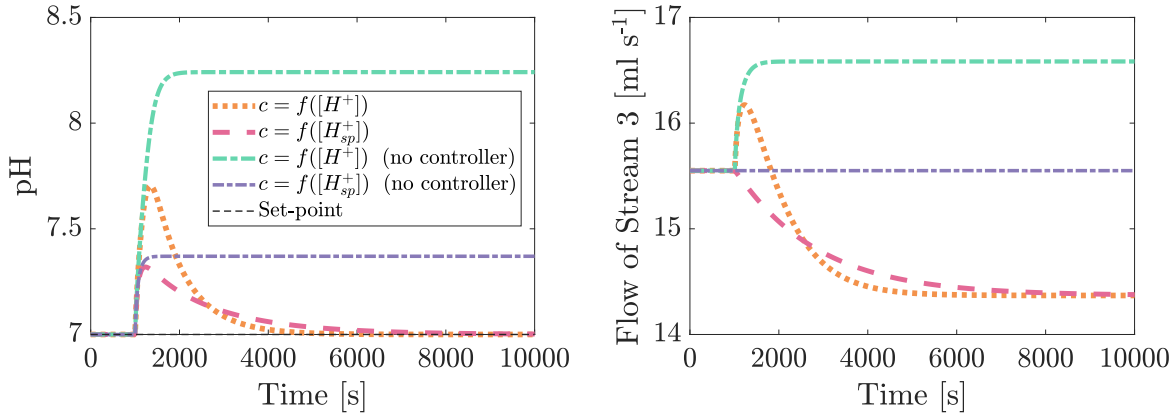


(d) Unmeasured Disturbance: $\Delta q_2 = +0.65\ ml\, s^{-1}$ at $t = 1000\ s$

Figure 7.8: Results for error and delay for pH system

## 7.4 Case Study Discussion

For this system, perfect disturbance rejection is expected as the disturbances only affect the internal variables. Applying the standard transformation procedure to the system does not satisfy this as there are multiple internal variables and one must be selected to base the system on. In this case, both $W_{a4}$ and $W_{b4}$. At nominal conditions, these are both of the order of magnitude $10^{-4}$ and therefore neither will have a substantially greater effect. Furthermore, if one of them had a stronger impact on the CV, i.e. a greater coefficient or order then it may be favourable to control this one and allow the other to 'catch-up'. In this case study, the CV is described by a static equation and the disturbances only directly affect the internal variables. The equations are also such that both internal variables may be combined to give another variable. These factors mean that perfect disturbance rejection is able to be achieved. Though, this is will not always be the case. From this it can be concluded that the transformation theory cannot be blindly applied to a system, it must be studied and understood properly in order to create a favourable control scheme.

Critically, this case study was originally simulated in order to study the possibility of using an 'output transform'. This was used since the measurement of pH is a nonlinear measurement, whereas this is easily converted to a linear measure, the hydrogen ion concentration. In this case, the output transform is well-known and simple to apply, but it can easily be extended to a more complex measurement. This simplifies the system, allowing the existing transformation theory to be applied and satisfactory control of the system.

# Chapter 8

# Case Study D: Chylla-Haase Reactor

This case study is an example of an applied industrial control problem. The Chylla-Haase Reactor is a multi-product semi-batch polymerization reactor set as a benchmark problem in order to compare different control schemes for this nonlinear system (Chylla and Haase, 1993). The aim of the benchmark problem is to keep the reactor temperature within a defined range ($\pm 0.6K$) by manipulating the valve position, which leads to the heating or cooling of the reactor jacket temperature. A short literature review of previously proposed methods is presented after the process model is introduced.

## 8.1 Process Model

Due to the abundance of equations to describe this system, only the key relations are presented in the main body, to provide an understanding of the process. Further relations and all nominal values are presented in Appendix C.

The system follows the flowsheet presented in Fig. 8.1, the symbols used are summarised in Table 8.1. Monomer is fed to the system at $t = 1800\,s$ and stopped at $t = 6000\,s$. The monomer reacts to form a polymer; a simple kinetic model is used as the temperature dynamics are the key aspect in this case study (Chylla and Haase, 1993). The polymerization reactor is heated/cooled by a jacket which is filled with either cooling water or steam, depending on the calculated valve position, $c$, which dictates the position of valve 1 and 2. The mass of monomer $m_M$, the mass of polymer $m_P$, the reactor temperature $T$, the jacket inlet temperature $T_j^{in}$ and the jacket outlet temperature $T_j^{out}$ are described by the ODEs in Eq. 8.1 - 8.5. Nomenclature used in these ODEs, and the corresponding equations are summarised in Table 8.1.

These models are based on data from an industrial pilot plant (Chylla and Haase, 1993).

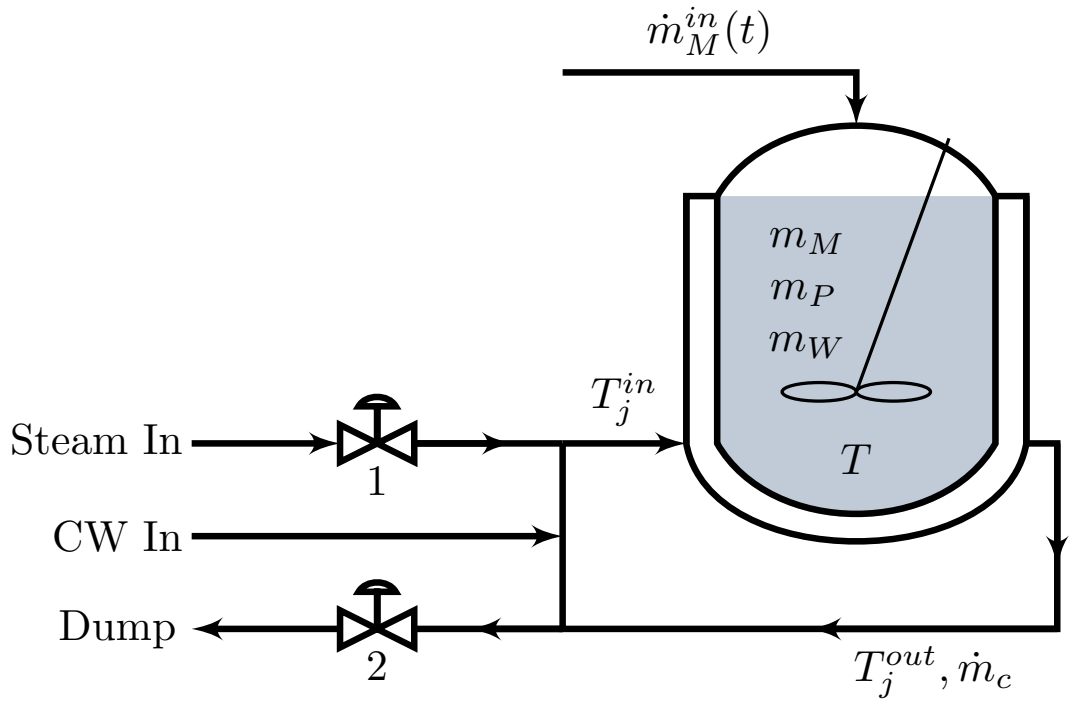


Figure 8.1: Chylla-Haase reactor (CW = cooling water). Adapted from (Graichen et al., 2006)

$$\frac{dm_M}{dt} = \dot{m}_M^{in}(t) + \frac{Q_{rea}}{\Delta H} \tag{8.1}$$

$$\frac{dm_P}{dt} = -\frac{Q_{rea}}{\Delta H} \tag{8.2}$$

$$\begin{aligned}\frac{dT}{dt} = \frac{1}{\sum_i m_i c_{P,i}} [&\dot{m}_M^{in}(t) c_{p,M}(T_{amb} - T) - UA(T - T_j) \\ &-(UA)_{loss}(T - T_{amb}) + Q_{rea}] \quad (i = M, P, W)\end{aligned} \tag{8.3}$$

$$\frac{dT_j^{in}}{dt} = \frac{dT_j^{out}(t - \theta_2)}{dt} + \frac{T_j^{out}(t - \theta_2) - T_j^{in}}{\tau_p} + \frac{K_p(c)}{\tau_p} \tag{8.4}$$

$$\frac{dT_j^{out}}{dt} = \frac{1}{m_C c_{p,C}} [\dot{m}_C c_{p,C}(T_j^{in}(t - \theta_1) - T_j^{out}) + UA(T - T_j)] \tag{8.5}$$

Table 8.1: Nomenclature and equations (if applicable) for Chylla-Haase Reactor ODEs.

| **Variable** | **Symbol** | **Unit** | **Equation** |
|---|---|---|---|
| Mass of monomer in reactor | $m_M$ | $kg$ | 8.1 |
| Mass of polymer in reactor | $m_P$ | $kg$ | 8.2 |
| Mass of water in reactor | $m_W$ | $kg$ | – |
| Temperature of reactor | $T$ | $K$ | 8.3 |
| Temperature of jacket inlet | $T_j^{in}$ | $K$ | 8.4 |
| Temperature of jacket outlet | $T_j^{out}$ | $K$ | 8.5 |
| Average jacket temperature | $T_j$ | $K$ | $C.1$ |
| Ambient temperature | $T_{amb}$ | $K$ | – |
| Heating/Cooling Function | $K_p(c)$ | $K$ | 8.6 |
| Heat of reaction | $Q_{rea}$ | $kW$ | $C.2$ |
| Overall heat transfer coefficient | $U$ | $kW\,m^{-2}\,K^{-1}$ | $C.9$ |
| Jacket heat transfer area | $A$ | $m^2$ | $C.8$ |
| Heat of polymerization | $\Delta H$ | $kJ\,kg^{-1}$ | – |
| Monomer inlet flow | $\dot{m}_M^{in}(t)$ | $kg\,s^{-1}$ | – |
| Coolant inlet flow | $\dot{m}_C$ | $kg\,s^{-1}$ | – |
| Specific heat capacity ($i$=monomer, polymer, coolant or water) | $c_{p,i}$ | $kJ\,kg^{-1}\,K^{-1}$ | – |
| Heat loss to surroundings coefficient | $(UA)_{loss}$ | $kW\,K^{-1}$ | – |
| Time delay 1 | $\theta_1$ | $s$ | – |
| Time delay 2 | $\theta_2$ | $s$ | – |
| Time constant for cooling/heating | $\tau_p$ | $s$ | – |

Special attention must be brought to the heating/cooling function, Eq. 8.6. Due to the fact that the jacket on the reactor is used for heating and cooling, depending if steam or cooling water is passed through it; the equation cannot be expressed as a single function over $c = [0,\ 100]$.

$$K_p(c) = \begin{cases} 0.8 \times 30^{(-c/50)}(T_{inlet} - T_j^{in}(t)) & c < 50\% \\ 0 & c = 50\% \\ 0.15 \times 30^{((c/50)-2)}(T_{steam} - T_j^{in}(t)) & c > 50\% \end{cases} \tag{8.6}$$

## 8.2 Control Scheme

The controlled variable in this case study was the reactor temperature, the manipulated variable is the valve position for the cooling/heating jacket. The disturbances to the system are not as explicit as previous case studies, but these are identified as;

- Initial monomer feed entry; the monomer feed enters the reactor at $t = 1800\ s$ and at ambient summer temperature. This cools the reactor since $T_{amb,S} < T_{set}$.

- Polymerization reaction; the exothermic polymerization reaction will heat the reactor. Meanwhile, the mass within the reactor is increasing due to monomer feed. The overall heat capacity is changing since quantities of monomer and polymer are changing, which both have different heat capacity.

- Monomer feed cessation; the monomer feed stops being fed to the reactor at $t = 6000\ s$. This stream has a cooling effect on the reactor as it enters at ambient temperature. The exothermic reaction will also cease shortly after this when all monomer is converted.

The reactor starts from the ambient summer temperature, $T_{amb,S}$, and follows the set-point governed by Eq. 8.7. This is supposed to guide the reactor to the correct temperature before the monomer starts being fed to the reactor. This benchmark problem states that the temperature is to stay within $\pm 0.6K$ of $T^*_{set}$ at all times.

$$T^*_{set} = \begin{cases} T_{amb,S} + (T_{set} - T_{amb,S}) \sum_{i=3}^{5} a_i (\frac{t}{1800})^i & t \leq 1800s \\ T_{set} & t > 1800s \end{cases} \tag{8.7}$$

### 8.2.1 Robustness

In the literature for this case study, there are a number of suggestions of possible parameter changes, or parameters that may not be accurately known, in order to test a system's robustness, these include;

- Time delays; there are already time delays incorporated into the measurement of the jacket temperatures, seen in Eqs. 8.4 and 8.5. Both $\theta_1$ and $\theta_2$ are predicted to change up to $\pm 25$ % from the nominal values of $\theta_1 = 22.8\ s$ and $\theta_2 = 15\ s$.

- Feed impurity factor; the feed impurity affects the rate of reaction within the reactor, indirectly affecting the temperature due to the exothermic reaction. This is expected to range from 0.8 to 1.2, where $i = 1$ is the nominal value. The value of $i$ is directly proportional to the rate of polymerisation and therefore also the reaction heat.

- Fouling factors; the reactor is proposed to be run five times before it is cleaned. After each batch there will be a degree of fouling on the walls of the reactor, impacting the heat transfer from the jacket. The fouling factor, $1/h_f\ [m^2\ K\ kW^{-1}]$, takes values of $[0.000, 0.176, 0.352, 0.528, 0.704]$ for batches 1-5 respectively.

- Ambient temperature; in the calculation for transformation it is assumed that the ambient temperature is the summer ambient temperature, $T_{amb,S}$. Clearly

this will not always be the case, and this will affect heat transfer to surroundings. The ambient temperature in summer, $T_{amb,S} = 305.282\ K$, and the ambient temperature in winter, $T_{amb,W} = 280.382\ K$.

### 8.2.2 Literature Review

This problem has been attempted many times in literature, many of which achieve the $\pm 0.6\ K$ error threshold, though they often bring a high degree of complexity to the problem. Most of the literature only covers the robustness in terms of a comparison between the first and fifth (most fouled) batch.

Helbig et al. (1996) make use of nonlinear MPC and an EKF to estimate the heat generated and the heat transfer coefficient. In a nominal case, both nonlinear MPC on its own and with an EKF kept the system within the error bounds. Although, even with the EKF added the reactor temperature varied outwith $\pm 0.6\ K$ when the process time constants are changed $+25\%$.

Clarke-Pringle and MacGregor (1997) proposed the use of a non-linear adaptive controller to adjust the jacket temperature, this controlled the system well at nominal conditions and then with an EKF robustness was provided and the system could deal with a fouled reactor.

Vasanthi et al. (2011) used a PI controller based on the jacket temperature error and also an artificial neural network (ANN) in order to estimate the heat generated and the heat transfer coefficient. This is used to give an estimate of the jacket temperature and is compared to the actual jacket temperature before corrective action is made. This was shown to stay within error bounds for both the first and the fifth batch. Furthermore, the same authors later proposed using the same control structure except using an Unscented Kalman filter (UKF) instead of the ANN (Vasanthi et al., 2012). Results for both ANN and UKF cases stay within $\pm 0.6\ K$ of reactor temperature error for the first and fifth batch. The UKF case had a lower IAE than the ANN for both the first batch and the fifth batch.

Li et al. (2014) achieve the best results seen in the literature for the Chylla-Haase benchmark problems in terms of error minimization. They use an ADRC method, along with an ESO, whereby they say the controller is model-free meaning a precise system model is not required. This, therefore, means that the robustness tests pose less of a threat. One of the proposed controllers is able to achieve below $\pm 0.2\ K$ reactor temperature error for both the clean reactor and the fouled reactor for batch

5. However, this method is more complicated, relative to the transformed input theory presented in this chapter and it appears that the control valve oscillates around $c = 50\%$ at all times, never reaching a steady value and alternating between heating and cooling.

Finkler et al. (2013) compare nonlinear MPC and a so-called "simple and efficient" optimizing control scheme are compared. The optimizing control scheme is an additional PI controller which alters the monomer flow into the reactor, which is indirectly able to control the temperature of the reactor. This is a change to the original benchmark problem as in all other literature the monomer flow is taken to be constant. The new control scheme keeps the reactor temperature within error bounds during the reaction, however once the monomer feed stops, and this degree of freedom is not available to control the system the reactor temperature deviates outwith the stipulated bounds. Similarly, Beyer et al. (2008) also state that a different monomer feed trajectory may improve control performance. However, they use the original stepped trajectory in simulations. They simulate a system using exact input/output linearization and a Sigma-Point Kalman filter to estimate the heat produced and the heat transfer coefficient online. Errors for both batches 1 and 5, in both summer and winter fall below $\pm 0.6\ K$.

Graichen et al. (2006) proposed an approach with some similarities to the theory used in this chapter. A feed-forward extension of cascade control was used along with an EKF to achieve online state estimation of the heat transfer coefficient and the reaction heat. The feed-forward aspect is inversion-based which incorporates the trajectories of the monomer and polymer flows into a numerically solvable equation to give a desired trajectory for the jacket temperature. This is shown to keep the temperature within the stipulated bound at all times for the nominal case. With the addition of the EKF, the system reaches the $\pm 0.6\ K$ error bound but does not cross it when all the robustness tests are applied.

### 8.2.3 Input Transformation Theory

#### 8.2.3.1 General Linear Transform

For this case study, the general cascade is used to control the system so that inversion of the transform is avoided. The control scheme follows Fig. 8.2.

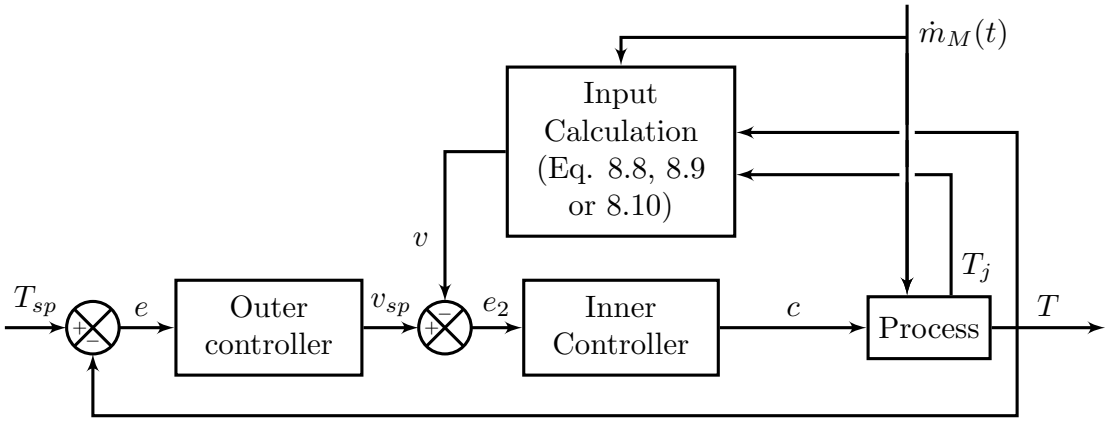


Figure 8.2: Control Scheme for Chylla-Haase Reactor

For the general linear transform, the calculation block contains Eq. 8.8. A second calculation block is not used in this case as the main disturbance to the system, $\dot{m}_M$ appears in the ODE for the output to the system, i.e. $\frac{dT}{dt}$, and as one of the key benefits of the transform is keeping the control scheme simple, this is unnecessary. For this case study, the tuning parameter for the transform is labelled $A_{tr}$ rather than $A$ as in previous cases, this is due to the fact $A$ is used in the original literature as the jacket heat transfer area.

$$\begin{aligned} v = \frac{1}{\sum_i m_i c_{P,i}} [\dot{m}_M^{in}(t) c_{p,M}(T_{amb} - T) - UA(T - T_j) \\ -(UA)_{loss}(T - T_{amb}) + Q_{rea}] - A_{tr}T \quad (i = M, P, W) \end{aligned} \tag{8.8}$$

Where,

$$A_{tr} = \left(\frac{df}{dT}\right)^* = 0.61\, s^{-1}$$

In all other case studies, the value of $A$ when calculated as $(df/dy)^*$ has been negative - which is not the case here. As it is unknown if the system will be able to cope with this, another system is simulated, where $A_{tr} = -1/220\, s^{-1}$, that is the negative reciprocal of ten times the largest delay in the system.

#### 8.2.3.2 Integrating and Static Transform

An integrating or static transform on this system follows the same block diagram as the general linear transform, Fig. 8.2, except for the substitution of $v_{FL}$ and $v_0$ respectively, and with a different calculation block. The calculation block for the integrating system follows Eq. 8.9 rather than Eq. 8.8, and the static system solves Eq. 8.10 for $v_0$

$$v_{FL} = \frac{1}{\sum_i m_i c_{P,i}} [\dot{m}_M^{in}(t) c_{p,M}(T_{amb} - T) - UA(T - T_j) \\ -(UA)_{loss}(T - T_{amb}) + Q_{rea}] \quad (i = M, P, W) \tag{8.9}$$

$$0 = \frac{1}{\sum_i m_i c_{P,i}} [\dot{m}_M^{in}(t) c_{p,M}(T_{amb} - v_0) - UA(v_0 - T_j) \\ -(UA)_{loss}(v_0 - T_{amb}) + Q_{rea}] \quad (i = M, P, W) \tag{8.10}$$

### 8.2.4 Controller Parameters

This system never reaches a true steady-state until the feed is stopped, at which point it is essentially a static single tank. The three key stages to the process occur at start-up, at the point of monomer flow and at the point of the cessation of monomer flow. Trying to undertake a step-response at any of these stages is not possible since there will always be dynamics, and all three would give different results. For this reason, it was decided to use a trial-and-error approach for controller parameters, tuning for each simulation until the best case is found. For the simple feedback-only case the controller parameters from Graichen et al. (2006) were used in order to validate simulations were running correctly. All controller parameters can be found in Table 8.2.

Table 8.2: Process and Tuning Parameters for all Chylla-Haase Reactor Simulations (Values with no units are dimensionless)

| **Case** | **Controller** | $K_c$ | $\tau_I$ |
|---|---|---|---|
| General ($A_{tr} = 0.61\,s^{-1}$) | Inner | $50\,s\,K^{-1}$ | $500\,s$ |
| | Outer | $120\,s^{-1}$ | $6 \times 10^4\,s$ |
| General ($A_{tr} = -1/220\,s^{-1}$) | Inner | $7.22 \times 10^3\,s\,K^{-1}$ | $160\,s$ |
| | Outer | $2 \times 10^{-3}\,s^{-1}$ | $220\,s$ |
| Static | Inner | $116\,K^{-1}$ | $475\,s$ |
| | Outer | 80 | $0.3\,s$ |
| Integrating | Inner | $6 \times 10^4\,s\,K^{-1}$ | $5 \times 10^3\,s$ |
| | Outer | $3.3 \times 10^{-2}\,s^{-1}$ | $120\,s$ |
| Feedback Only | Inner | $20\,K^{-1}$ | $40\,s$ |
| | Outer | 4 | $20\,s$ |

## 8.3 Results

### 8.3.1 Normal Operation

The results for the case where only feedback is used to control the system can be seen in Fig. 8.3. From the valve position, Fig. 8.3b, and jacket temperature, Fig. 8.3c, the two points of monomer feed entry and cessation, at $t = 1800\ s$ and $t = 6000\ s$, can clearly be seen to disturb the system. It can be seen that the system never reaches a steady-state until the reaction has stopped at $t = 9000\ s$. From Fig. 8.3a the temperature appears to track the set-point reasonably well, although the problem states that the temperature must never move outwith $\pm 0.6\,K$ of the set-point. It can clearly be seen in Fig. 8.3d that this is not the case and peaks at almost $1.5\,K$ twice. Therefore this control scheme is not satisfactory.

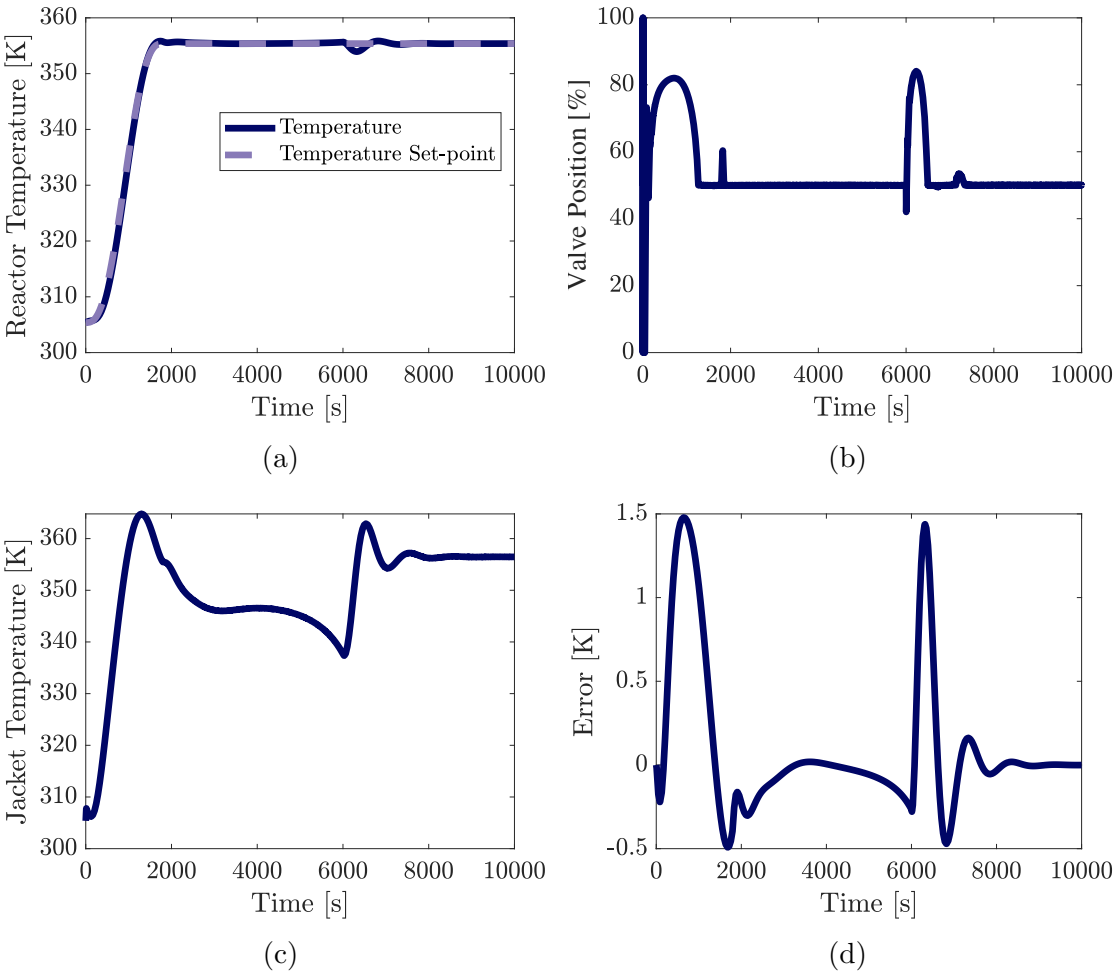


Figure 8.3: Results for Chylla-Haase Reactor with Feedback Only Cascade Control

The results for the general linear transform using the regular method to calculate the tuning parameter $A_{tr}$, i.e. $A_{tr} = (df/dT)^* = 0.61\,s^{-1}$, can be seen in Fig. 8.4. The error stays within the $\pm 0.6\,K$ band until $t = 6000\ s$, when the monomer feed ceases. From this point the system becomes unstable and the reactor temperature oscillates around 355 $K$. This is clearly not acceptable and means that this control scheme cannot be used. Before the oscillation the valve position follows a similar shape to the valve position for the feedback-only system, albeit with some extra oscillation which kept the error lower.

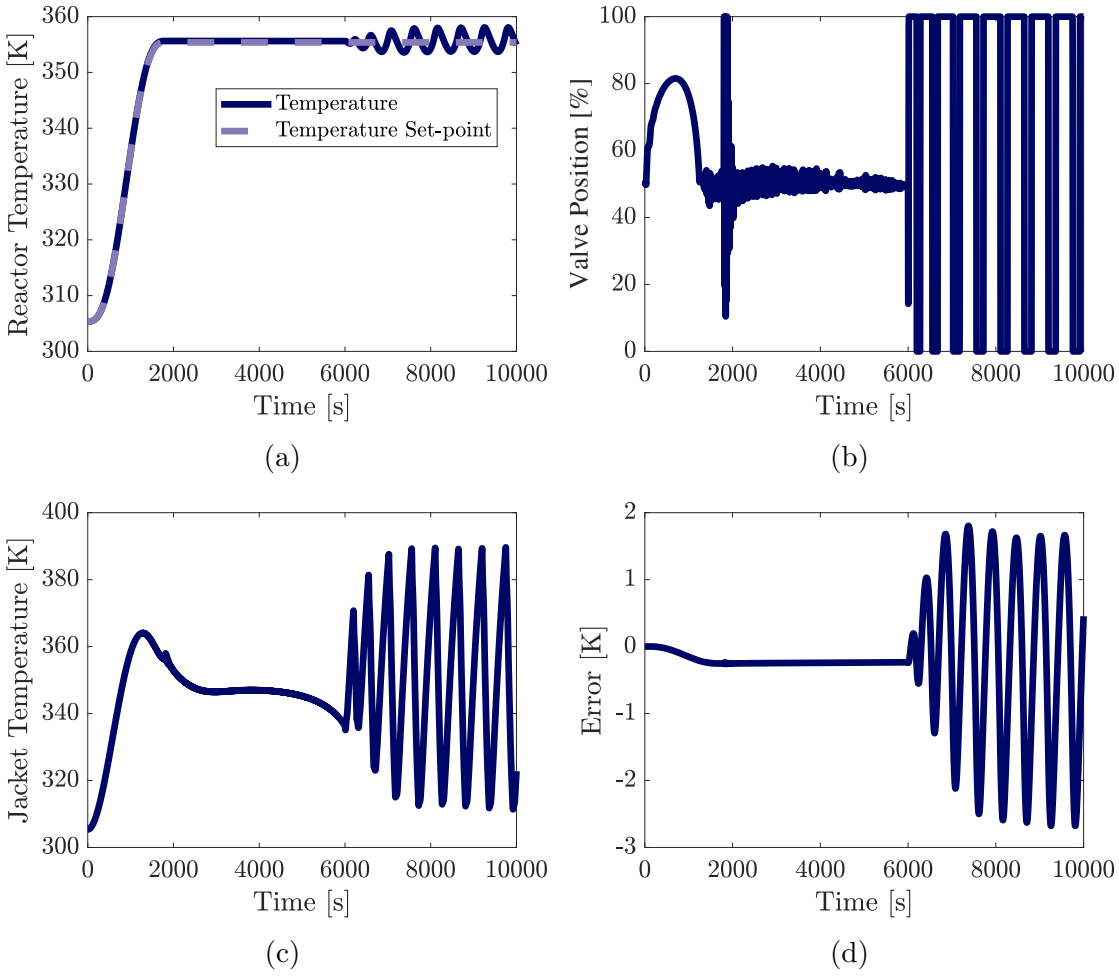


Figure 8.4: Results for Chylla-Haase Reactor with General Linear Transform ($A_{tr} = 0.61\,s^{-1}$)

The results for simulations with the static transform can be seen in Fig. 8.5. This is the first simulation that stays within the $\pm 0.6\ K$ limit, and peaks at an error of $0.4\ K$. This does however come at the cost of heavy valve oscillation after $t = 6000\ s$, though this settles after $2000\ s$, unlike the general linear transform. Throughout the reaction period ($1800\,s$ to $6000\,s$) the error is kept close to 0 too.

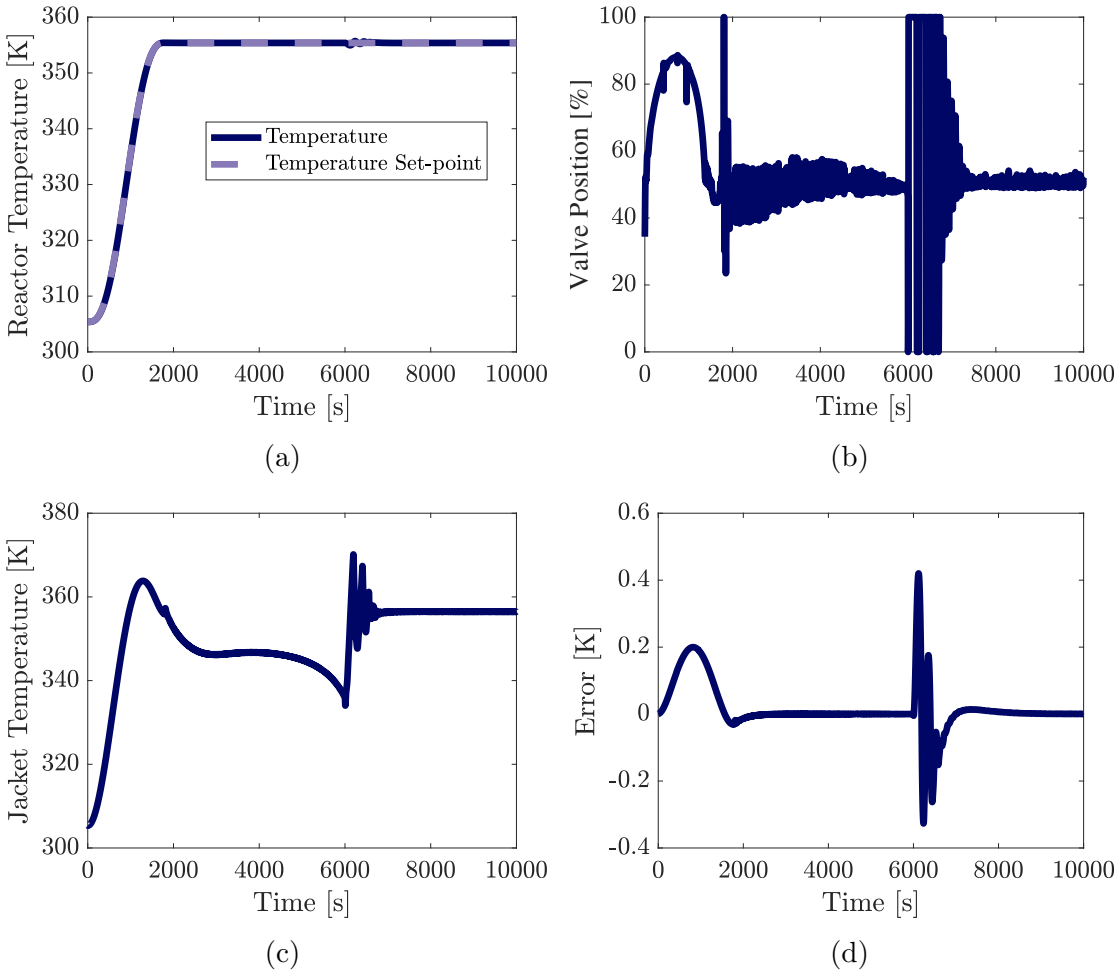


Figure 8.5: Results for Chylla-Haase Reactor with Static Transform

The results for the simulations with the integrating transform can be seen in Fig. 8.6. The error peaks at a value of $0.34K$, within the provided bounds by almost half. For this case there is a lot less oscillation seen in the valve position and the jacket temperature after the monomer feed has ceased. The error settles to 0 by $t = 6700\ s$ too.

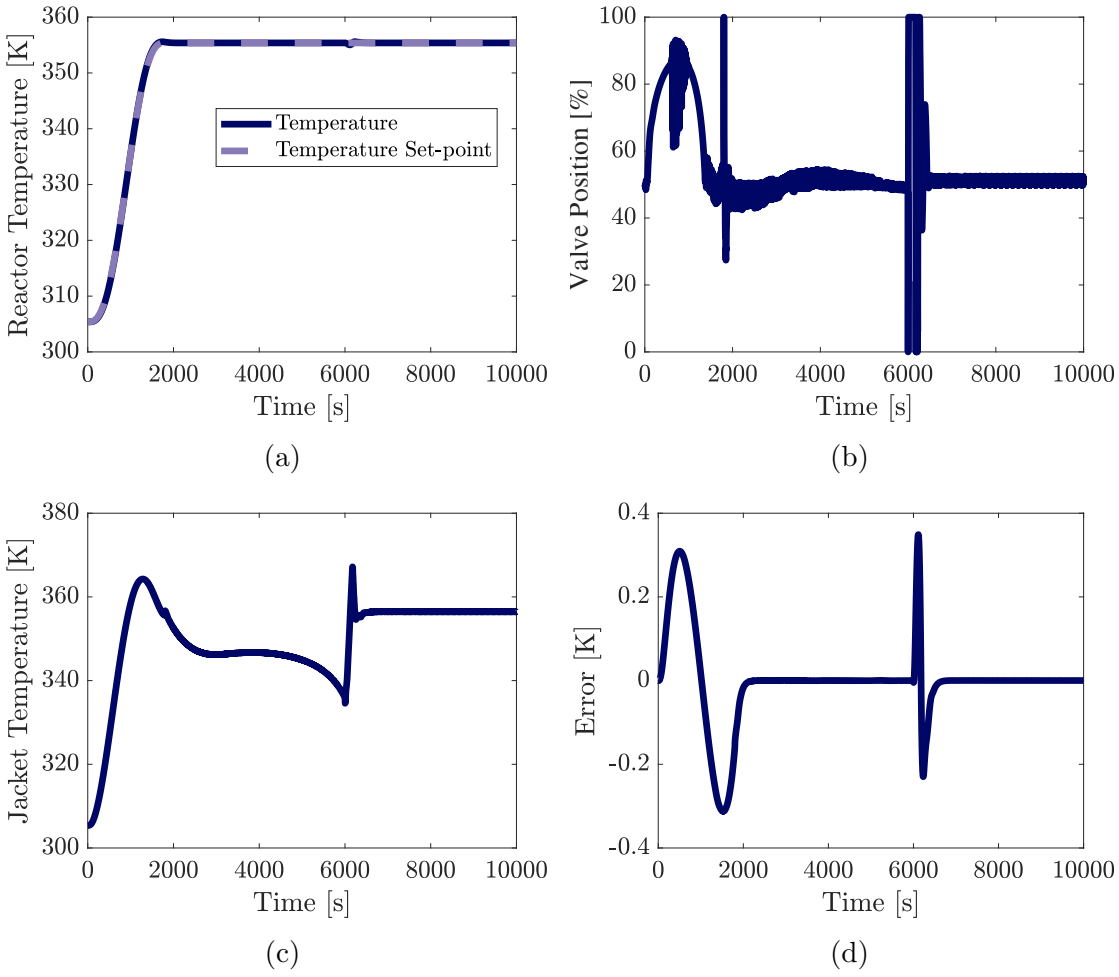


Figure 8.6: Results for Chylla-Haase Reactor with Integrating Transform

The simulation results for the general linear transform where the $A_{tr} = -1/220\,s^{-1}$ can be seen in Fig. 8.7. For this case it can clearly be seen from the reactor temperature graph, Fig. 8.7a, the system does not track the set-point as accurately as the other systems. This is reflected in the error graph, Fig. 8.7d, where the error peaks at $19K$ - clearly outwith the desired $\pm 0.6K$ range and therefore unacceptable. A zoomed-in version of the error graph, with the accepted error bound as the y-axis, can be seen in Fig. 8.8. From this it can clearly be seen that for the general linear transform with $A_{tr} = -1/220\,s^{-1}$ that the system actually still responds well to the cessation of monomer flow at $t = 6000\ s$, which acts as a disturbance. Therefore for this system, it can be seen that it responds well to disturbances but does not track a set-point change as accurately as required.

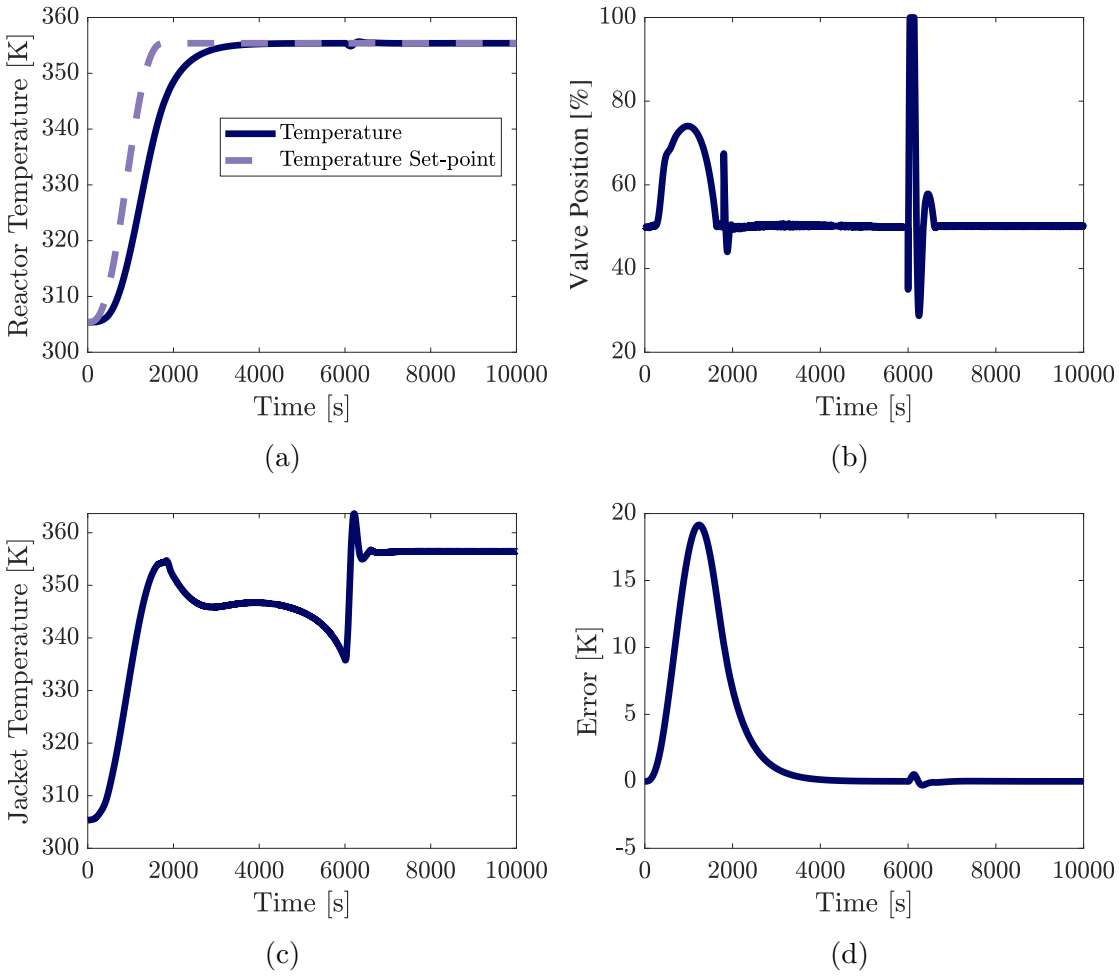


Figure 8.7: Results for Chylla-Haase Reactor with General Linear Transform ($A_{tr} = -1/220$)

The errors for all cases are summarised in Fig. 8.8. For the system to be 'acceptable', the error must stay within the plotted y-axis limits at all times. Therefore, by this measure the cascade control and both general linear transforms are not acceptable. Both the static and integrating systems fulfil requirements. However, it must be

noted that for the general linear transform with $A_{tr} = -1/220\,s^{-1}$ that for a similar error around $t = 6000\ s$, there is much less valve oscillation - clearly also a desirable outcome. Out of the static and integrating systems, the integrating transform had the least oscillation.

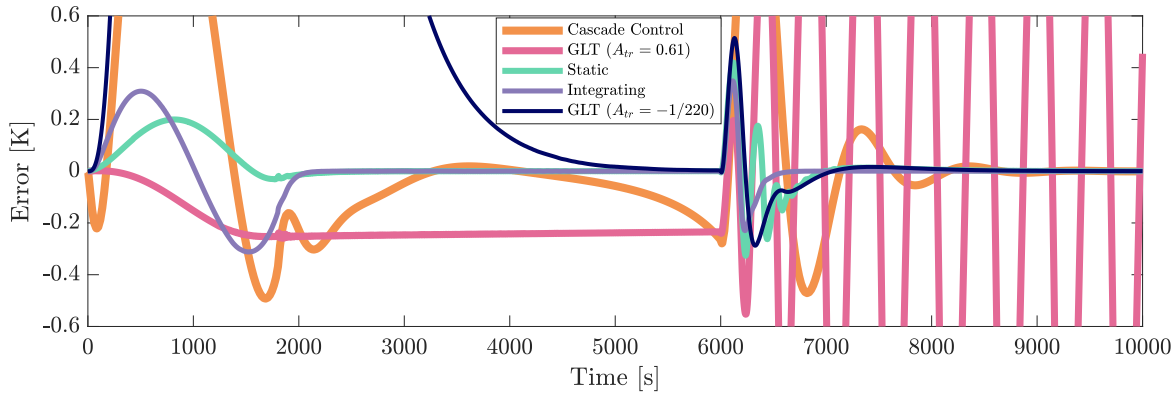


Figure 8.8: Summary of errors. ($\pm 0.6\ K$ is the accepted error bound)

### 8.3.2 Robustness

In order to measure the robustness of the systems, the integral absolute error (IAE) is used. This is calculated by $IAE = \int_0^\infty \mid e(t) \mid dt$, where $e(t) = T^*_{set} - T$. IAE values for the robustness tests set out in Section 8.2.1 can be seen in Table 8.3. The GLT case has $A_{tr} = -1/220\,s^{-1}$ rather than $A_{tr} = 0.61\,s^{-1}$ due to the stability concerns seen above.

Table 8.3: IAE Values for Robustness Tests. († symbolises an unstable system)

| **Case** | **Parameter** | **Value Change** | **Unit** | **IAE** | | |
|---|---|---|---|---|---|---|
| | | | | **Static** | **Int.** | **GLT** |
| Base Case | – | – | – | 331.8 | 444.4 | $2.52 \times 10^4$ |
| 1 | $\theta_1$ | $22.8 \rightarrow 17.1$ | $s$ | 331.8 | 444.4 | $2.52 \times 10^4$ |
| 2 | $\theta_1$ | $22.8 \rightarrow 28.5$ | $s$ | 331.8 | 444.4 | $2.52 \times 10^4$ |
| 3 | $\theta_2$ | $15 \rightarrow 11.25$ | $s$ | 331.8 | 444.4 | $2.52 \times 10^4$ |
| 4 | $\theta_2$ | $15 \rightarrow 18.75$ | $s$ | 331.8 | 444.4 | $2.52 \times 10^4$ |
| 5 | $i$ | $1.0 \rightarrow 0.8$ | – | 278.4 | 443.6 | $2.62 \times 10^4$ |
| 6 | $i$ | $1.0 \rightarrow 1.2$ | – | 381.0 | 484.6 | $2.50 \times 10^4$ |
| 7 | $1/h_f$ | $0.000 \rightarrow 0.176$ | $m^2K\,kW^{-1}$ | 365.1 | 527.0 | $2.50 \times 10^4$ |
| 8 | $1/h_f$ | $0.000 \rightarrow 0.352$ | $m^2K\,kW^{-1}$ | 348.7 | 609.8 | $2.50 \times 10^4$ |
| 9 | $1/h_f$ | $0.000 \rightarrow 0.528$ | $m^2K\,kW^{-1}$ | 409.3 | 695.1 | $2.55 \times 10^4$ |
| 10 | $1/h_f$ | $0.000 \rightarrow 0.704$ | $m^2K\,kW^{-1}$ | 431.3 | 781.8 | $2.64 \times 10^4$ |
| 11 | $T_{amb}$ | $305.382 \rightarrow 280.382$ | $K$ | $2.45 \times 10^5$† | $1.20 \times 10^5$† | $9.02 \times 10^4$ |

A lower value of IAE symbolises better performance. It can be seen that for all systems a change in delay, Cases 1-4, does not affect the IAE. This is thought to be due

to the fact that neither delay terms, $\theta_1$ or $\theta_2$, appear in the transform. Furthermore, as these are small delays relative to the time the system runs for, i.e. 10000 $s$, they do not have much impact on the feedback loop either.

For all feed impurities and the fouling factors cases, except Case 5, the IAE for the static and integrating cases increase compared to the base case. Increasing the fouling factor means that the overall heat transfer coefficient will decrease, and therefore less heat will be conducted from the jacket to the reactor. The transform will calculate the amount of heat required at 'clean' conditions, and therefore under-calculate the amount actually required. This will be corrected by the feedback loop. Interestingly, in Case 5 it is seen that the IAE decreases for the static and integrating systems. Decreasing the impurity factor for the system means that the reaction rate in the reactor is lower, and therefore the rate that heat is expelled from the reaction is lower too. It is expected that this makes the most impact at the point where the monomer feed ceases. A lower rate of heat production by the reaction is equivalent to a smaller disturbance impacting the system when it is withdrawn, and therefore it is easier for the control system to correct it.

Some of the IAE results for the general linear transform are the opposite of what is expected; an increase from the Base Case in Case 5, and a decrease in Cases 6-8. The IAE values are around two orders of magnitude larger than the other two transforms, and from Figs. 8.7d and 8.8 it can be seen that around $t = 6000\,s$ the error is low. Therefore, it may be concluded that the majority of the error contribution takes place during the start-up and reaction phases, rather than during the monomer cessation period of the other two transforms and therefore it is hard to compare them. For example, for Case 6 the IAE value is seen to decrease from the Base Case, meaning that the error is lower. This may be explained by the fact that a larger value of $i$ means that the rate of heat expelled from the reaction is higher. The GLT case struggled to match the set-point in the initial stages when the monomer is added, seen in Fig. 8.7a, and therefore if more heat is produced, the reactor heats up faster and assists the control scheme reach the set-point, reducing the error and IAE.

The change in the ambient temperature has the most profound effect on all three systems, although interestingly the general linear transform still remains stable. The ambient temperature appears directly in the transformed equation and therefore has an important impact. Although, in a real-life scenario out of the four robustness tests the ambient temperature is the easiest to measure. Therefore the measurement could possibly be included in the transform in order to avoid the instability.

## 8.4 Case Study Discussion

From this more applied, industrial case study some limitations have been identified. Firstly, choosing $A_{tr} = (df/dy)^*$ will not always work. In this case, applying this gave a positive $A_{tr}$ value - in the past case studies, where ODEs were derived from mass and energy balances where the controlled variable for the system was always the 'out' term. This meant that when the ODE was differentiated with respect to $y$ it was always negative. In Chapter 3 it was shown that for the transfer function $G(s) = y(s)/v(s)$ the gain and time constant of the system were equal to $-1/A_{tr}$. Therefore with a positive value of $A_{tr}$ a right-hand plane pole is created - giving rise to an unstable system. This is exactly what was seen in the simulations with instability after $t = 6000\ s$. This is the reason a negative value of $A_{tr}$ was chosen - giving rise to a stable system. This value of $A$ is also able to be used as a tuning parameter for the system.

The complexity in the process model for this system resulted in extra complexity in trying the transform the inputs to the system. The jacket temperature, i.e. the internal variable, was not able to be directly controlled and meant the general cascade control structure had to be used rather than the alternative cascade control structure. The fact that the jacket was able to both heat and cool the reactor also caused problems - meaning at valve positions less than 50% steam was injected whereas at valve positions more than 50% cooling water was injected. This means that, ideally, separate transforms would be required depending if the system required heating or cooling - though this deviates from the simplicity of the theory in the first place.

It has been seen for this case study that the transformation theory has not worked as well as for other case studies, though it has still been shown to perform better than the basic cascade control, and in a much simpler manner than other cases which are seen in literature. Both the static and integrating transforms have been able to stay within the $\pm 0.6\ K$ limit and may be seen as viable alternatives for systems with $A > 0$.

# Chapter 9

# Conclusion

This thesis has shown the application of the new input transformation method for controlling nonlinear processes in a cascaded manner. If the previous assumptions of the theory are breached, i.e. if the system has a relative order greater than one and/or the system is not invertible, then the new input transformation method can still be used if applied with cascade control. This has been achieved in a simple manner that is easy to implement, especially in comparison to other nonlinear control techniques.

Throughout, different control configurations have been simulated, namely the general cascade structure, the alternative cascade structure, the 'double-linearized' cascade structure and the chain of transforms - comparisons have been shown in Chapter 4 and 6. All have proved to give a stable system, and will give similar results for most systems - especially the general cascade structure and the alternative cascade structures, which were directly compared in Chapter 4 (Fig. 4.4). The choice between the general or alternative structure depends on the system. For a system that is not invertible, and to avoid numerical solvers the general structure should be used. However, the alternative cascade is a more intuitive option, with both controllers acting on realisable variables. This means that controller tuning may be easier if a model is known.

In Chapter 5 it was shown that the theory is able to be adapted to suit systems where not all process variables are known - namely the internal variable which the cascade usually relies on. This was a key assumption in the original theory. In industry this may be a common occurrence for variables that cannot be measured, or it is not economical to measure them, and therefore being able to adapt the control structure to suit this is important - a problem that not all other nonlinear techniques can handle.

Both the double-linearized structure and the chain of transforms were shown, in

Chapter 6 (Fig. 6.6), to have the capability of perfect disturbance rejection for special cases where the disturbance appears directly in the model equation for the internal variable, rather than that of the controlled variable. For this case, the general cascade structure and the alternative cascade structures are able to tend towards perfect disturbance rejection for a fast inner loop. If the special case is not met then the simpler option of the general or alternative cascade may be used over the chain of transforms or double-linearized structures.

This control method is model-based but not completely model-reliant as it has robustness to model mis-match. As shown in Chapter 6 and 7, the new input transformation theory is able to handle cases of unmeasured disturbances and unexpected time delay when the outer controller is used (Fig. 6.8 and 7.8). This is an important factor as it means that the control structure is able to operate without a completely accurate process model - which is not normally known. For this to be achieved the outer feedback loop must be utilised so that the outer PI controller is able to correct the system back to its set-point. The cascade control works for all cases, and is more robust than the simple case which only has one calculation block and one feedback loop.

Although mainly focused on systems that are nonlinear in the inputs, the new theory has also been shown to work for systems that are nonlinear in the outputs. pH control, shown in Chapter 8, is a difficult task due to the nonlinearities of its measurement. Through the use of a simple output transformation, the existing transformed input theory is able to be easily applied and achieve both disturbance rejection and set-point tracking.

## 9.1 Future Work

This thesis has studied single-input single-output (SISO) systems with a relative order greater than one. In reality, many systems will be multiple-input multiple-output (MIMO). Bjorvand (2020) has previously studied transformed manipulated variables for MIMO systems which had relative orders of one, which showed the possibility of decoupling between variables. Perfect disturbance rejection was exhibited for perfect models too. The natural progression for this thesis would be to assess the capability of the application of Transformed Manipulated Variables to MIMO systems that have relative order(s) greater than one. It is anticipated that there would be a degree of interference between the variables and perfect disturbance would be lost. Decoupling may be possible, depending on the system.

# Bibliography


Ahlgren, T. D. and Stevens, W. F. (1971). "Adaptive control of a chemical process system". In: *AIChE Journal* 17.2, pp. 428–435. ISSN: 15475905. DOI: 10.1002/aic.690170235.

Anandanatarajan, R., Chidambaram, M., and Jayasingh, T. (2006). "Limitations of a PI controller for a first-order nonlinear process with dead time". In: *ISA Transactions* 45.2. ISSN: 00190578. DOI: 10.1016/S0019-0578(07)60189-X.

Aslam, F. and Kaur, G. (2011). "Comparative analysis of conventional, P, PI, PID and fuzzy logic controllers for the efficient control of concentration in CSTR". In: *International journal of computer applications* 17.6, pp. 12–16.

Åström, K. J. and Wittenmark, B. (2008). *Adaptive control*. Courier Corporation. ISBN: 0486319148.

Bastin, G. and Dochain, D. (1990). *On-line Estimation and Adaptive Control of Bioreactors*. Elsevier. DOI: 10.1016/c2009-0-12088-3.

Bequette, B. W. (July 1991). "Nonlinear Control of Chemical Processes: A Review". In: *Industrial and Engineering Chemistry Research* 30.7, pp. 1391–1413. ISSN: 15205045. DOI: 10.1021/ie00055a001. URL: https://pubs.acs.org/doi/abs/10.1021/ie00055a001.

Beyer, M. A., Grote, W., and Reinig, G. (2008). "Adaptive exact linearization control of batch polymerization reactors using a Sigma-Point Kalman Filter". In: *Journal of Process Control* 18.7-8, pp. 663–675. ISSN: 09591524. DOI: 10.1016/j.jprocont.2007.12.002.

Bjorvand, S. (2020). *Control Structures with Embedded Process Knowledge*. Tech. rep. NTNU. URL: https://folk.ntnu.no/skoge/diplom/diplom20/simen-bjorvand/thesis.pdf.

Bošković, D. M. and Krstić, M. (2002). "Backstepping control of chemical tubular reactors". In: *Computers and Chemical Engineering* 26.7-8, pp. 1077–1085. ISSN: 00981354. DOI: 10.1016/S0098-1354(02)00026-1.

Brown, A. and Zhang, J. (2014). "Active disturbance rejection control of a neutralisation process". In: *Computer Aided Chemical Engineering*. Vol. 33. Elsevier B.V., pp. 739–744. DOI: 10.1016/B978-0-444-63456-6.50124-1.

Chabni, F., Taleb, R., Benbouali, A., and Amin, M. (2016). "The Application of Fuzzy Control in Water Tank Level Using Arduino". In: *International Journal of Advanced Computer Science and Applications* 7.4. ISSN: 2158107X. DOI: 10.14569/ijacsa.2016.070432.

Chen, L., Bastin, G., and Van Breusegem, V. (1995). "A case study of adaptive nonlinear regulation of fed-batch biological reactors". In: *Automatica* 31.1, pp. 55–65. ISSN: 00051098. DOI: 10.1016/0005-1098(94)00068-T.

Chen, Z., Zheng, Q., and Gao, Z. (2007). "Active disturbance rejection control of chemical processes". In: *Proceedings of the IEEE International Conference on Control Applications*, pp. 855–861. ISBN: 1424404436. DOI: 10.1109/CCA.2007.4389340.

Chylla, R. W. and Haase, D. R. (1993). "Temperature control of semibatch polymerization reactors". In: *Computers and Chemical Engineering* 17.3, pp. 257–264. ISSN: 00981354. DOI: 10.1016/0098-1354(93)80019-J.

Clarke-Pringle, T. and MacGregor, J. F. (1997). "Nonlinear adaptive temperature control of multi-product, semi-batch polymerization reactors". In: *Computers and Chemical Engineering* 21.12, pp. 1395–1409. ISSN: 00981354. DOI: 10.1016/S0098-1354(97)00013-6.

Cohen, G. H. and Coon, G. A. (1953). "Theoretical consideration of retarded control". In: *Trans. Asme* 75, pp. 827–834.

Desoer, C. A. and Lin, C. A. (1985). "Tracking and Disturbance Rejection of MIMO Nonlinear Systems with PI Controller". In: *IEEE Transactions on Automatic Control* 30.9. ISSN: 15582523. DOI: 10.1109/TAC.1985.1104078.

Finkler, T. F., Lucia, S., Dogru, M. B., and Engell, S. (2013). "Simple control scheme for batch time minimization of exothermic semibatch polymerizations". In: *Industrial and Engineering Chemistry Research* 52.17, pp. 5906–5920. ISSN: 15205045. DOI: 10.1021/ie302321k. URL: https://pubs.acs.org/doi/abs/10.1021/ie302321k.

Fogler, H. S. (2016). *Elements of chemical reaction engineering*. eng. Fifth edition.. Prentice-Hall international series in the physical and chemical engineering sciences. Boston: Prentice Hall. ISBN: 9780133887518.

Gao, Z., Huang, Y., and Han, J. (2001). "An alternative paradigm for control system design". In: *Proceedings of the IEEE Conference on Decision and Control* 5, pp. 4578–4585. ISSN: 01912216. DOI: 10.1109/CDC.2001.980926.

Graichen, K., Hagenmeyer, V., and Zeitz, M. (2006). "Feedforward control with online parameter estimation applied to the Chylla-Haase reactor benchmark". In: *Journal of Process Control* 16.7, pp. 733–745. ISSN: 09591524. DOI: 10.1016/j.jprocont.2006.01.001.

Hall, R. C. and Seborg, D. E. (1989). "Modelling and self-tuning control of a multivariable ph neutralization process part i: Modelling and multiloop control". In: *1989 American Control Conference*. IEEE, pp. 1822–1827.

Han, J., Yu, S., and Yi, S. (2019). "Oxygen excess ratio control for proton exchange membrane fuel cell using model reference adaptive control". In: *International Journal of Hydrogen Energy* 44.33, pp. 18425–18437. ISSN: 03603199. DOI: 10.1016/j.ijhydene.2019.05.041.

Han, J. (2009). "From PID to active disturbance rejection control". In: *IEEE Transactions on Industrial Electronics*. Vol. 56. 3, pp. 900–906. DOI: 10.1109/TIE.2008.2011621.

Hangos, K. M., Bokor, J., and Szederkényi, G. (Apr. 2006). "Feedback and Input-output Linearization of Nonlinear Systems". In: *Analysis and Control of Nonlinear Process Systems*. Springer-Verlag, pp. 227–251.

Helbig, A., Abel, O., M'hamdi, A., and Marquardt, W. (1996). "Analysis and nonlinear model predictive control of the Chylla-Haase benchmark problem". In: *IEE Conference Publication*. 427 /2. IEE, pp. 1172–1177. DOI: 10.1049/cp:19960719.

Henson, M. A. and Kurtz, M. J. (1995). "Feedback Linearizing Controller Design for Chemical Processes: Challenges and Recent Advances". In: *IFAC Proceedings Volumes* 28.14, pp. 167–172. ISSN: 14746670. DOI: 10.1016/s1474-6670(17)46825-x.

Henson, M. A. and Seborg, D. E. (1994). "Adaptive nonlinear control of a pH neutralization process". In: *IEEE transactions on control systems technology* 2.3, pp. 169–182. ISSN: 1063-6536.

Henson, M. A. and Seborg, D. E. (1997). *Nonlinear process control*. Prentice Hall PTR Upper Saddle River, New Jersey. ISBN: 013625179X.

Hua, C., Liu, P. X., and Guan, X. (2009). "Backstepping control for nonlinear systems with time delays and applications to chemical reactor systems". In: *IEEE*

*Transactions on Industrial Electronics* 56.9, pp. 3723–3732. ISSN: 02780046. DOI: 10.1109/TIE.2009.2025713.

Huang, H., Wu, L., Han, J., Feng, G., and Lin, Y. (2004). "A new synthesis method for unit coordinated control system in thermal power plant - ADRC control scheme". In: *2004 International Conference on Power System Technology, POWERCON 2004*. Vol. 1, pp. 133–138. ISBN: 0780386108. DOI: 10.1109/icpst.2004.1459980.

Isidori, A. (1995). *Nonlinear control systems*. eng. Third edition.. Communications and control engineering series. Berlin ; London: Springer. ISBN: 3540199160.

Jha, S., Karthika, S., and Radhakrishnan, T. (2017). "Modelling and control of crystallization process". In: *Resource-Efficient Technologies* 3.1, pp. 94–100. ISSN: 24056537. DOI: 10.1016/j.reffit.2017.01.002.

Kanellakopoulos, I., Kokotovic, P. V., and Morse, A. S. (Feb. 1992). "A toolkit for nonlinear feedback design". In: *Systems and Control Letters* 18.2, pp. 83–92. ISSN: 01676911. DOI: 10.1016/0167-6911(92)90012-H.

Khalil, H. K. (2002). *Nonlinear Systems*. Upper Saddle River, NJ: Prentice Hall. ISBN: 9780130675309.

Kokotović, P. V. (1992). "The Joy of Feedback: Nonlinear and Adaptive". In: *IEEE Control Systems* 12.3, pp. 7–17. ISSN: 1066033X. DOI: 10.1109/37.165507.

Li, D., Li, Z., Gao, Z., and Jin, Q. (2014). "Active disturbance rejection-based high-precision temperature control of a semibatch emulsion polymerization reactor". In: *Industrial and Engineering Chemistry Research* 53.8, pp. 3210–3221. ISSN: 08885885. DOI: 10.1021/ie402544n. URL: https://pubs.acs.org/doi/abs/10.1021/ie402544n.

Monroy-Loperena, R. and Alvarez-Ramirez, J. (2004). "Backstepping-based cascade control scheme for batch distillation columns". In: *AIChE Journal* 50.9, pp. 2113–2129. ISSN: 00011541. DOI: 10.1002/aic.10184.

Morari, M., Zafiriou, M., and Zafiriou, E. (1989). *Robust Process Control*. Prentice Hall. ISBN: 9780137821532.

Najim, K., Najim, M., Dahhou, B., Youlal, H., and Unbehauen, H. (1985). "Adaptive Control in Chemical Industry". In: *IFAC Proceedings Volumes* 18.9, pp. 47–53. ISSN: 14746670. DOI: 10.1016/s1474-6670(17)60258-1.

Nguyen, N. T. (2018). *Model-Reference Adaptive Control*. Advanced Textbooks in Control and Signal Processing. Cham: Springer International Publishing. ISBN:

978-3-319-56392-3. DOI: 10.1007/978-3-319-56393-0. URL: http://link.springer.com/10.1007/978-3-319-56393-0.

Nijmeijer, H. and Van der Schaft, A. (1990). *Nonlinear dynamical control systems*. Springer. ISBN: 978-0-387-97234-3.

Passino, K. M. and Yurkovich, S. (1998). *Fuzzy control*. Pearson. ISBN: 020118074X.

Patel, R., Deb, D., Dey, R., and E. Balas, V. (2020). "Model Reference Adaptive Control of Microbial Fuel Cells". In: *Adaptive and Intelligent Control of Microbial Fuel Cells. Intelligent Systems Reference Library*. Vol. 161. Springer, pp. 109–121.

Pitalúa-Díaz, N., Herrera-López, E., Valencia-Palomo, G., González-Angeles, A., Rodríguez-Carvajal, R., and Cazarez-Castro, N. (2015). "Comparative Analysis between Conventional PI and Fuzzy LogicPI Controllers for Indoor Benzene Concentrations". In: *Sustainability* 7.5, pp. 5398–5412. ISSN: 2071-1050. DOI: 10.3390/su7055398. URL: http://www.mdpi.com/2071-1050/7/5/5398.

Pivojika, P. (2000). "Analysis and design of fuzzy pid controller based on classical pid controller approach". In: *Advances in Soft Computing*. Vol. 6. Springer Verlag, pp. 186–199. URL: https://link.springer.com/chapter/10.1007/978-3-7908-1841-3_14.

Rivera, D. E., Morarl, M., and Skogestad, S. (1986). "Internal Model Control: Pid Controller Design". In: *Industrial and Engineering Chemistry Process Design and Development* 25.1, pp. 252–265. ISSN: 01964305. DOI: 10.1021/i200032a041. URL: https://pubs.acs.org/sharingguidelines.

Schipanov, G. V. (1939). *Theory and methods of designing automatic regulators*. Tech. rep., pp. 49–66.

Seborg, D. E., Mellichamp, D. A., Edgar, T. F., and Doyle III, F. J. (2010). *Process dynamics and control*. John Wiley & Sons. ISBN: 0470128674.

Sira-Ramirez, H., Luviano-Juarez, A., Remirez-Neria, M., and Zurita-Bustamante, E. W. (2017). *Active Disturbance Rejection Control of Dynamic Systems*. Elsevier. DOI: 10.1016/c2016-0-01983-6.

Skogestad, S. (2003). "Simple analytic rules for model reduction and PID controller tuning". In: *Journal of process control* 13.4, pp. 291–309. ISSN: 0959-1524.

Tyreus, B. D. and Luyben, W. L. (1992). "Tuning PI controllers for integrator/dead time processes". In: *Industrial & Engineering Chemistry Research* 31.11, pp. 2625–2628. ISSN: 0888-5885.

Vaidyanathan, S. and Azar, A. (2021). *Backstepping Control of Nonlinear Dynamical Systems*. Elsevier. DOI: 10.1016/c2018-0-02049-6.

Van Der Zalm, G. M. (2004). *Tuning of PID-type controllers: literature overview*. Tech. rep. Technische Universiteit Eindhoven.

Vasanthi, D., Pranavamoorthy, B., and Pappa, N. (2011). "Artificial neural network tuned cascade control for temperature control of polymerization reactor". In: *IEEE International Symposium on Intelligent Control - Proceedings*, pp. 1367–1372. ISBN: 9781457711046. DOI: 10.1109/ISIC.2011.6045421.

Vasanthi, D., Pranavamoorthy, B., and Pappa, N. (2012). "Design of a self-tuning regulator for temperature control of a polymerization reactor". In: *ISA Transactions* 51.1, pp. 22–29. ISSN: 00190578. DOI: 10.1016/j.isatra.2011.07.009. URL: https://pubmed.ncbi.nlm.nih.gov/21862006/.

Wang, Y. and Zhu, X. (2004). "Temperature control of the batch polypropylene Reactor by ADRC". In: *IFAC Proceedings Volumes (IFAC-PapersOnline)*. Vol. 37. 1. IFAC Secretariat, pp. 935–938. DOI: 10.1016/s1474-6670(17)38854-7.

Zadeh, L. A. (1965). "Fuzzy sets". In: *Information and Control* 8.3, pp. 338–353. ISSN: 00199958. DOI: 10.1016/S0019-9958(65)90241-X.

Zheng, Q., Daluom, A., Xu, W., and Zheng, Y. (2012). "Reduced-order active disturbance rejection control for multivariable chemical processes". In: *Conference Record - IAS Annual Meeting (IEEE Industry Applications Society)*. ISBN: 9781467303309. DOI: 10.1109/IAS.2012.6374014.

Ziegler, J. G. and Nichols, N. B. (1942). "Optimum settings for automatic controllers". In: *trans. ASME* 64.11.

Zotică, C., Alsop, N., and Skogestad, S. (2020). "Transformed Manipulated Variables for Linearization, Decoupling and Perfect Disturbance Rejection." In: *IFAC-PapersOnLine*.

# Appendix A

# Open-Loop Step Responses

## A.1 Tanks-in-Series Tuning

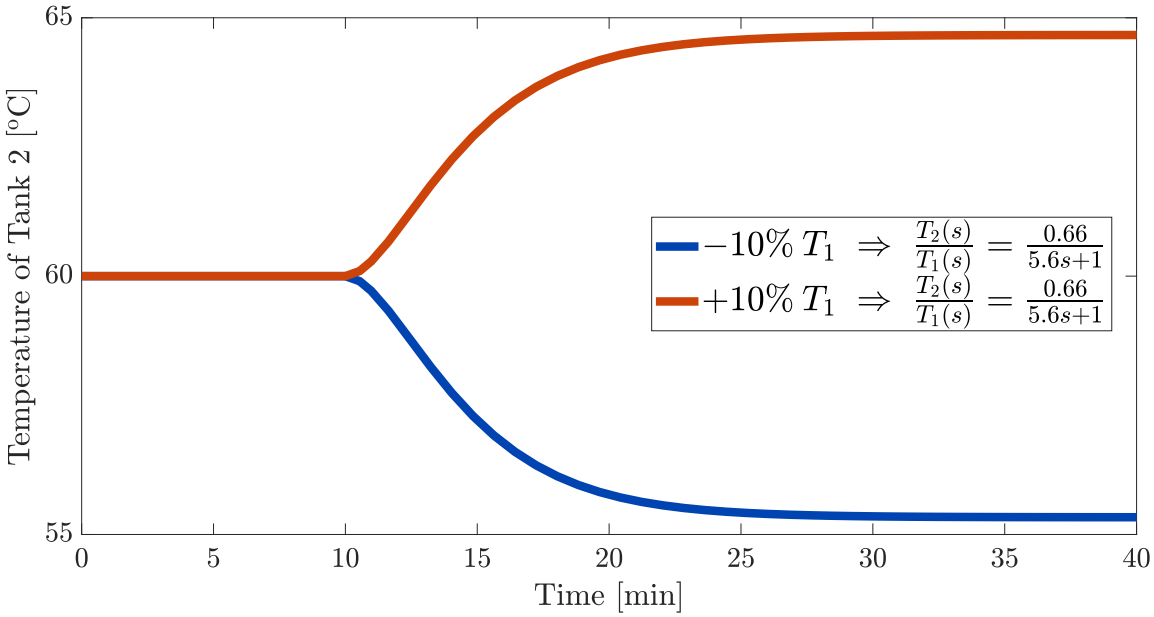


Figure A.1: Open-loop Response to Step-Changes in $T_1$ at $t = 10min$ for a Pure Feedback System

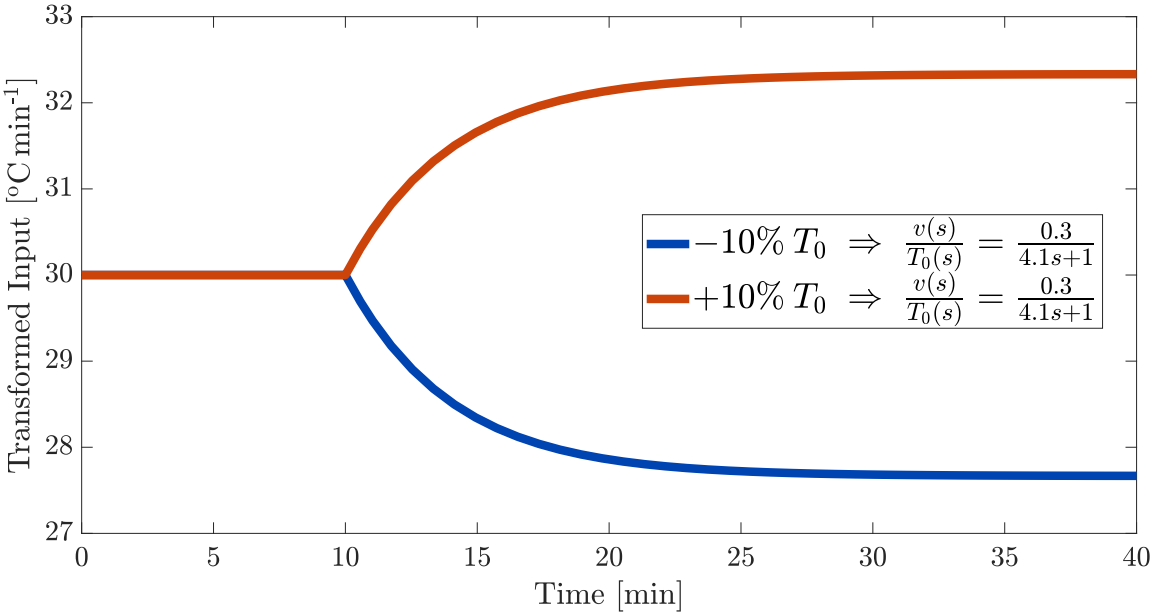


Figure A.2: Open-loop Response to Step-Changes in $T_0$ at $t = 10min$ for General Cascade System

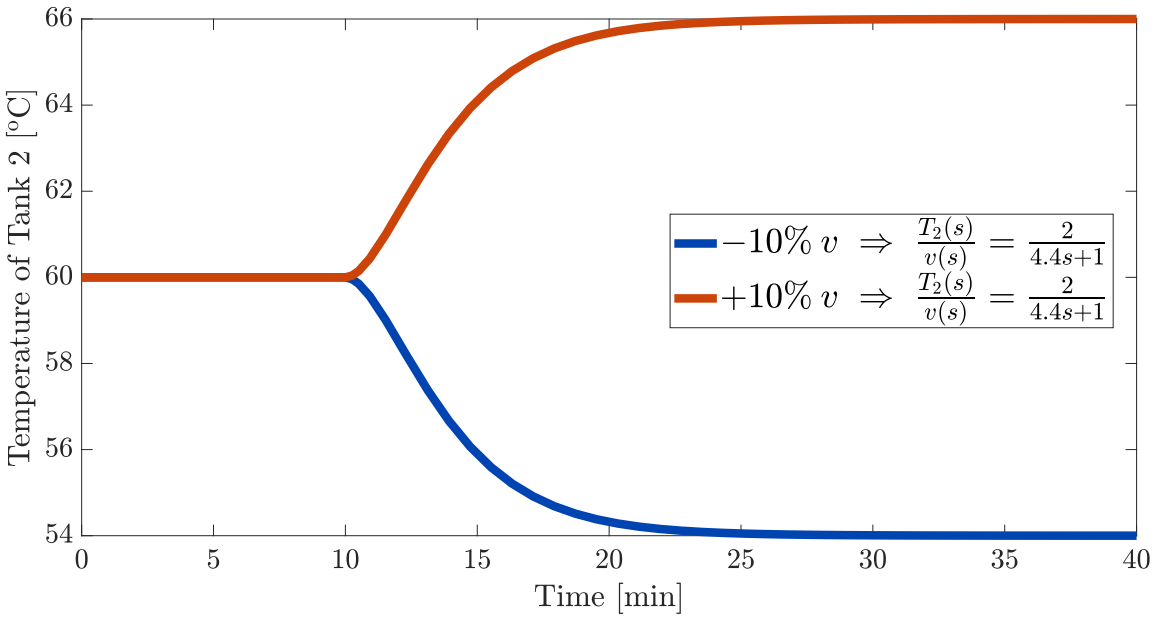


Figure A.3: Open-loop Response to Step-Changes in $v$ at $t = 10min$ for General Cascade System

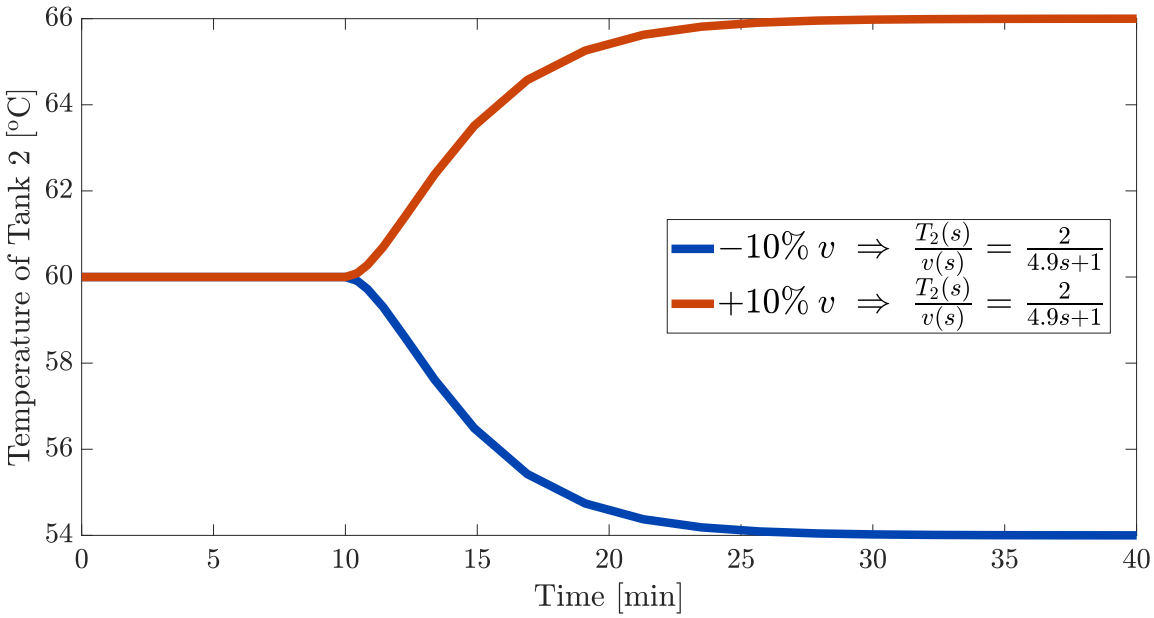


Figure A.4: Open-loop Response to Step-Changes in $v$ at $t = 10min$ for Alternative Cascade System

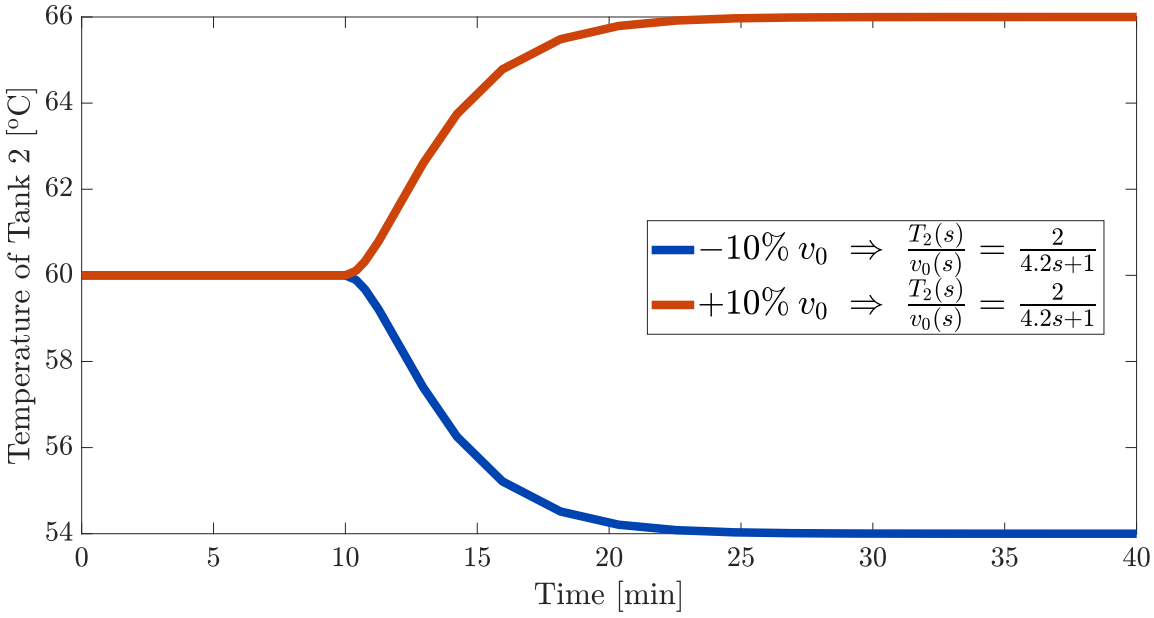


Figure A.5: Open-loop Response to Step-Changes in $v$ at $t = 10min$ for Static Alternative Cascade System

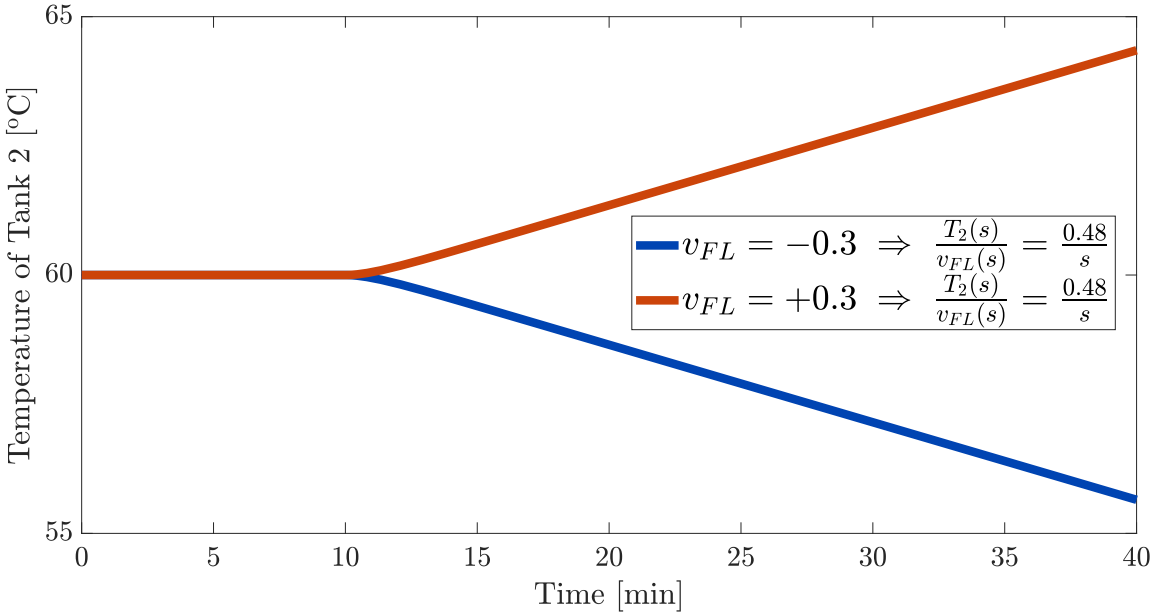


Figure A.6: Open-loop Response to Step-Changes in $v$ at $t = 10min$ for Integrating Alternative Cascade System

## A.2 Tanks-in-Series Extension Tuning

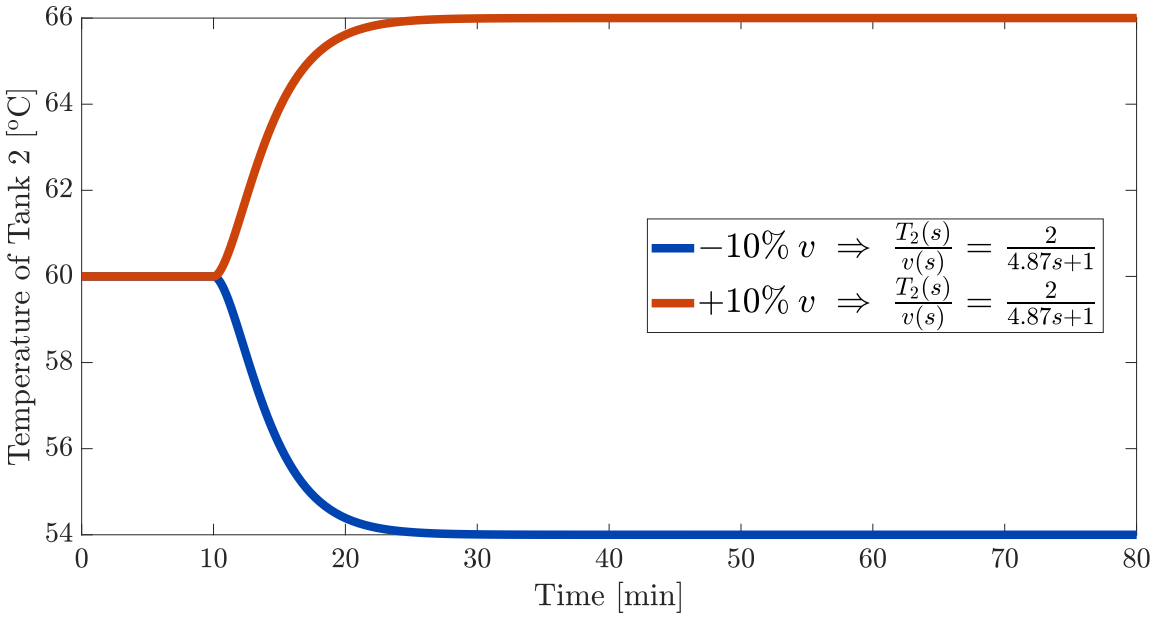


Figure A.7: Open-loop Response to Step-Changes in $v$ at $t = 10min$ for Cascade System 1

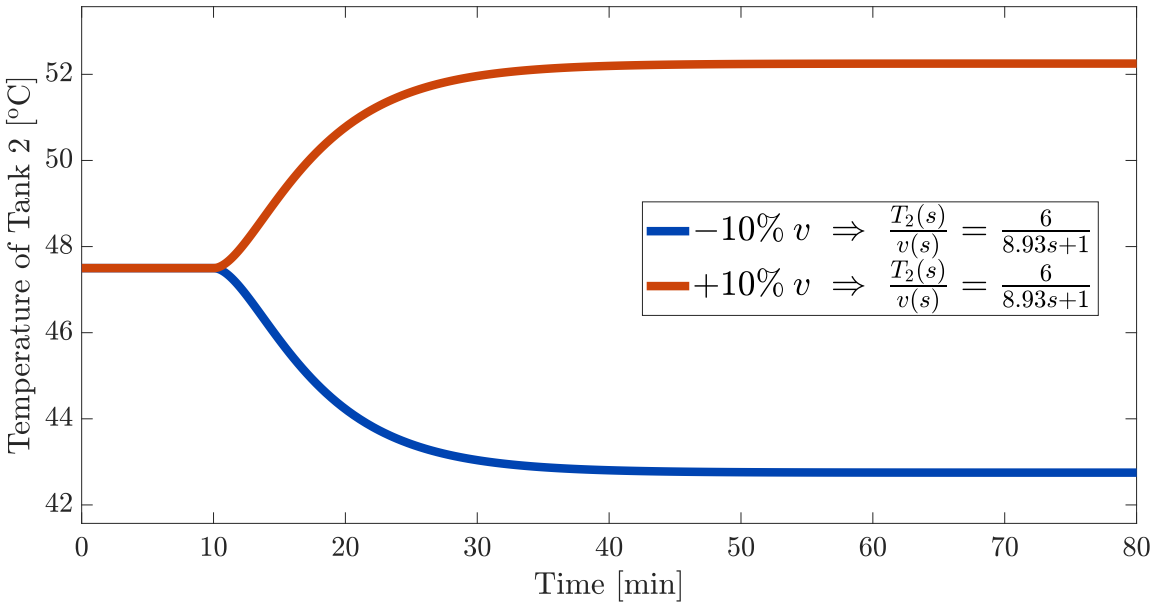


Figure A.8: Open-loop Response to Step-Changes in $v$ at $t = 10min$ for Cascade System 2

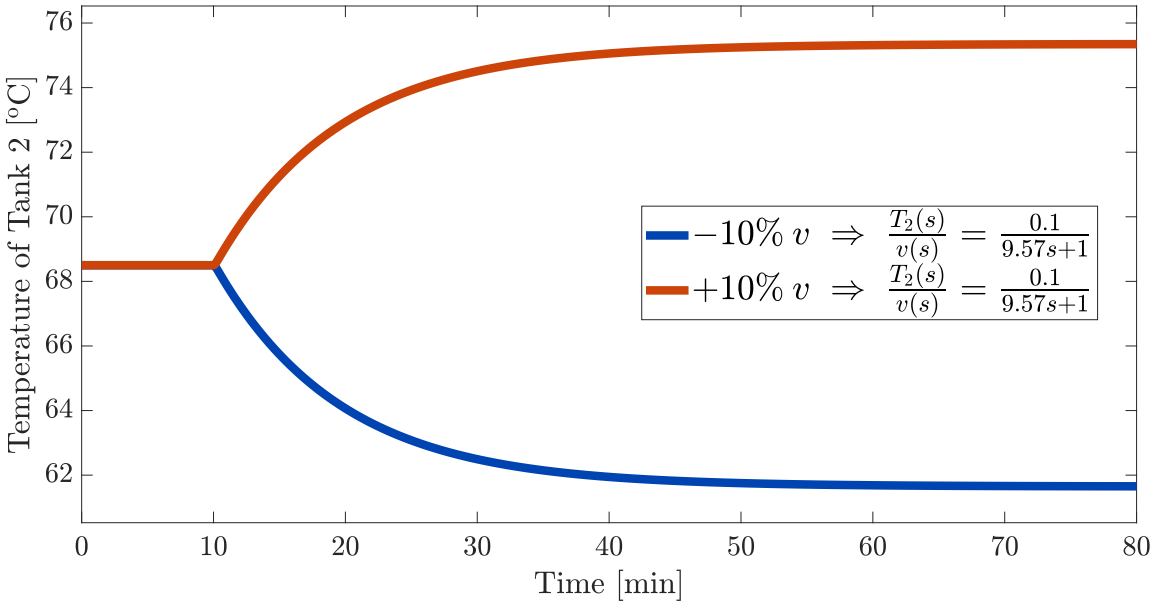


Figure A.9: Open-loop Response to Step-Changes in $v$ at $t = 10min$ for Cascade System 3

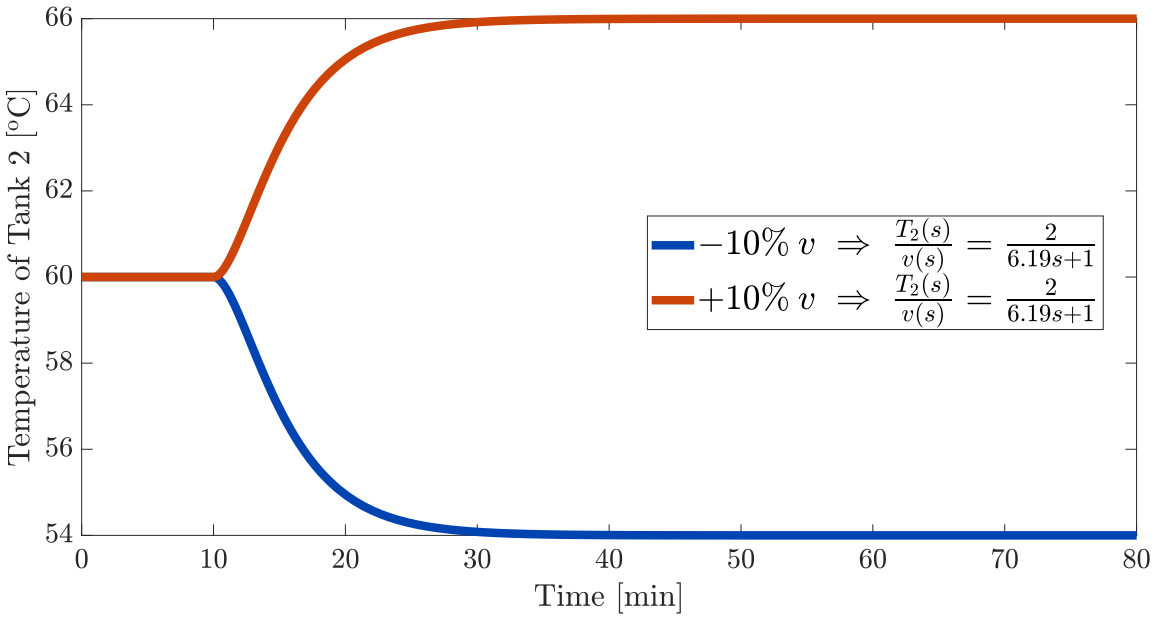


Figure A.10: Open-loop Response to Step-Changes in $v$ at $t = 10min$ for Case 1 System 1

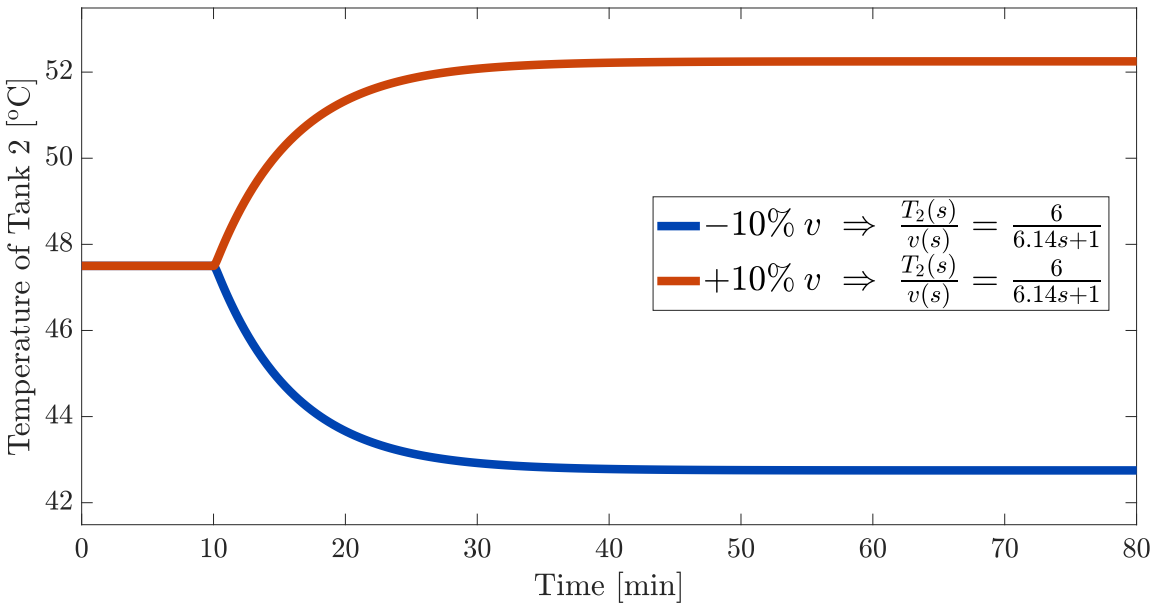


Figure A.11: Open-loop Response to Step-Changes in $v$ at $t = 10min$ for Case 1 System 2

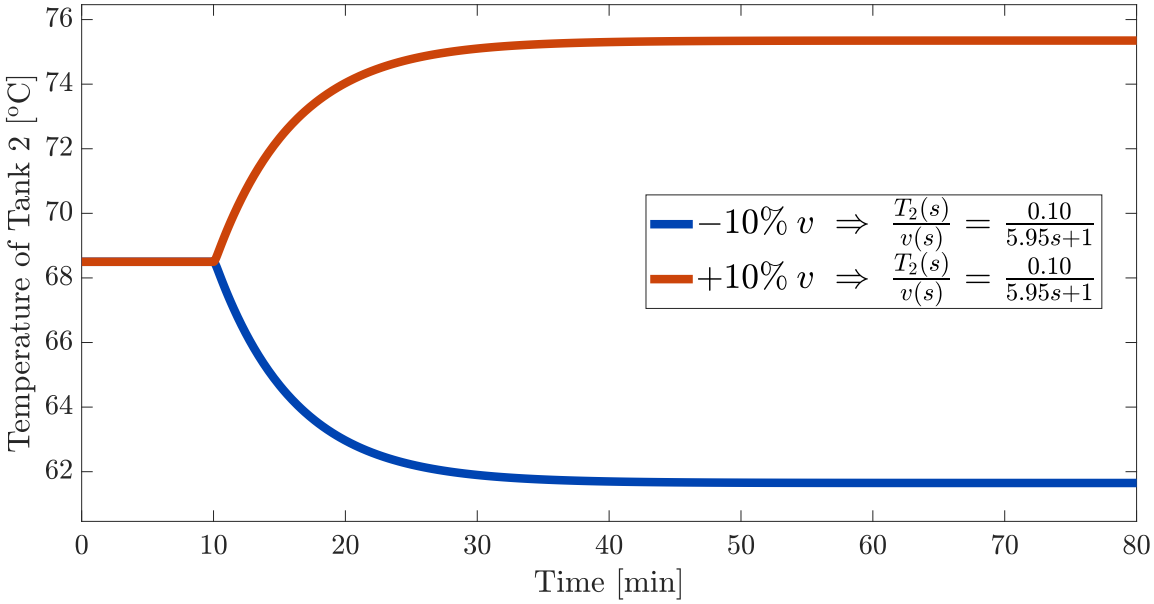


Figure A.12: Open-loop Response to Step-Changes in $v$ at $t = 10min$ for Case 1 System 3

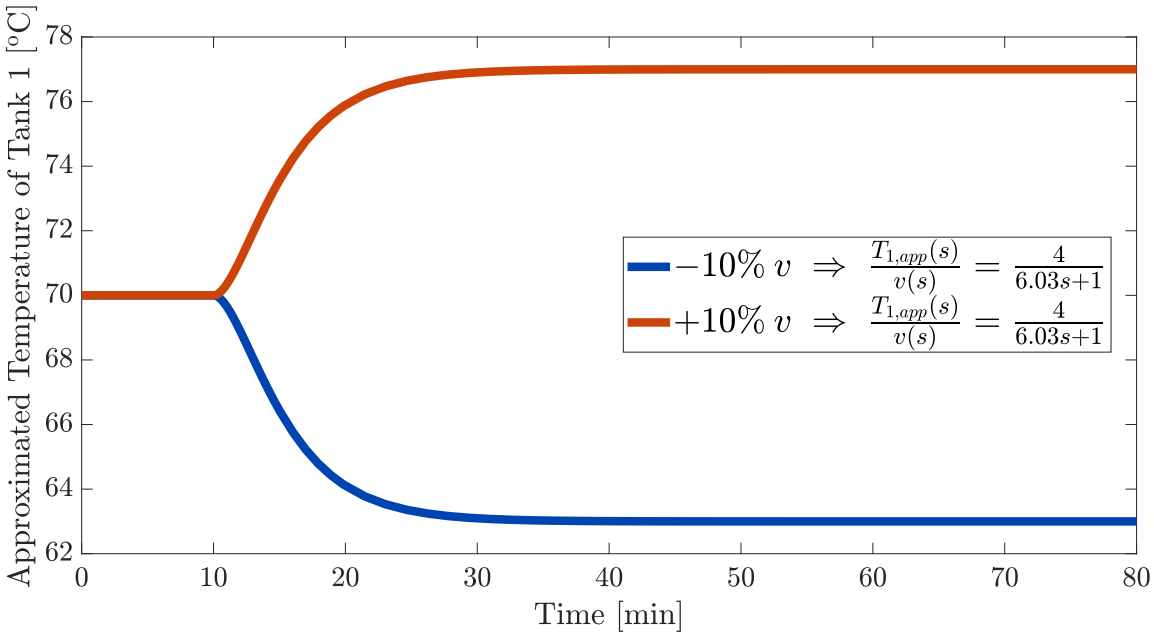


Figure A.13: Open-loop Response to Step-Changes in $v$ at $t = 10min$ for Case 2 System 1

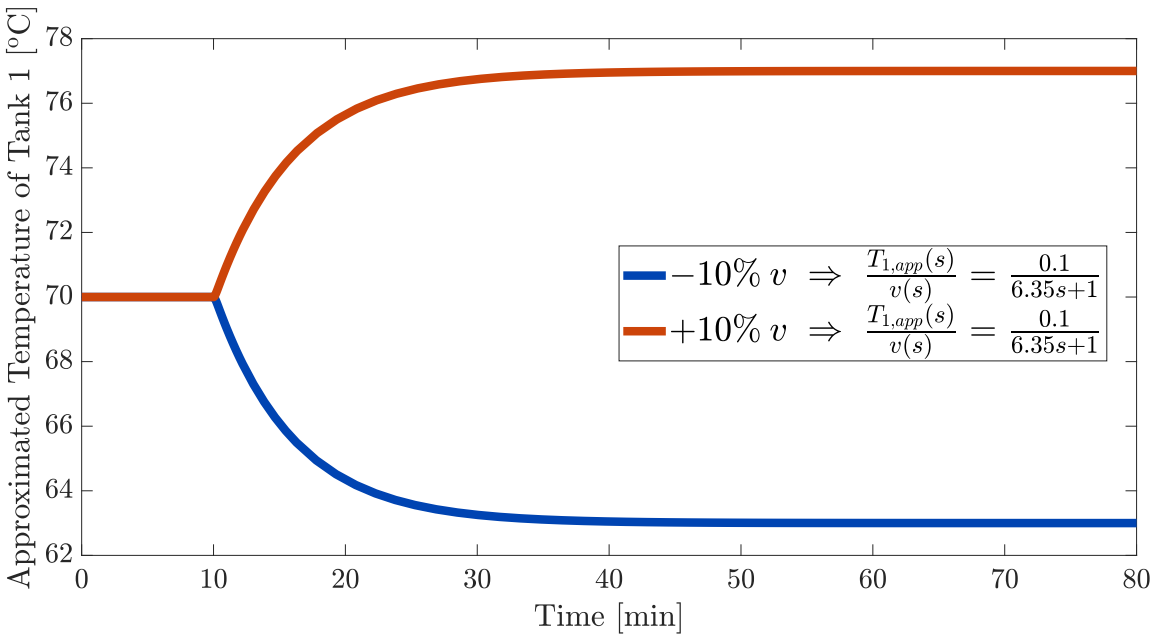


Figure A.14: Open-loop Response to Step-Changes in $v$ at $t = 10min$ for Case 2 System 2

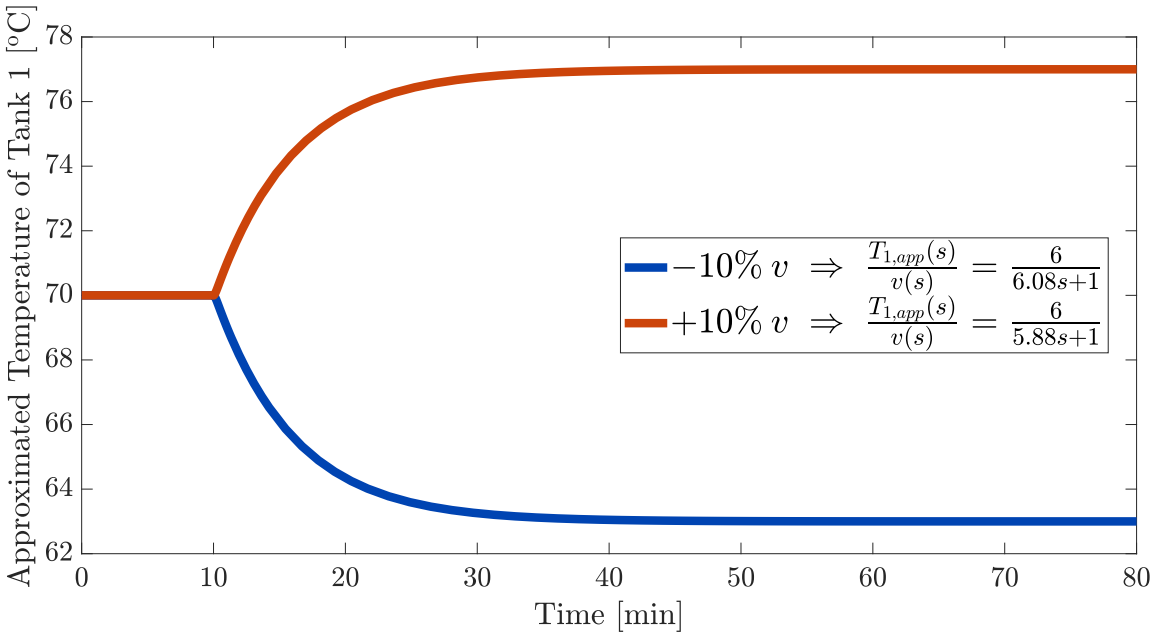


Figure A.15: Open-loop Response to Step-Changes in $v$ at $t = 10min$ for Case 2 System 3

## A.3 CSTR Tuning

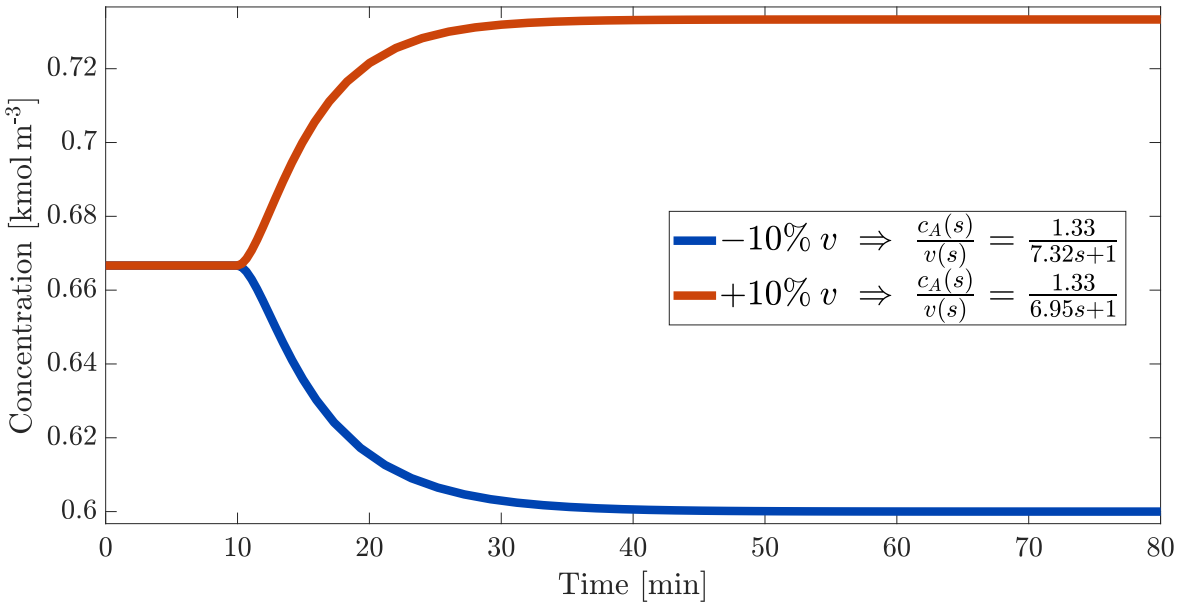


Figure A.16: Open-loop Response to Step-Changes in $v$ at $t = 10min$ for Chain of Transforms

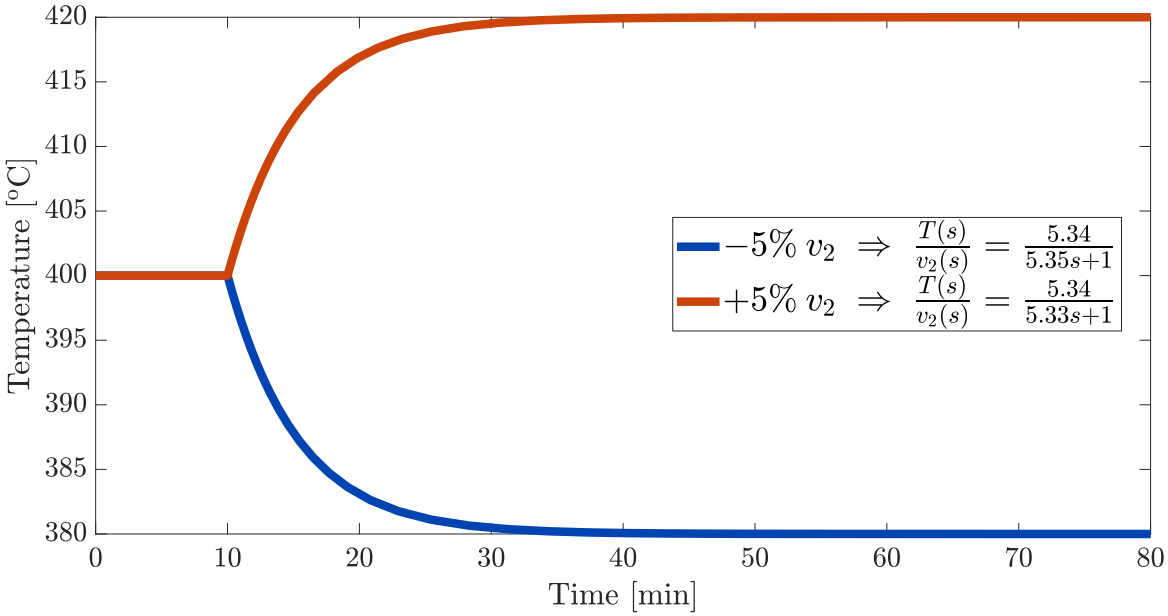


Figure A.17: Open-loop Response to Step-Changes in $v_2$ at $t = 10min$ for Double-Linearized Alternative Cascade System. (limited to 5% to avoid saturation)

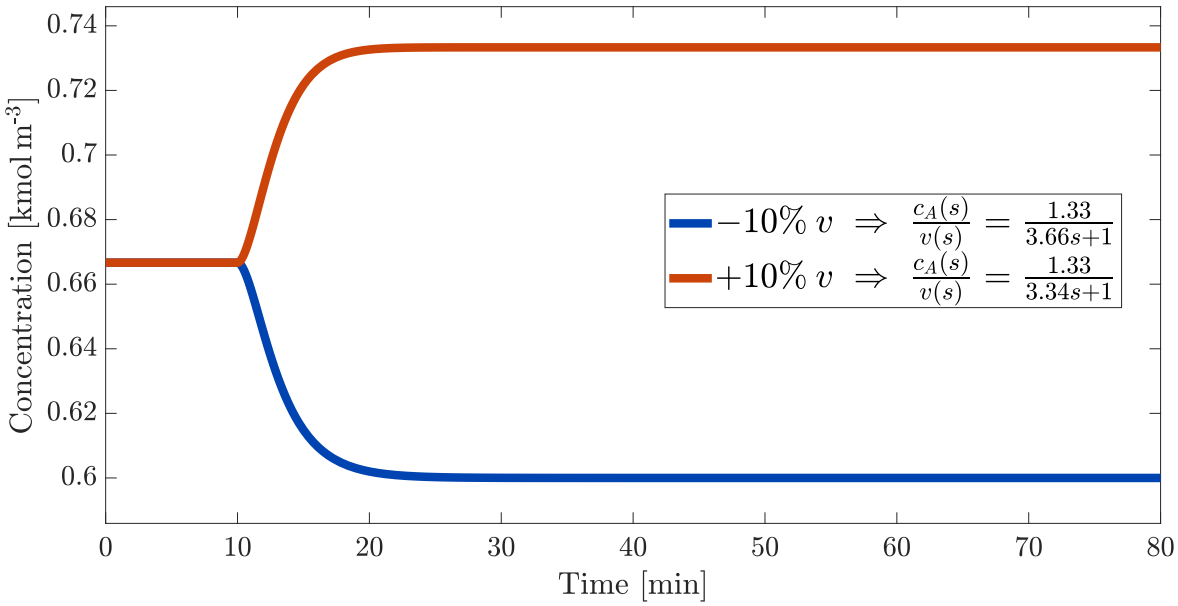


Figure A.18: Open-loop Response to Step-Changes in $v$ at $t = 10min$ for Double-Linearized Alternative Cascade System

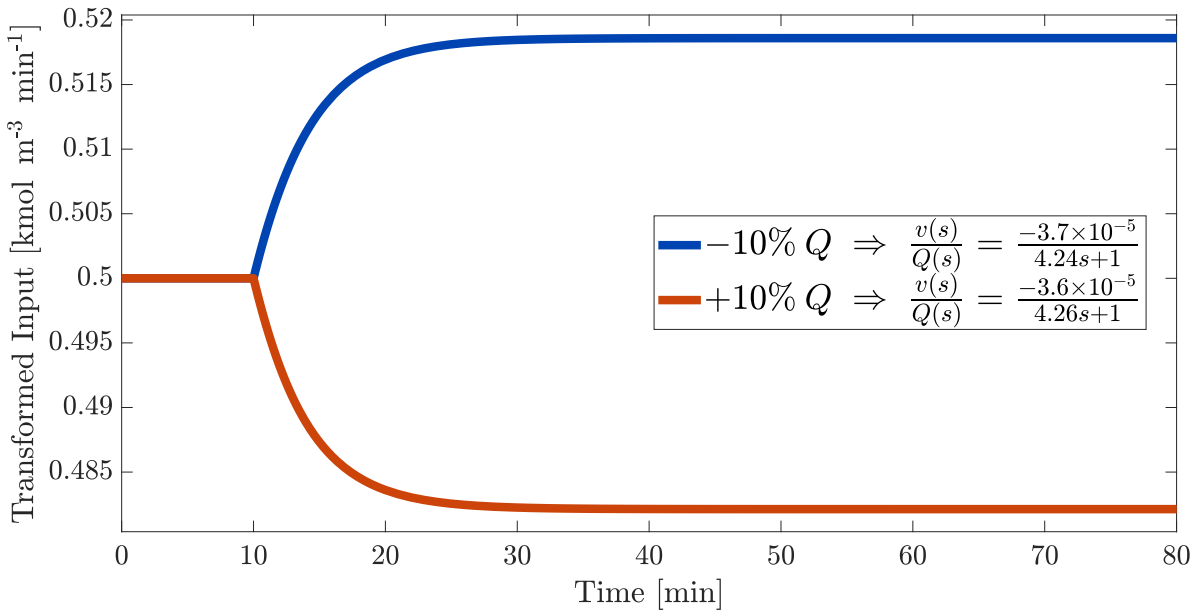


Figure A.19: Open-loop Response to Step-Changes in $Q$ at $t = 10min$ for General Cascade System

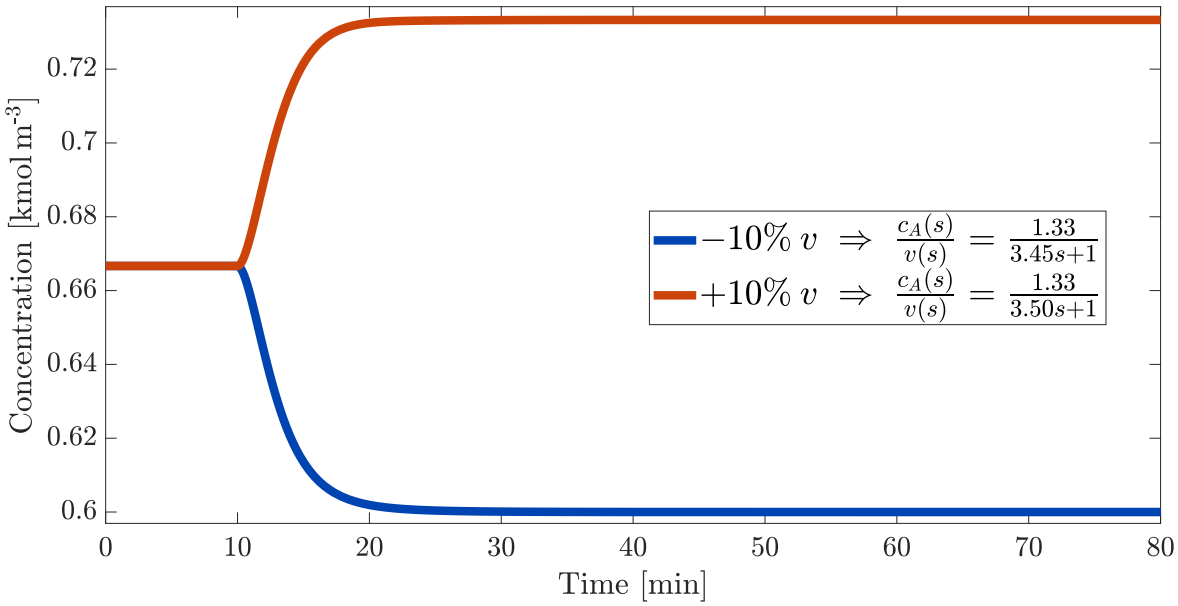


Figure A.20: Open-loop Response to Step-Changes in $v$ at $t = 10min$ for General Cascade System

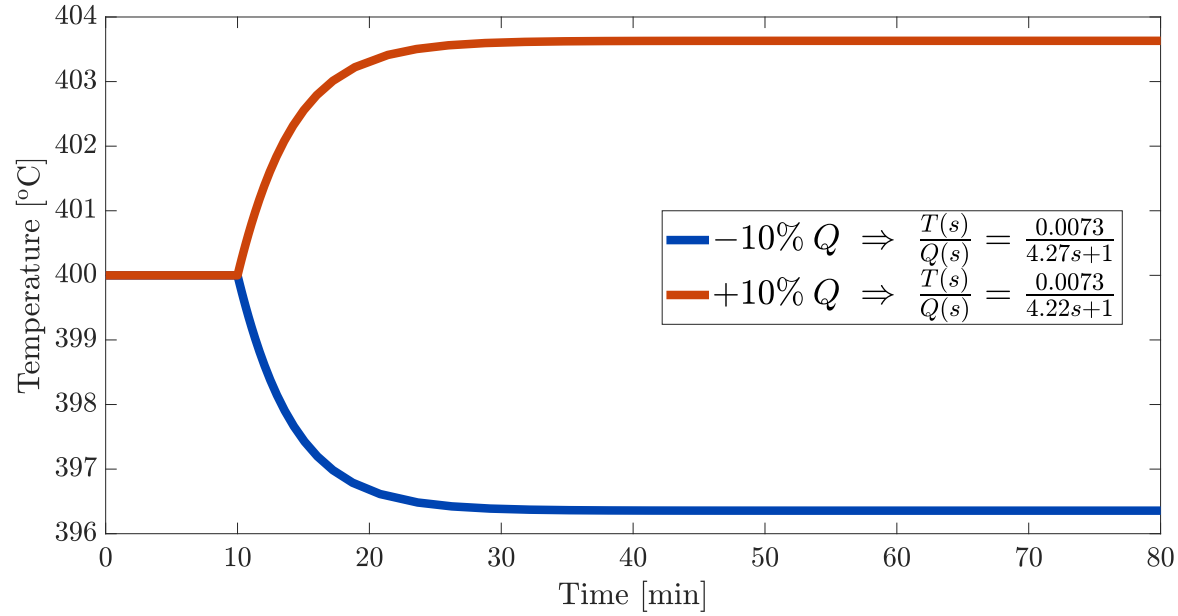


Figure A.21: Open-loop Response to Step-Changes in $Q$ at $t = 10min$ for Feedback Only System

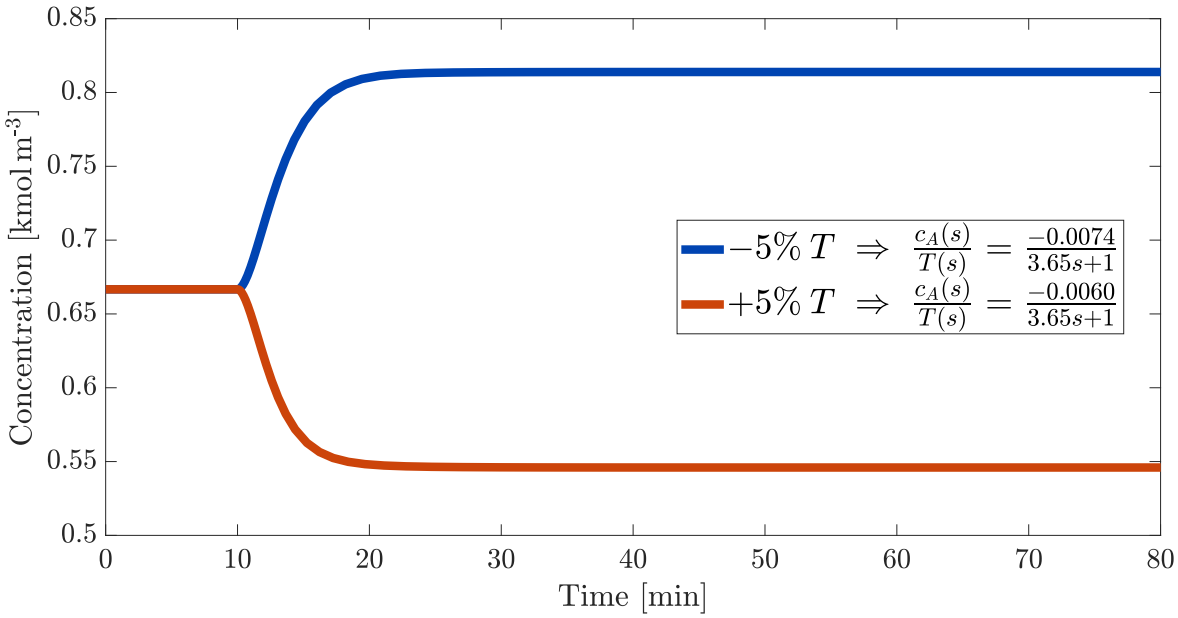


Figure A.22: Open-loop Response to Step-Changes in $T$ at $t = 10min$ for Feedback Only System. (Limited to 5% to avoid saturation)

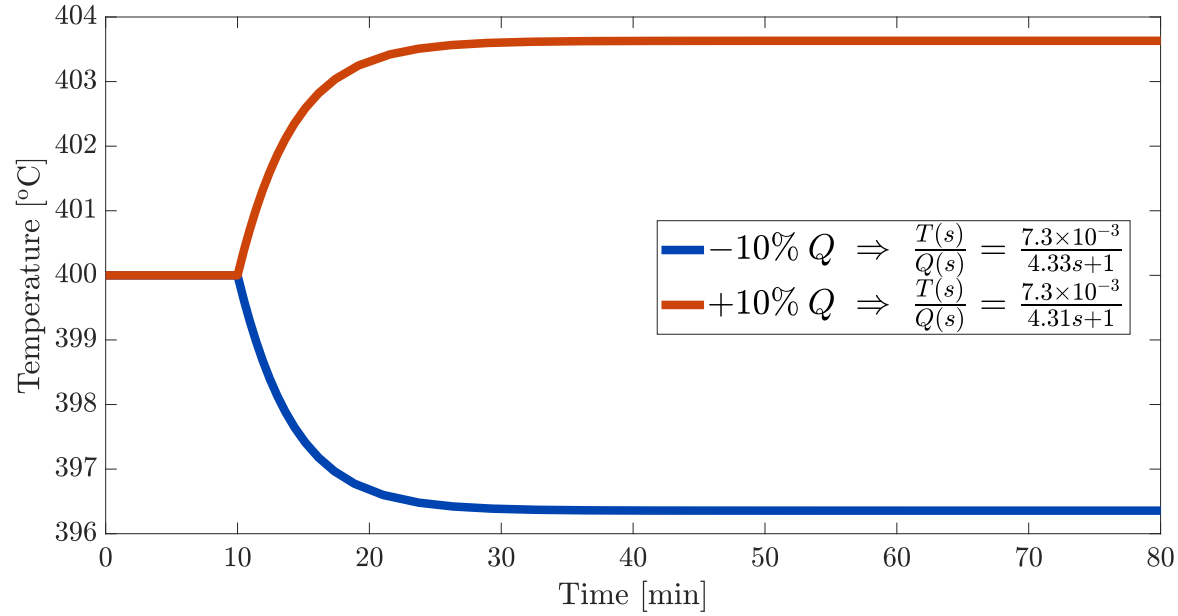


Figure A.23: Open-loop Response to Step-Changes in $Q$ at $t = 10min$ for Alternative Fitted Cascade System

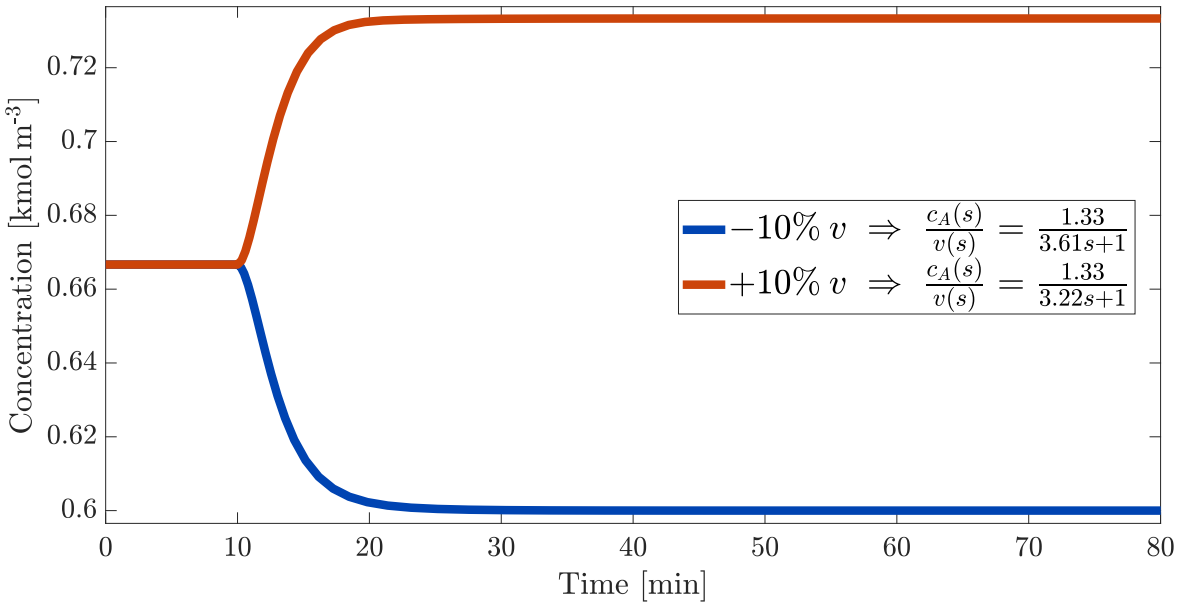


Figure A.24: Open-loop Response to Step-Changes in $v$ at $t = 10min$ for Alternative Fitted Cascade System

## A.4 pH Neutralisation Tuning

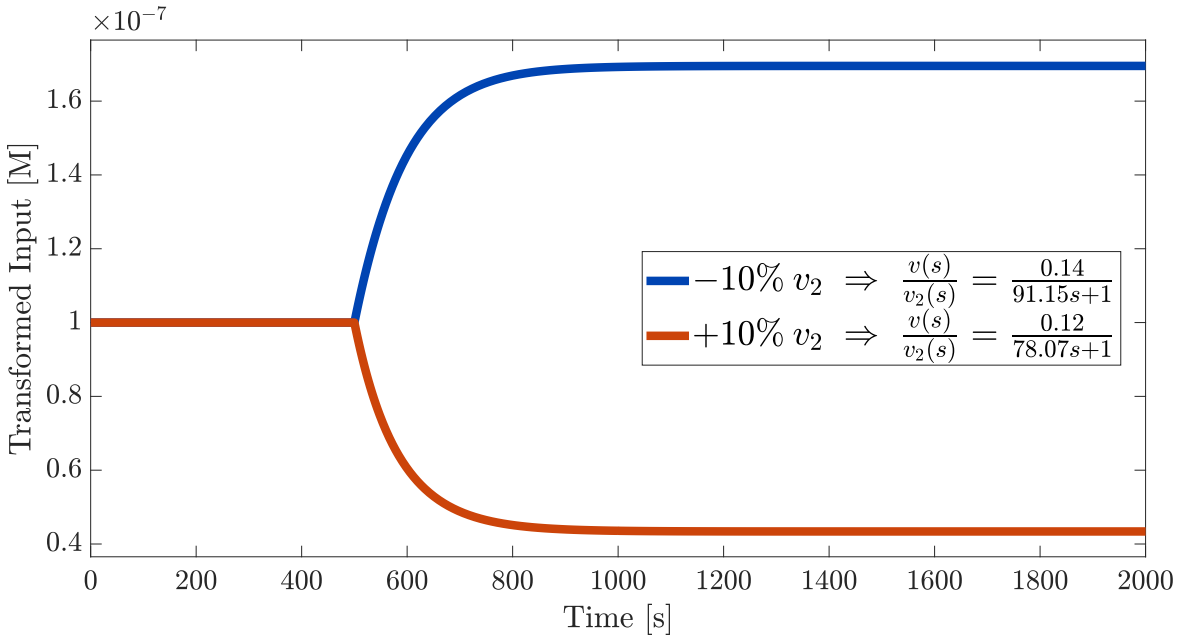


Figure A.25: Open-loop Response to Step-Changes in $v_2$ at $t = 10min$ for General Cascade System

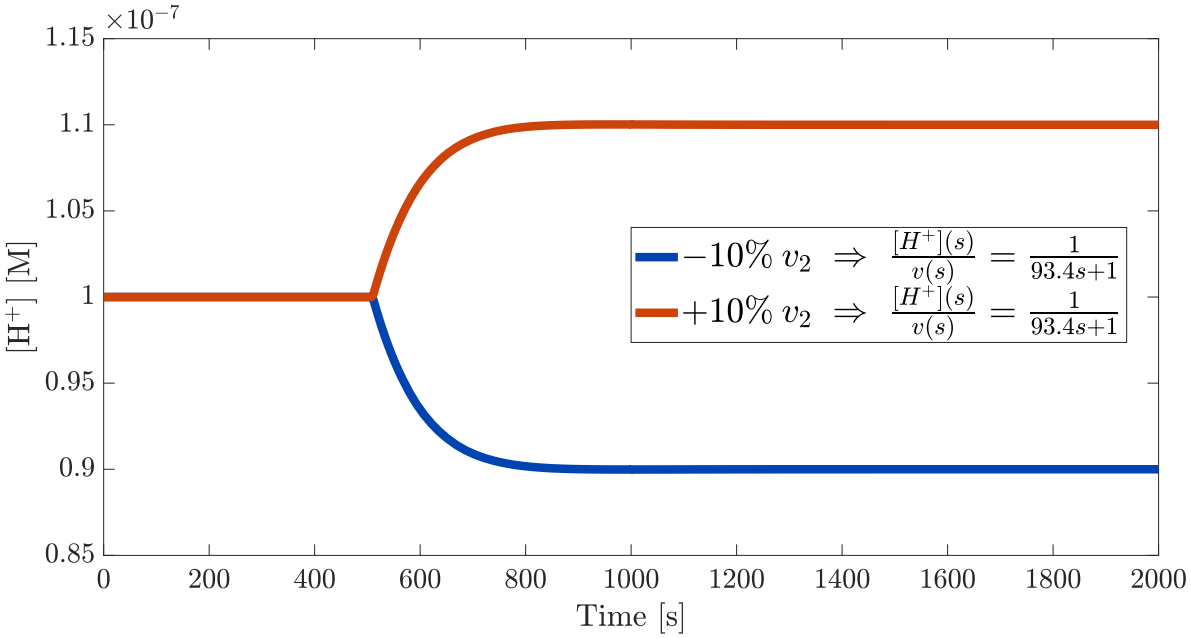


Figure A.26: Open-loop Response to Step-Changes in $v$ at $t = 10min$ for General Cascade System

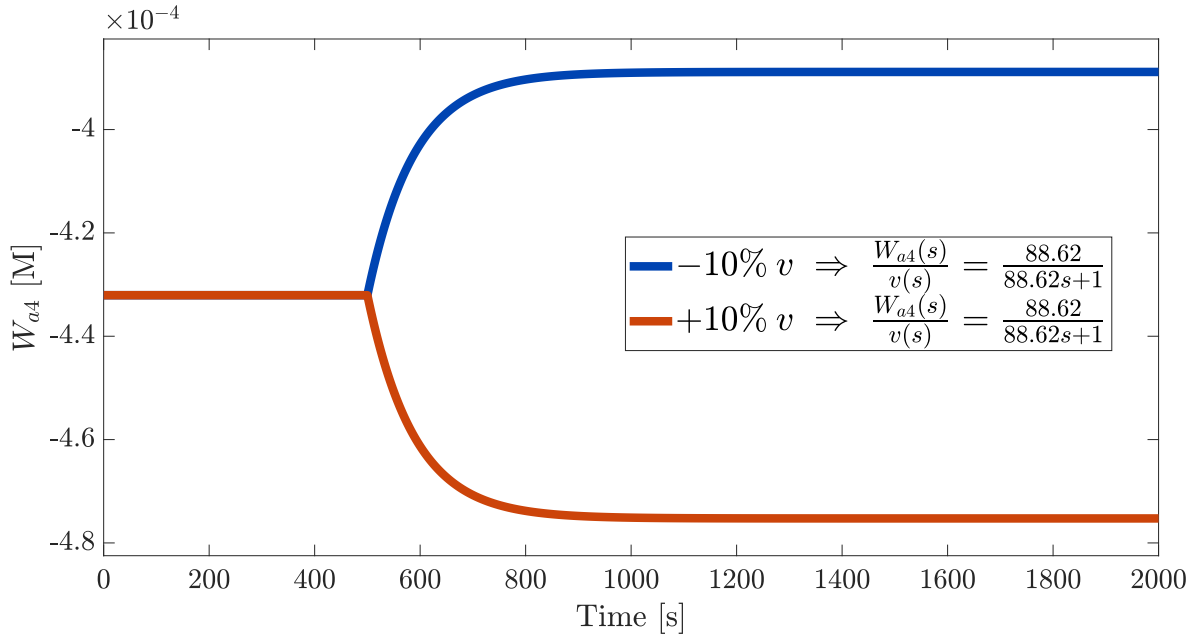


Figure A.27: Open-loop Response to Step-Changes in $v$ at $t = 10min$ for Alternative Cascade on $W_{a4}$ system

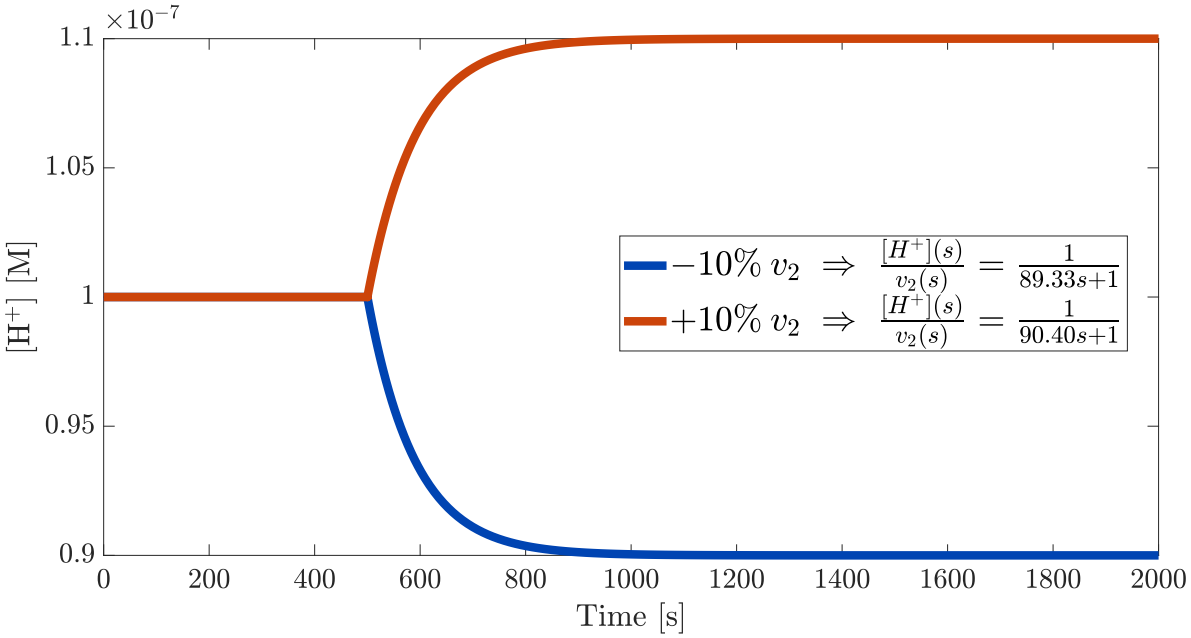


Figure A.28: Open-loop Response to Step-Changes in $v_2$ at $t = 10min$ for Alternative Cascade on $W_{a4}$ system

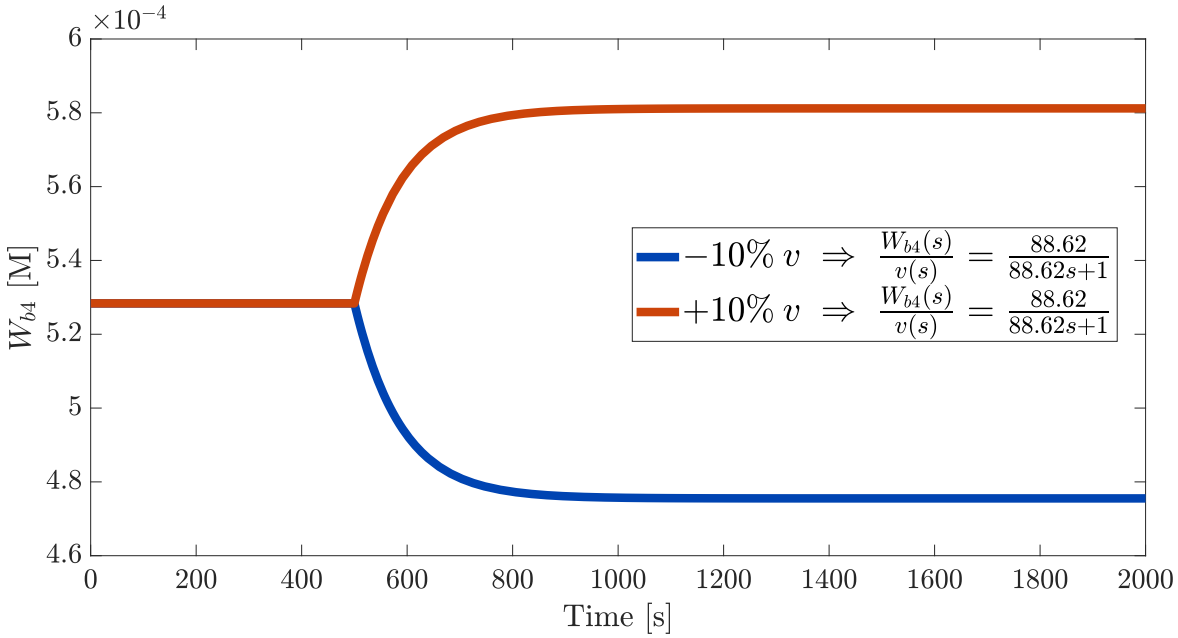


Figure A.29: Open-loop Response to Step-Changes in $v$ at $t = 10min$ for Alternative Cascade on $W_{b4}$ system

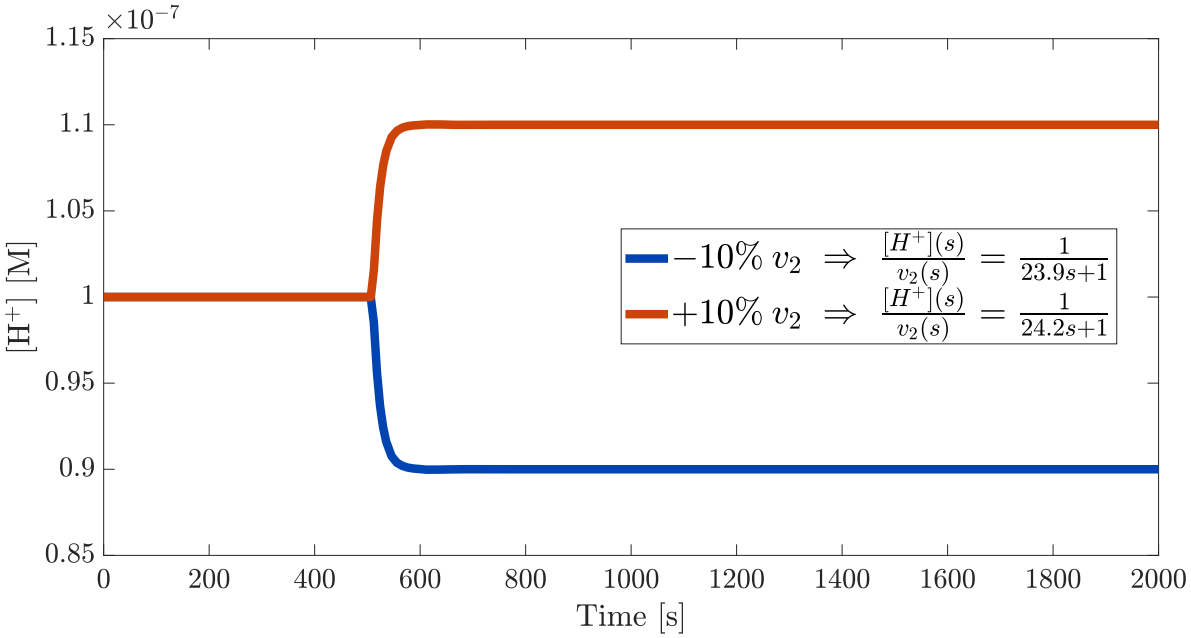


Figure A.30: Open-loop Response to Step-Changes in $v_2$ at $t = 10min$ for Alternative Cascade on $W_{b4}$ system

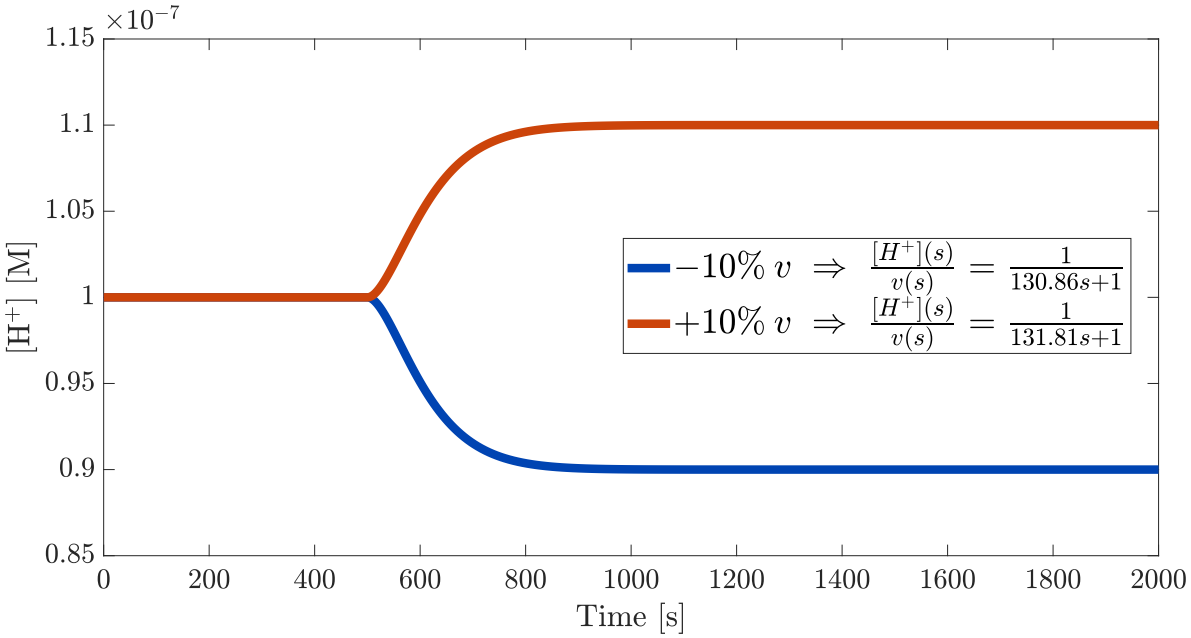


Figure A.31: Open-loop Response to Step-Changes in $v$ at $t = 10min$ for Chain of Transforms System

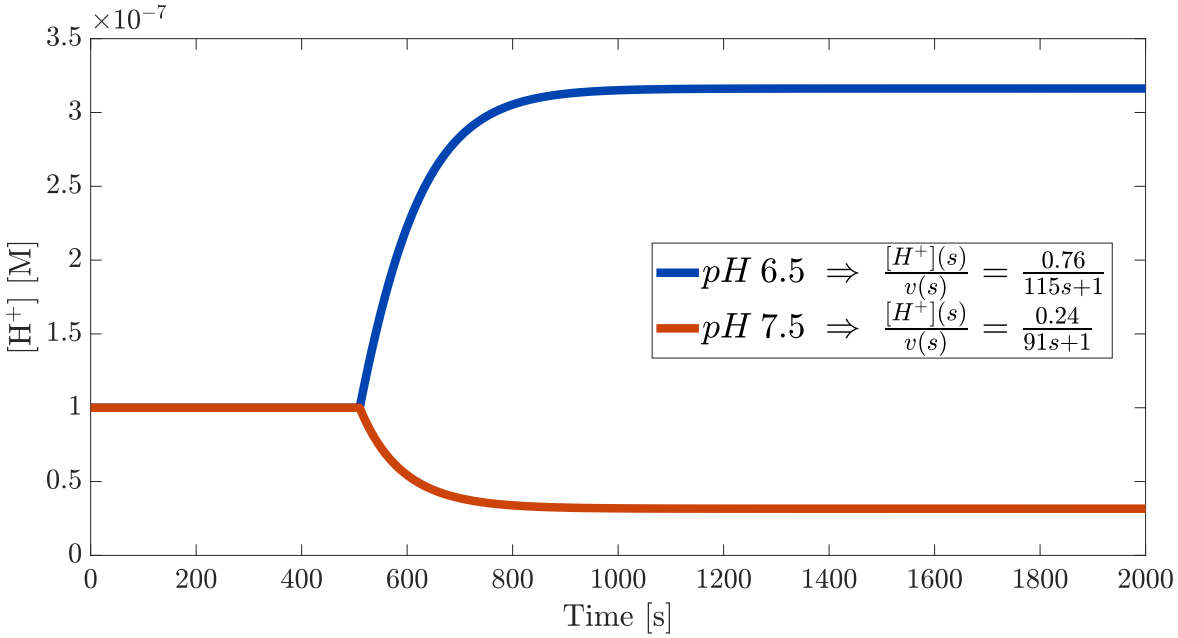


Figure A.32: Open-loop Response to Step-Changes in $v$ at $t = 10min$ for Combination System

# Appendix B

# Derivations

## B.1 Case Study A Derivations

Assumptions used;

*A1*: Perfect mixing in both tanks

*A2*: Constant density, $\rho$, and specific heat, $c_p$.

*A3*: Inlet temperature, $T_0$, may be manipulated sufficiently fast by the heat added, $Q$.

*A4*: Constant pressure and volume

In the derivations below, subscript $i = [0, 1, 2, d]$, where subscript 0 symbolises stream into tank 1, subscript 1 symbolises the stream out of tank 1, subscript 2 symbolises the stream out of tank 2 and subscript $d$ symbolises the disturbance stream into tank 2.

### B.1.1 Mass Balances

From a mass balance around tank 1;

$$\frac{dm_1}{dt} = w_0 - w_1$$

Where, $m_1$ $[kg]$ is the mass hold-up in tank 1, and $w_i$ $[kg\,min^{-1}]$ is the mass flow of stream $i$. Substituting $m_1 = \rho V_1$, $V_1 = A_1 h_1$ and $w_i = \rho F_i$, where $\rho$ is the density of the fluid $[kg\,m^{-3}]$, $V_1$ is the volume of tank 1, $A_1$ $[m^2]$ is the cross-sectional area of tank 1, $h_1$ $[m]$ is the level of the fluid in tank 1 and $F_i$ $[m^3\,min^{-1}]$ is the volumetric flow of stream $i$.

$$\frac{d(\rho A_1 h_1)}{dt} = \rho(F_0 - F_1)$$

Dividing by $\rho A_1$, as neither vary with time gives the mass balance over tank 1;

$$\frac{dh_1}{dt} = \frac{1}{A_1}(F_0 - F_1) \tag{B.1}$$

In a similar manner for tank 2, including the flow in of the disturbance stream, the mass balance becomes;

$$\frac{dm_2}{dt} = w_1 + w_d - w_2$$

Where, $m_2$ $[kg]$ is the mass hold-up in tank 2 $[kg]$. Substituting $m_2 = \rho V_2$, $V_2 = A_2 h_2$ and $w_i = \rho F_i$, where $V_2$ $[m^3]$ is the volume of tank 2, $A_2$ $[m^2]$ is the cross-sectional area of tank 2 and $h_2$ $[m]$ is the level of the fluid in tank 2 and dividing by $\rho A_2$ gives the mass balance over tank 2, Eq. B.2.

$$\frac{dh_2}{dt} = \frac{1}{A_2}(F_d + F_1 - F_2) \tag{B.2}$$

### B.1.2 Energy Balances

From an energy balance around tank 1, with no heat or shaft work;

$$\frac{d(m_1 H_1)}{dt} = w_0 H_0 - w_1 H_1$$

Where $H_0$ and $H_1$ $[J\,kg^{-1}]$ are the specific enthalpies of the inlet stream to tank 1 and outlet stream of tank 1 respectively, and other parameters have same meanings as above. For an absence of phase change the two equations below hold:

$$H_i = H(T_{ref}) + \int_{T_{ref}}^{T_i} c_p\, dT$$

$$\frac{dH_i}{dt} = c_p \frac{dT_i}{dt}$$

Where, $c_p$ $[J\,K^{-1}\,kg^{-1}]$ is the specific heat capacity, and $H(T_{ref})$ $[J\,kg^{-1}]$ is the enthalpy at reference temperature (both are assumed constant). Enthalpy of mixing is assumed negligible. Therefore, using the equations for $H_i$ and $dH_i/dt$ in the original energy balance and product rule on LHS;

$$m_1 c_p \frac{dT_1}{dt} + \Big(H(T_{ref}) + \int_{T_{ref}}^{T_1} c_p\, dT\Big)\frac{dm_1}{dt} = w_0\Big(H(T_{ref}) + \int_{T_{ref}}^{T_0} c_p\, dT\Big) - w_1\Big(H(T_{ref}) + \int_{T_{ref}}^{T_1} c_p\, dT\Big)$$

Noting that $dm_1/dt = w_0 - w_1$ and $m_1 = \rho A_1 h_1$ , where parameters have same

meanings as above. Performing the integration gives;

$$\rho A_1 h_1 c_p \frac{dT_1}{dt} + \big(H(T_{ref}) + c_p(T_1 - T_{ref})\big)(w_0 - w_1) = \\ w_0\big(H(T_{ref}) + c_p(T_0 - T_{ref})\big) - w_1\big(H(T_{ref}) + c_p(T_1 - T_{ref})\big)$$

Multiplying out brackets gives;

$$\rho A_1 h_1 c_p \frac{dT_1}{dt} + H(T_{ref})w_0 - H(T_{ref})w_1 + c_p T_1 w_0 - c_p T_{ref} w_0 - c_p T_1 w_1 + c_p T_{ref} w_1 = \\ w_0 H(T_{ref}) + w_0 c_p T_0 - w_0 c_p T_{ref} - w_1 H(T_{ref}) - w_1 c_p T_1 + w_1 c_p T_{ref}$$

Which, after cancelling out like terms, gives;

$$\rho A_1 h_1 c_p \frac{dT_1}{dt} = w_0 c_p (T_0 - T_1)$$

Noting that $w_0 = \rho F_0$, this gives the energy balance over tank 1 after rearranging; Eq. B.3.

$$\frac{dT_1}{dt} = \frac{F_0 c_p (T_0 - T)}{A_1 h_1} \tag{B.3}$$

Similarly for tank 2, but with the addition of the disturbance stream, applying a mass balance over tank 2 gives;

$$\frac{d(m_2 H_2)}{dt} = w_1 H_1 + w_d H_d - w_2 H_2$$

Using the same procedure as above;

$$m_2 c_p \frac{dT_2}{dt} + \big(H(T_{ref}) + c_p(T_2 - T_{ref})\big)\frac{dm_2}{dt} = w_1\big(H(T_{ref}) + c_p(T_1 - T_{ref})\big) + \\ w_d\big(H(T_{ref}) + c_p(T_d - T_{ref})\big) - w_2\big(H(T_{ref}) + c_p(T_2 - T_{ref})\big)$$

Noting that $dm_2/dt = w_1 + w_d - w_2$ and cancelling like terms, as in tank 1 energy balance derivation, gives;

$$m_2 c_p \frac{dT_2}{dt} = w_1 c_p (T_1 - T_2) + w_d c_p (T_d - T_2)$$

Noting that $m_2 = \rho A_2 h_2$ and $w_i = \rho F_i$, then dividing through by $\rho A_2 h_2 c_p$ gives the energy balance over tank 2, Eq. B.4.

$$\frac{dT_2}{dt} = \frac{F_1(T_1 - T_2) + F_d(T_d - T_2)}{A_2 h_2} \tag{B.4}$$

## B.2 Case Study A Extension Derivations

For the Case Study A extension the same assumptions as Case Study A, above, are made. In this section however, subscript $i = [0, 1, 2, 1d, 2d]$, where subscript 0 symbolises the stream into tank 1, subscript 1 symbolises the stream out of tank 1, 2 symbolises the stream out of tank 2, subscript $1d$ symbolises the disturbance stream to tank 1 and $2d$ symbolises the disturbance stream to tank 2.

### B.2.1 Mass Balances

For a mass balance over tank 1;

$$\frac{dm_1}{dt} = w_0 + w_{1d} - w_1$$

Using the same nomenclature as Section B.1.1, subbing in $m_1 = \rho A_1 h_1$ and $w_i = \rho F_i$;

$$\frac{d(\rho A_1 h_1)}{dt} = \rho(F_0 + F_{1d} - F_1)$$

Dividing by $\rho A_1$ gives us the mass balance over tank 1;

$$\frac{dh_1}{dt} = \frac{1}{A_1}(F_0 + F_{1d} - F_1) \tag{B.5}$$

The mass balance for tank 2 is exactly the same as the mass balance derivation for tank 2 in Section B.1.1 except for substitute of $d$ with $2d$, giving;

$$\frac{dh_2}{dt} = \frac{1}{A_2}(F_{2d} + F_1 - F_2) \tag{B.6}$$

### B.2.2 Energy Balances

For an energy balance over tank 1;

$$\frac{d(m_1 H_1)}{dt} = w_0 H_0 + w_{1d} H_{1d} - w_1 H_1$$

Using the same method as Section B.1.2;

$$m_1 \frac{dH_1}{dt} + H_1 \frac{dm_1}{dt} = w_0 H_0 + w_{1d} H_{1d} - w_1 H_1$$

Applying the equations for $H_i$ and $dH_i/dt$ as above;

$$m_1 c_p \frac{dT_1}{dt} + \Big(H(T_{ref}) + \int_{T_{ref}}^{T_1} c_p \, dT\Big)\frac{dm_1}{dt} =$$
$$w_0\Big(H(T_{ref}) + c_p \int_{T_{ref}}^{T_0} dT\Big) + w_{1d}\Big(H(T_{ref}) + c_p \int_{T_{ref}}^{T_{1d}} dT\Big) - w_1\Big(H(T_{ref}) + c_p \int_{T_{ref}}^{T_1} dT\Big)$$

Performing the integration, noting that $m_1 = \rho A_1 h_1$ and $w_i = \rho F_i$ and dividing through by $\rho A_1 h_1 c_p$ gives the energy balance for over tank 1, Eq. B.7;

$$\frac{dT_1}{dt} = \frac{F_0(T_0 - T_1) + F_{1d}(T_{1d} - T_1)}{A_1 h_1} \tag{B.7}$$

The energy balance over tank 2 is exactly the same as described in Section B.1.2, except for the substitute of $d$ with $2d$, giving Eq. B.8.

$$\frac{dT_2}{dt} = \frac{F_1(T_1 - T_2) + F_d(T_{2d} - T_2)}{A_2 h_2} \tag{B.8}$$

## B.3 Case Study B Derivations

The molar balance and energy balance for the CSTR case study are derived here with the following assumptions;

*B1*: Perfect volume control, i.e. $q_1 = q_2$

*B2*: Constant density, $\rho$, and specific heat, $c_p$

*B3*: Control of heat added is sufficiently fast

*B4*: Perfect mixing within tank

*B5*: Constant pressure and volume

*B6*: Negligible shaft work

### B.3.1 Component Molar Balance

For a component molar balance of $A$ over a reactor;

$$\frac{dN_A}{dt} = q_1 c_{Af} - q_2 c_A - rV \tag{B.9}$$

Where, $N_A$ $[kmol]$ is the number of moles in the reactor, $q_1$ and $q_2$ $[m^3\,min^{-1}]$are the inlet and outlet flowrates respectively, $c_{Af}$ and $c_A$ $[kmol\,m^{-3}]$ are the concentrations of the inlet and outlet respectively, $r$ $[kmol\,m^{-3}\,min^{-1}]$ is the rate of reaction and

$V$ $[m^3]$ is the volume of the reactor. From the assumptions, $q_1 = q_2$. Using this and the fact that $N_A = c_A V$ the balance becomes;

$$\frac{d(c_A V)}{dt} = q_1(c_{Af} - c_A) - rV$$

As the reaction is first order, $A \rightarrow B$, $r = k(T)c_A$, where $k(T)$ $[min^{-1}]$ is the reaction rate constant and calculated by the Arrhenius equation, $k(T) = k_0 e^{-\frac{E}{R}(\frac{1}{T} - \frac{1}{T_0})}$. Taking $V$ out of the derivative as it is constant and dividing by V gives the final equation;

$$\frac{dc_A}{dt} = \frac{q_1}{V}c_{Af} - \Big(\frac{q_1}{V} + k(T)\Big)c_A \tag{B.10}$$

### B.3.2 Energy Balance

For an energy balance over a reactor with constant pressure and volume with negligible work done/added (Fogler, 2016);

$$\frac{d(\sum(m_i H_i))}{dt} = Q + \sum(F_{io}H_{io}) - \sum(F_i H_i)$$

Where $\sum = \sum_{i=1}^{n}$ for brevity and $i = [1, 2]$, corresponding to species $A$ and $B$ respectively. $m_i$ $[kg]$ is the mass in the reactor, $Q$ $[kJ\,min^{-1}]$ is the heat added to the reactor, $F_{i0}$ and $F_i$ $[kg\,min^{-1}]$ are the inlet and outlet mass flows of species $i$ and $h_{i0}$ and $h_0$ $[kJ\,kg^{-1}]$ are the specific enthalpies, on a mass basis, of species $i$ in the inlet and outlet flows. Applying product rule to the left-hand side differential gives;

$$\sum\Big(m_i\frac{dH_i}{dt}\Big) + \sum\Big(H_i\frac{dm_i}{dt}\Big) = Q + \sum(F_{io}H_{io}) - \sum(F_i H_i)$$

For an absence of phase change;

$$H_i = H(T_{ref}) + \int_{T_{ref}}^{T} c_{pi}\,dT$$

$$\frac{dH_i}{dt} = c_{pi}\frac{dT}{dt}$$

Where $c_{pi}$ $[kJ\,kg^{-1}\,K^{-1}]$ is the specific heat capacity of species $i$ and $T$ $[K]$ is the temperature of the reactor. Substituting this into the energy balance equation gives;

$$\sum\Big(m_i c_{pi}\frac{dT}{dt}\Big) + \sum\Big(H_i\frac{dm_i}{dt}\Big) = Q + \sum(F_{io}H_{io}) - \sum(F_i H_i)$$

From a component mass balance over the tank, similar to Eq. B.9 but on a mass basis;

$$\frac{dm_i}{dt} = -\nu_i r_A V + F_{io} - F_i$$

Where, $m_i$ $[kg]$ is the mass of species $i$ in the reactor, $\nu_i$ [-] is the stoiciometric coefficient of species $i$ in the reaction, $r_A$ $[kmol\,m^{-3}\,min^{-1}]$ is the reaction rate of species A and $V$ $[m^3]$ is the volume of the reactor. Substituting this into the energy balance equation gives;

$$\sum\left(m_i c_{pi}\frac{dT}{dt}\right)+\sum\left(\nu_i H_i(-r_A V)\right)+\sum(F_{i0}H_i)-\sum(F_i H_i) = Q+\sum(F_{io}H_{io})-\sum(F_i H_i)$$

Collecting like terms, noting that $\sum(\nu_i h_i) = \Delta H_{rx}$, where $\Delta H_{rx}$ $[kJ\,kmol^{-1}]$ is the heat of reaction, and dividing by $\sum m_i c_{pi}$ gives;

$$\frac{dT}{dt} = \frac{Q - \sum(F_{i0}(H_i - H_{io})) - \Delta H_{rx}(-r_A V)}{\sum m_i c_{pi}}$$

With the assumption that $c_{pi}$ $[kJ\,kg^{-1}\,K^{-1}]$ is constant for all species in the liquid phase $A \rightarrow B$ reaction, i.e. $c_{pi} = c_p \;\forall\; i$, and there is no mass accumulation in the reactor since density is constant and there is perfect volume control, it can be said that $\sum(m_i c_{pi}) = mc_p$, where $m$ $[kg]$ is the mass in the reactor. Also, the reaction rate, $-r_A$ $[kmol\,m^{-3}\,min^{-1}]$ can be described by $-r_A = k(T)c_A$ for the first-order reaction, where $k(T)$ $[min^{-1}]$ follows the Arrenhius equation. Applying these equations reduces the energy balance to;

$$\frac{dT}{dt} = \frac{Q - \sum(F_{i0}(H_i - H_{io})) - \Delta H_{rx}k(T)c_A V}{mc_p}$$

For a constant heat capacity, $H_i - H_{io} = c_p(T - T_{io})$, and as the inlet stream will only contain reactant, $F_{i0} = F_{A0}$ $[kg\,min^{-1}]$, then $\sum(F_{i0}(H_i - H_{io})) = F_{A0}c_p(T - T_1)$, where $T_1$ $[K]$ is the temperature of the feed stream and the outlet stream temperature, $T$ $[K]$ is the same as the tank temperature and $F_{A0}$ $[kg\,min^{-1}]$ is the mass flowrate of the inlet stream. Giving;

$$\frac{dT}{dt} = \frac{Q - F_{A0}c_p(T - T_1) - \Delta H_{rx}k(T)c_A V}{mc_p}$$

Using $m = \rho V$, splitting the fraction up and cancelling terms gives the energy balance for the reactor;

$$\frac{dT}{dt} = \frac{Q}{\rho V c_p} - \frac{q_1}{V}(T - T_1) - \frac{\Delta H_{rx}c_A k(T)}{\rho c_p} \tag{B.11}$$

Where,

$$k(T) = k_0 e^{-\frac{E}{R}(\frac{1}{T}-\frac{1}{T_0})}$$

and where $q_1$ $[m^3\,min^{-1}]$ is the volumetric flowrate into of the reactor, $k_0$ $[min^{-1}]$ is the reference rate constant, $T_0$ $[K]$ is the temperature at which the reference rate constant is taken, $E$ $[kJ\,kmol^{-1}]$ is the activation energy of the reaction and $R$ $[kJ\,K^{-1}\,kmol^{-1}]$ is the universal gas constant.

# Appendix C

# Chylla-Haase Reactor Full Model

$$T_j = \frac{T_j^{in} + T_j^{out}}{2} \tag{C.1}$$

$$Q_{rea} = -\Delta H \; R_p \tag{C.2}$$

$$R_p = ikm_M \tag{C.3}$$

$$\Delta H = \frac{\Delta H_p}{MW_M} \tag{C.4}$$

$$k = k_0 \exp\left( - \frac{E}{RT} \right) (k_1 \mu)^{k_2} \tag{C.5}$$

$$\mu = c_0 \exp(c_1 f) \; 10^{\left(c_2 (\frac{a_0}{T} - c_3)\right)} \tag{C.6}$$

$$f = \frac{m_P}{m_M + m_P + m_W} \tag{C.7}$$

$$A = \left( \frac{m_M}{\rho_M} + \frac{m_p}{\rho_P} + \frac{m_W}{\rho_W} \right) \frac{P}{B_1} + B_2 \tag{C.8}$$

$$U = \frac{1}{h^{-1} + h_f^{-1}} \tag{C.9}$$

$$h = d_0 \exp(d_1 \mu_{wall}) \tag{C.10}$$

$$\mu_{wall} = c_0 \exp(c_1 f) \; 10^{\left(c_2 (\frac{a_0}{T_{wall}} - c_3)\right)} \tag{C.11}$$

$$T_{wall} = \frac{T + T_j}{2} \tag{C.12}$$

Table C.1: Chylla-Haase Reactor Full Process Parameters

| **Variable** | **Symbol** | **Unit** | **Value** |
|---|---|---|---|
| Initial mass of monomer | $m_{M,0}$ | $kg$ | 0 |
| Initial mass of molymer | $m_{P,0}$ | $kg$ | 11.227 |
| Initial mass of water | $m_{W,0}$ | $kg$ | 42.75 |
| Density of monomer | $\rho_M$ | $kg\,m^{-3}$ | 900 |
| Density of polymer | $\rho_P$ | $kg\,m^{-3}$ | 1040 |
| Density of water | $\rho_W$ | $kg\,m^{-3}$ | 1000 |
| Heat capacity of monomer | $c_{p,M}$ | $kJ\,kg^{-1}\,K^{-1}$ | 1.675 |
| Heat capacity of polymer | $c_{p,P}$ | $kJ\,kg^{-1}\,K^{-1}$ | 3.14 |
| Heat capacity of water | $c_{p,W}$ | $kJ\,kg^{-1}\,K^{-1}$ | 4.187 |
| Molecular weight of monomer | $MW_M$ | $kg\,kmol^{-1}$ | 104 |
| Mass of coolant in jacket | $m_C$ | $kg$ | 21.455 |
| Mass flowrate of coolant in jacket | $\dot{m}_C$ | $kg/s$ | 0.9412 |
| Heat capacity of coolant | $c_{p,C}$ | $kJ\,kg^{-1}\,K^{-1}$ | 4.187 |
| Pre-exponential rate constant | $k_0$ | $s^{-1}$ | 55 |
| Rate constant correction | $k_1$ | $ms\,kg^{-1}$ | 1000 |
| Rate constant correction | $k_2$ | - | 0.4 |
| Activation energy | $E$ | $kJ\,kmol^{-1}$ | 29560.89 |
| Batch viscosity correction | $c_0$ | $kg\,m^{-1}\,s^{-1}$ | 0.000052 |
| Batch viscosity correction | $c_1$ | - | 16.4 |
| Batch viscosity correction | $c_2$ | - | 2.3 |
| Batch viscosity correction | $c_3$ | - | 1.563 |
| Batch viscosity correction | $a_0$ | $K$ | 555.556 |
| Heat of polymerization | $\text{-}\Delta H_p$ | $kJ\,kmol^{-1}$ | $-70152.16$ |
| Heat transfer coefficient correction | $d_0$ | $kW\,m^{-2}\,K^{-1}$ | 0.814 |
| Heat transfer coefficient correction | $d_1$ | $ms\,kg^{-1}$ | $-5.13$ |
| Mass flowrate of monomer | $\dot{m}_M^{in}$ | $kg\,s^{-1}$ | 0.00756 |
| Monomer flow schedule | $[t_{M,0}^{in}, t_{M,1}^{in}]$ | $s$ | $[1800, 6000]$ |
| Set point of reactor temperature | $T_{set}$ | $K$ | 355.382 |
| Universal gas constant | $R$ | $kJ\,kmol^{-1}\,K^{-1}$ | 8.314 |
| Heat loss to surroundings | $(UA)_{loss}$ | $kW\,K^{-1}$ | 0.00567567 |
| Time constant for heating/cooling | $\tau_p$ | $s$ | 40.2 |
| Time delay 1 | $\theta_1$ | $s$ | 22.8 |
| Time delay 2 | $\theta_2$ | $s$ | 15 |
| Impurity range | $i$ | - | $[0.8, 1.2]$ |
| Fouling factors | $1/h_f$ | $m^2K\,kW^{-1}$ | $[0.000, 0.176, 0.352, 0.528, 0.704]$ |
| Summer ambient temperature | $T_{amb,S}$ | $K$ | 305.382 |
| Winter ambient temperature | $T_{amb,W}$ | $K$ | 280.382 |
| Inlet cooling water temperature | $T_{inlet}$ | $K$ | 294.26 |
| Inlet steam temperature | $T_{steam}$ | $K$ | 449.82 |
| Temperature set-point parameter | $a_3$ | - | 10 |
| Temperature set-point parameter | $a_4$ | - | $-15$ |
| Temperature set-point parameter | $a_5$ | - | 6 |
| Reactor bottom area | $B_1$ | $m^2$ | 0.193 |
| Jacket perimeter | $P$ | $m$ | 1.594 |
| Jacket bottom area | $B_2$ | $m^2$ | 0.167 |

# Appendix D

# Roles and Responsibilities

(At the request of University of Edinburgh)

Throughout the placement at NTNU I worked both independently and collaboratively with Prof. Sigurd Skogestad and Cristina Zotică. The original transformed input theory had previously been studied and worked on and my main contribution was the process modelling and simulation for case studies, which did not fit into previous assumptions, i.e. relative order greater than 1, and identifying any problems or opportunities. For the case studies, the main procedure was that Cristina and/or Sigurd supplied me with an outline of the case study to get started, e.g. for the CSTR it was a list of steady-state parameters.

I then spent the next week deriving equations where applicable, and then moving onto MATLAB and Simulink to code the simulations. I had weekly meetings with Cristina, which were mainly used to troubleshoot case study problems, e.g. with some code or some theory, which I could not overcome myself. Frequent meetings were held with Sigurd too to discuss progress and sometimes go over my monthly reports.